Modelling of turbulence within vegetation canopies

Sogachev Andrey

Division of Atmospheric Sciences, Department of Physical Sciences, University of Helsinki, POBox 68, FIN-00014, Helsinki, Finland (e–mail: Andrei.Sogachev@helsinki.fi).

Outline

1. Introduction
2. Local diffusion models
   - phenomenological models
   - first- and an one-and-a-half closure models
3. Governing equations for canopy flow
4. Non-local closure models
   - second-order and higher closure models
   - LES
5. **Two-equation models**
6. **SCADIS model and its applications**
7. Summary

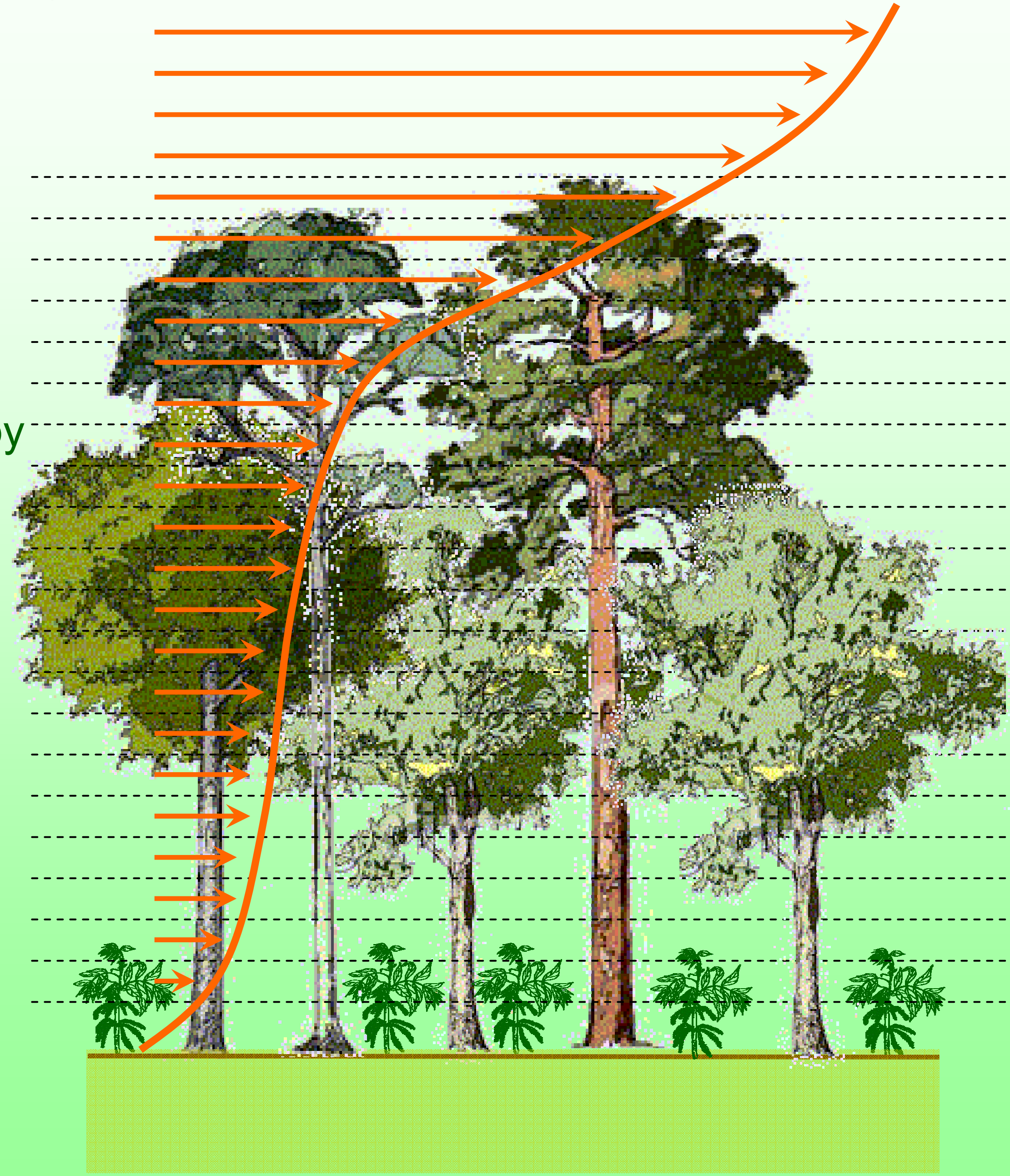

(Figure from Oltchev et al., 2004)

Introduction

Turbulence in plant canopies

Vegetation interacts with and influences the wind flow of the lowest atmospheric layers primarily in four ways: 1) in extracting momentum from the flow due to the aerodynamic drag of the plant parts; 2) in converting kinetic energy of the mean flow into turbulent kinetic energy in the wakes formed behind obstructions to the flow; 3) in breaking down large-scale turbulent motions into smaller scale motions, again in the wake flow; and 4) in providing a buoyant contribution to the "production" of turbulent energy due to the convective transfer of sensible heat between the plant parts and the airstream.

Useful review sources

Raupach, M. R., and A.S. Thom. 1981. Annual Review of Fluid Mechanics **13:** 97-129
Raupach, M. R., and R. H. Shaw. 1982. Boundary-Layer Meteorology **22:** 79-90.
Gross, G. 1993. Springer Verlag, Berlin, 168 pp.
Kaimal J.C. and J.J. Finnigan. 1994. Oxford University Press.. 289 pp (III chapter)
Finnigan, J. J. 2000. Annual Review of Fluid Mechanics **32:** 519-571.
Nato Science Series. 2007. Springer. (Eds. Y. Gayev and J.C.R. Hunt) V236.pp 414
http:/www.met.rdg.ac.uk/urb_met/NATO_ASI/talks.html

A ‘family portrait’

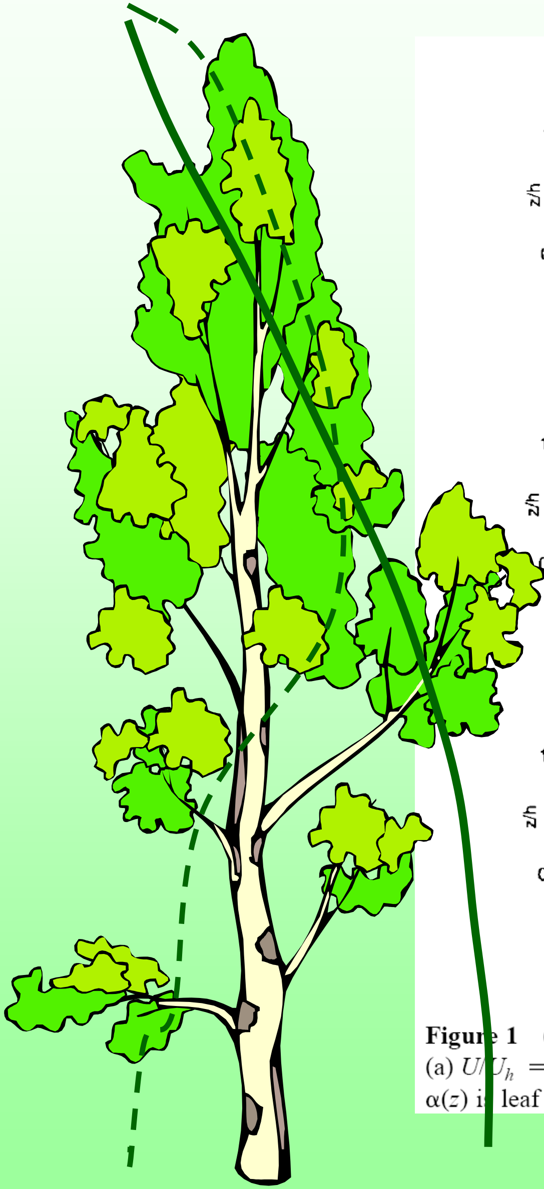

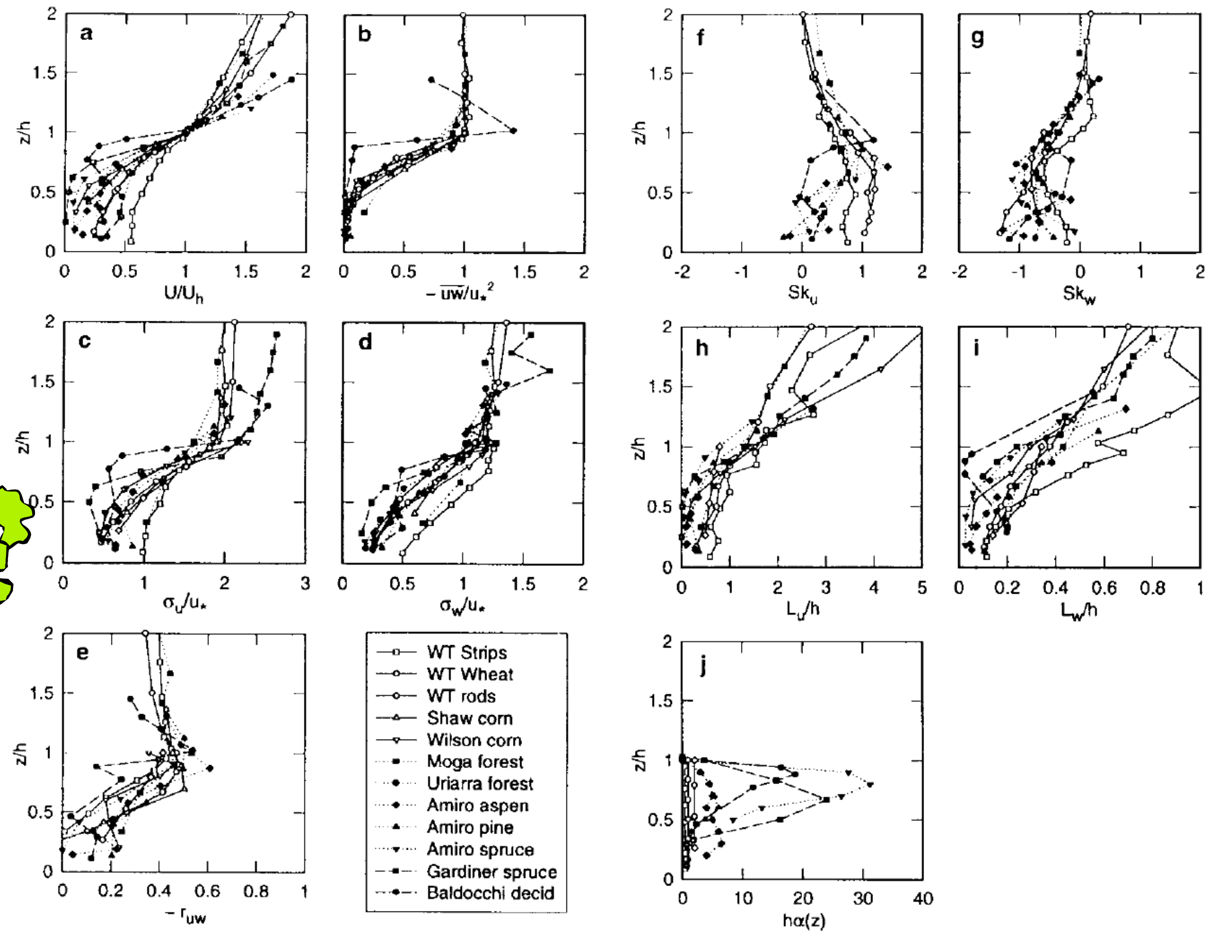

Figure 1 (a–e) A “family portrait” of canopy turbulence for canopies A to L in Table (1), showing profiles with normalized height z/h of (a) $U/U_h = \langle \overline{u_1} \rangle(z)/\langle \overline{u_1} \rangle(h)$; (b) $-\overline{u'w'}/u^*$; (c) σ_u/u^*; (d) σ_w/u^*; (e) $-r_{uw} = -\overline{u'w'}/\sigma_u\sigma_w$; (f) Sk_u; (g) Sk_w; (h) L_u; (i) L_w; (j) $h\alpha(z)$ where $\alpha(z)$ is leaf area per unit volume. L_u and L_w are defined in equation (3.1). Figure from Raupach et al (1996)

A(z) [м^2 м$^{-3}$]   LAI [м^2 м$^{-2}$]

(Raupach et al., 1996, Finnigan, 2000)

Wind profiles

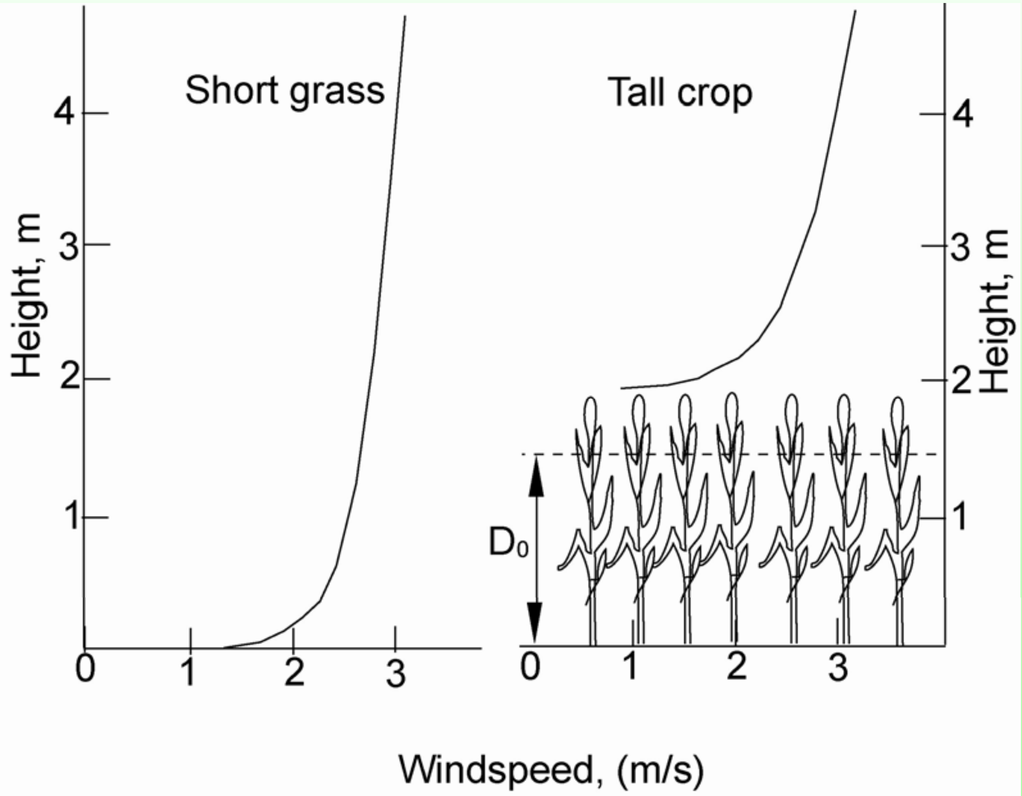

$$u(z) = \frac{u_*}{k}\left[\ln\left(\frac{z-d}{z_{0m}}\right) - \psi_m\right]$$

Estimation of *d* and z_0

Approach 1

(Thom, 1971)

$$d = \frac{\int_0^h z\left(\mathrm{d}\left\langle \overline{u'w'} \right\rangle / \mathrm{d}z\right)\mathrm{d}z}{\int_0^h \left(\mathrm{d}\left\langle \overline{u'w'} \right\rangle / \mathrm{d}z\right)\mathrm{d}z}$$

where h is the canopy height and $\langle \overline{u'w'} \rangle$, the kinematic momentum flux. The correction for the drag associated with the surface (Shaw and Pereira, 1982) yields the following:

$$d = h - \frac{1}{u_*^2}\int_0^h \left\langle \overline{u'w'} \right\rangle \mathrm{d}z.$$

The expression assumes $\langle \overline{u'w'} \rangle(0) \ll \langle \overline{u'w'} \rangle(h) = u_*^2$

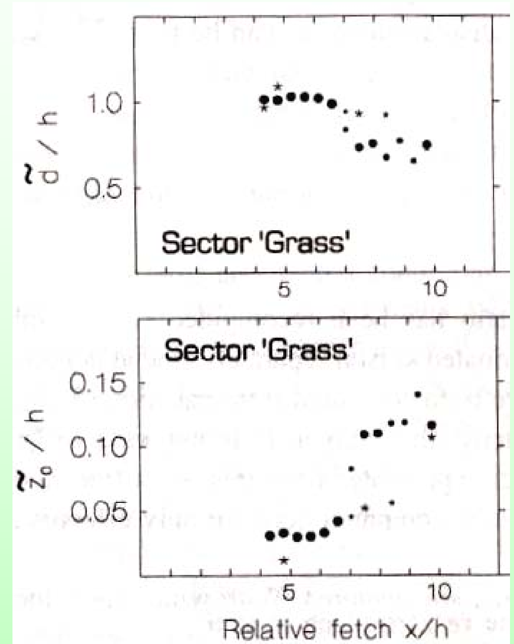

(Kruijt, 1994)

Approach 2

(Raupach et al., 1986):

$$d = \frac{\int_0^h zU^2\mathrm{d}z}{\int_0^h U^2\mathrm{d}z}$$

derived assuming the form drag to be the main drag mechanism.

$$z_0 = \frac{z_\mathrm{r} - d}{\exp\left(kU(z_\mathrm{r})/u_*\right)}.$$

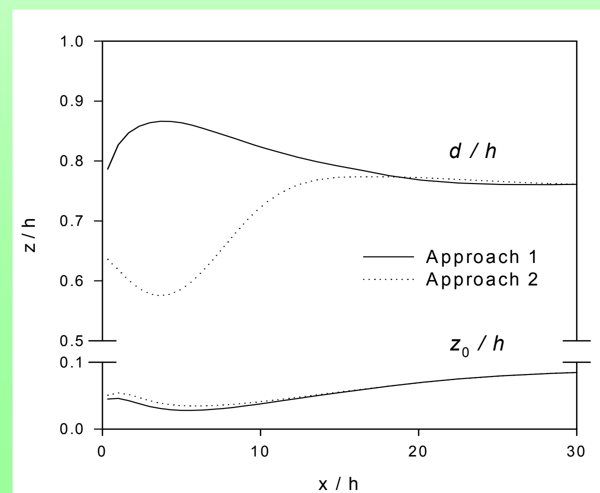

(Sogachev et al.,, 2005; 2006)

Local diffusion models

Phenomenological Models

The simplest response, almost universally used hitherto, is to dose the conservation equations at first order by using the diffusion equation, together with a plausible assumption about the diffusivity *K.*

$$\partial\tau/\partial z = c_M(U)a(z)U^2(z) \qquad \tau(z) = -\langle u'\overline{w'}\rangle \qquad U = \langle \bar{u} \rangle$$

The variations in leaf area, the random orientation and mutual interference of leaves, as well as the effects of turbulence are all subsumed in C_M (or C_d), the effective drag coefficient, and *a*(*z*), the leaf area per unit volume of space.

$$\tau(z) = K_M \frac{\partial U}{\partial z} \qquad \frac{\partial K_M}{\partial z}\frac{\partial U}{\partial z} + K_M \frac{\partial^2 U}{\partial z^2} = c_M(U)a(z)U^2$$

To solve this second-order differential equation in *U(z),* one must specify $c_M(U)$, *a(z),* and two boundary conditions for *U*, usually *U(h)* and *U*(0) (which is zero by the no-slip condition). Also, K_M must plausibly related to the other variables in the equation.

There are two general ways of doing this, which leads to an analytical wind profile in the special case of a uniform canopy *[a(z) = constant]* and a velocity-independent drag coefficient [$c_M(U)$ = constant].

The mixing-length approach is based upon Prandtl-von Karman mixing-length theory

(Inoue1963, Cionco 1965)

$$K_M = \ell^2 \frac{\partial U}{\partial z}$$

$$U(z)/U(h) = \exp\left[\alpha_1(z/h - 1)\right] \quad (1)$$

α_1 is equal to $(\frac{1}{2} c_M a h^3 \ell^{-2})^{1/3}$

This is the exponential wind profile. There are too many assumptions in its derivation for it to be regarded as any more than a single-parameter empirical fit, but it is nevertheless widely used, largely because it describes the upper part of most canopy wind profiles quite well when a_1 is suitably chosen. Cionco (1972) has summarized the best values of a_1 for numerous canopies; it usually lies between 2 and 3.

In the *diffusivity approach*, K_M is constructed directly from known variables without recourse to a mixing-length assumption.

Cowan(1968) $K_M \propto U$

$$\frac{U(z)}{U(h)} = \left(\frac{\sinh(\alpha_2 z/h)}{\sinh \alpha_2} \right)^{\frac{1}{2}} \quad (2)$$

Landsberg & James (1971), Thom (1971)

$$K_M = \text{constant}$$

(3)

$$U(z)/U(h) = \left[1 + \alpha_3(1 - z/h)\right]^{-2}$$

$$\alpha = h\frac{\sqrt{(C_d u_h L)}}{6K}$$

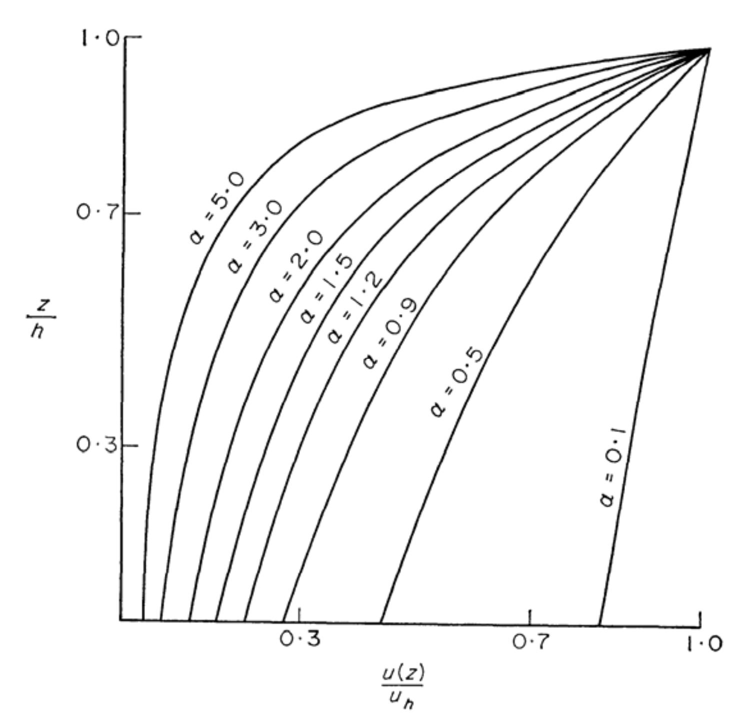

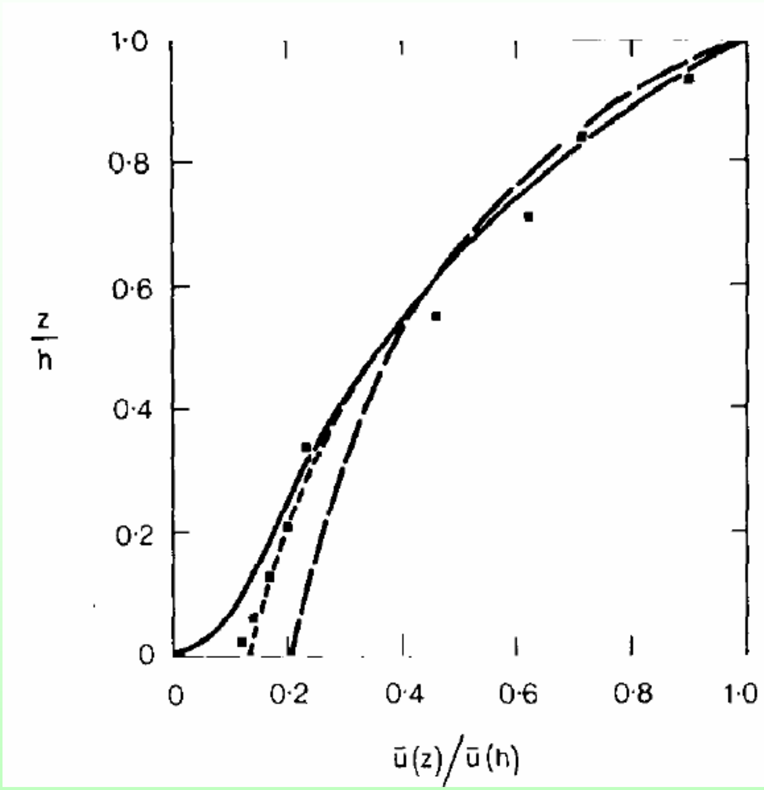

Comparison of analytical wind profiles from diffusion theory with measurements (squares) of Seginer et al (1976) in a uniform canopy of cylindrical rods.
Dotted line, Inoue(1963) with a_1=2;
Solid line, Cowan (1968) with a_2=4;
Dashed line, Thom (1971) with a_3-1.2.

After Raupach and Thom (1981)

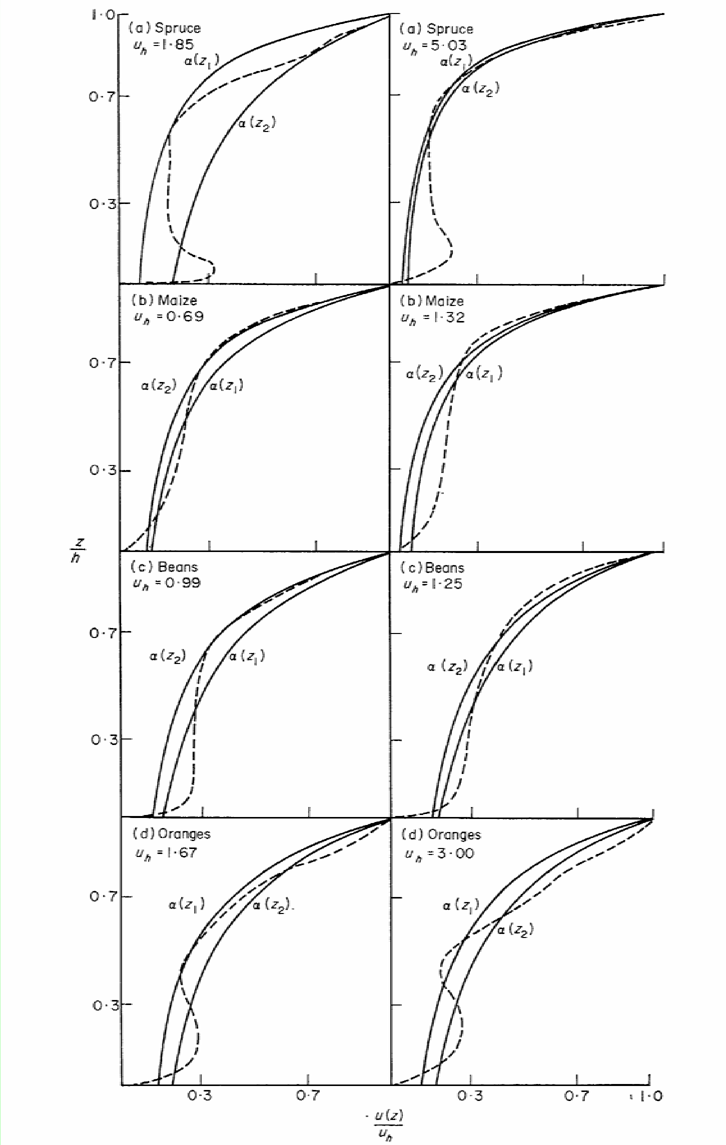

FIG. 5. Measured and calculated wind profiles on dimensionless scales. The numbers refer to the profile numbers given in Table 2. (a) Spruce, profiles 2 and 16; (b) maize, profiles 3 and 6; (c) beans, profiles 3 and 6; (d) oranges, profiles 1 and 4.

Landsberg & James (1971)

Smith et al. (1972) showed that, in descending through the forest, the stress and wind vectors turn through an angle which depends on the forest characteristics and on the stability and the speed of the airflow above the forest.

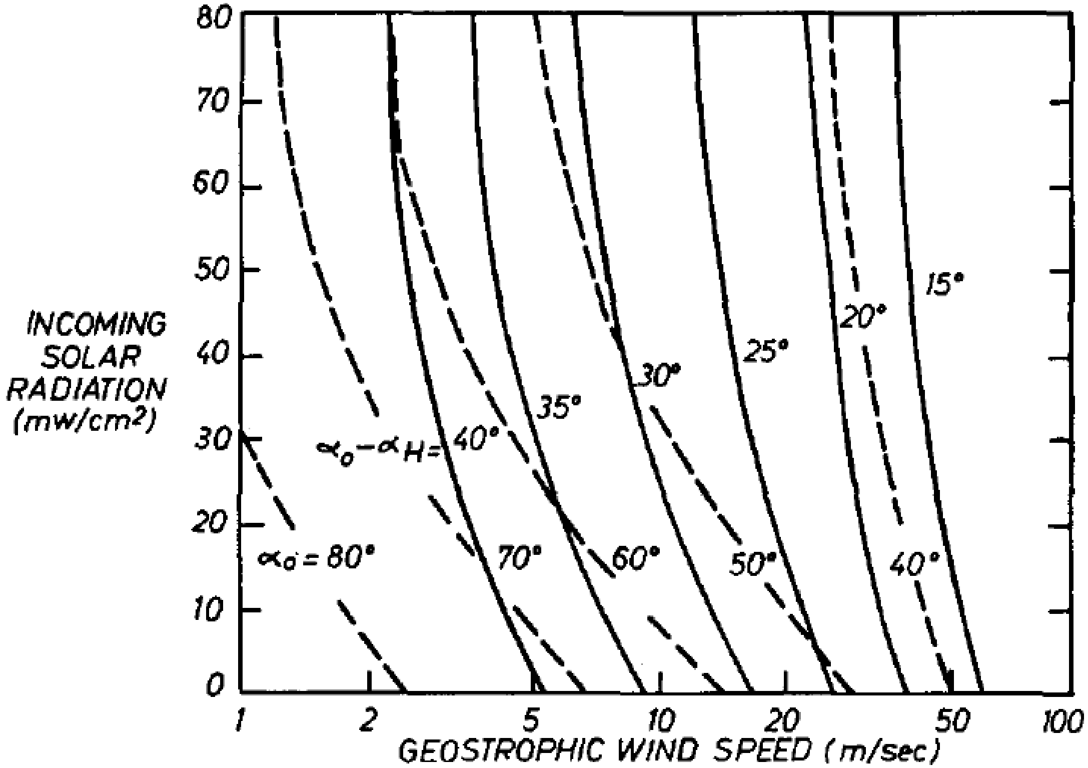

Fig. 7. The full lines show the predicted turning of the wind through the Thetford forest as a function of geostrophic wind speed and incoming solar radiation. The dashed lines show the full turning of the predicted surface wind from the geostrophic wind direction.

Albini (1981) argued that “all models involve the introduction of a length scale in one form or another; none make extensive use of an intrinsic length scale of the vegetation cover in deriving the shear stress. This scale is the inverse of the drag area per unit volume of the vegetation cover layer viewed as a continuum”.

Albini (1981) modelled the wind speed within the canopy as an exponential function of cumulative leaf drag area per unit planform area

$$\frac{u(z)}{u_h} = e^{-n\left\{1-\frac{\zeta(z)}{\zeta(h)}\right\}}, \tag{14}$$

where ξ is the cumulative leaf drag area per unit planform area:

$$\zeta(z) = \int_0^z \left[\frac{C_d(z')a(z')}{P_m(z')}\right] dz' \tag{15}$$

and $\zeta(h)$ is the drag area index. Here $P_m(z)$ is the foliage shelter factor for momentum as a function of height within the canopy.

Albini (1981) derive the phenomenological model for the mean wind speed and Reynolds shear stress profiles with height in a vegetation cover layer from forms suggested by truncation of the equations of turbulent fluid motion at second order in fluctuating velocity products

Using Albini's model Massman (1987, 1997) and Massman and Weil (1999) formulated an analytical one-dimensional second-order closure model to describe the within canopy velocity variances, turbulent intensities, dissipation rates, Lagrangian time scale and Lagrangian far field diffusivities for vegetation canopies of arbitrary structure and

$$\frac{-\overline{u'w'}(z)}{-\overline{u'w'}(h)} = \frac{u^2(h)\zeta(h)}{2n(-\overline{u'w'}(h))} e^{-2n(1-\zeta(z)/\zeta(h))}$$

$$u(z)/u(h) = e^{-n(1-\zeta(z)/\zeta(h))}$$

$$\zeta(z) = \int_0^z [C_d(z')a(z')/P_m(z')]dz'$$

$$z_0/h = (1-d/h)e^{(-ku(h)/u_*+\psi)}$$

$$d/h = 1-\int_0^1 e^{-2n(1-\zeta(z)/\zeta(h))}d\xi$$

where $\xi = z/h$.

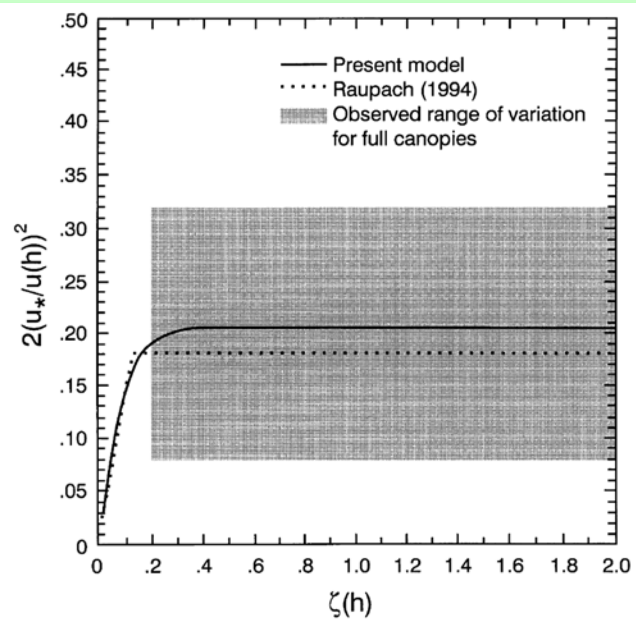

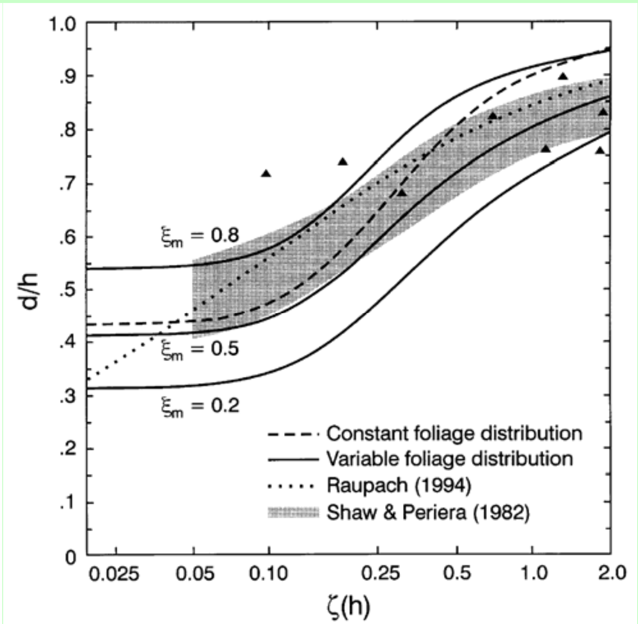

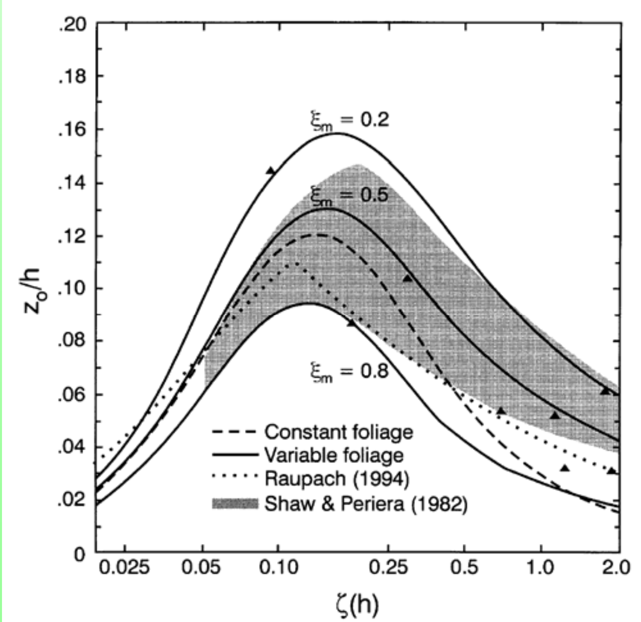

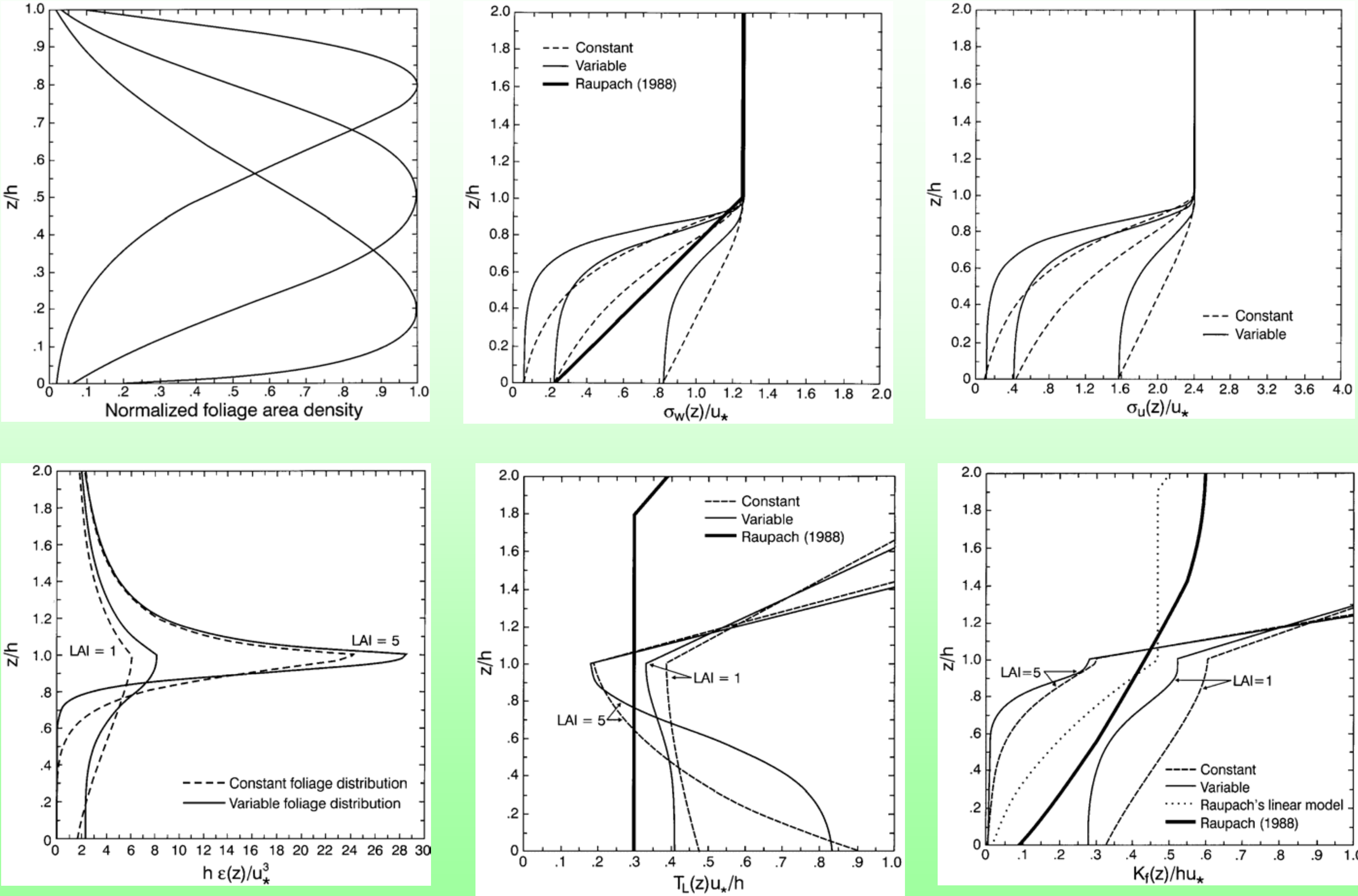

(Massman, 1997; Massman and Weil, 1999)

Further development of the model by Mohan and M K Tiwari, 2004

Lalic (1997), Lalic and Mihailovic (1998) and Mihailovic et al. 1999 derived a general equation for the wind speed profile in a roughness sublayer under neutral conditions

$$u(z) = \frac{u_*}{k} \ln \frac{z-d}{z_0}$$

$$u(z) = \frac{u_*}{k} a \left(\frac{z}{z_k} - 1 \right)^n \quad h < z < z_t$$

$$u(z) = \begin{cases} u_h \left[\dfrac{\cosh \beta \left(\dfrac{z - z_d}{h} \right)}{\cosh \beta \left(1 - \dfrac{z_d}{h} \right)} \right]^{\frac{5}{2}} & z_d < z \le h \\ C_h u_h & z_0 < z \le z_d \end{cases}$$

$$K_m(z) = \begin{cases} \sigma(z) u_h \left[\dfrac{\cosh \beta \left(\dfrac{z - z_d}{h} \right)}{\cosh \beta \left(1 - \dfrac{z_d}{h} \right)} \right]^{\frac{5}{2}} & z_d < z \le h \\ \sigma_d C_h u_h & z_0 < z \le z_d \end{cases}$$

$$\sigma(z) = \frac{2 C_d LAI \ h}{7 \beta^2 ch^6 \beta \left(\dfrac{z - z_d}{h} \right)} \left[1 + \sinh^2 \beta \left(\frac{z - z_d}{h} \right) + \frac{3}{5} \sinh^4 \beta \left(\frac{z - z_d}{h} \right) + \frac{1}{7} \sinh^6 \beta \left(\frac{z - z_d}{h} \right) \right]$$

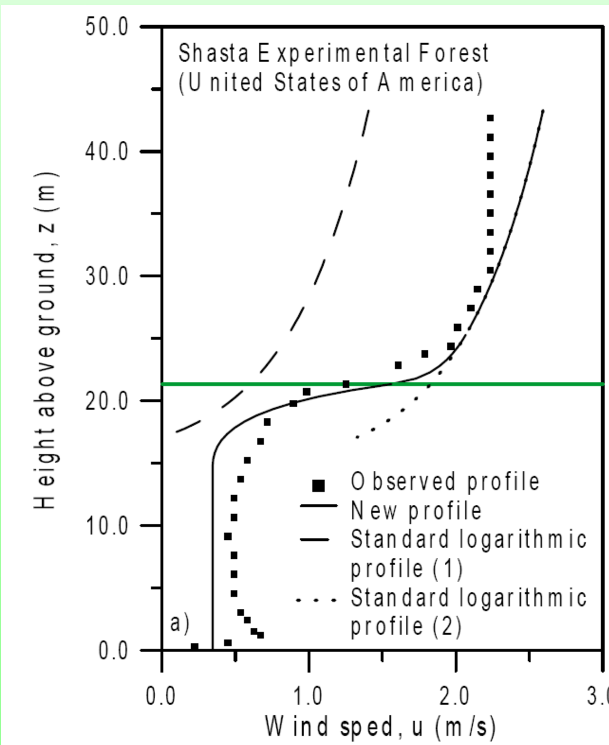

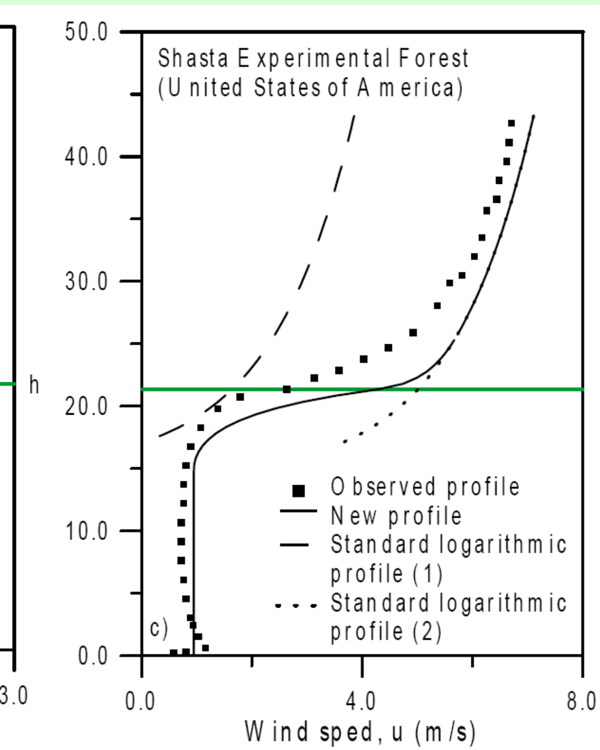

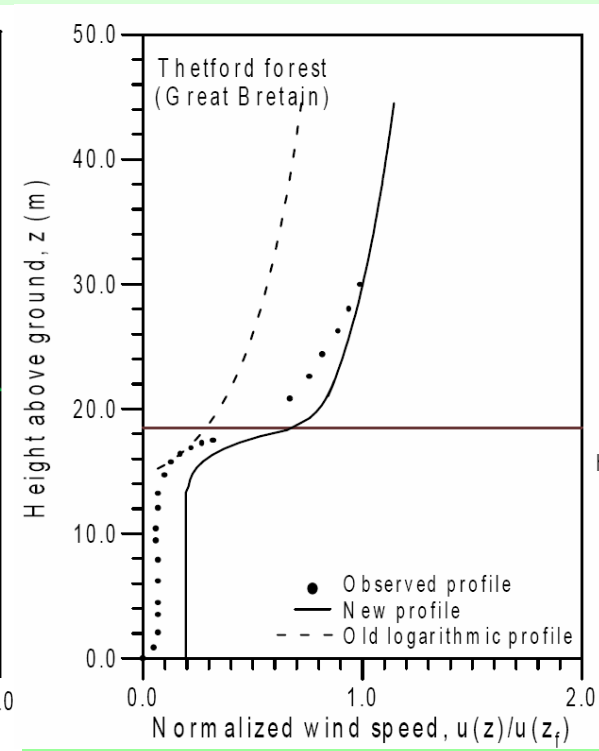

Belcher et al. 2003 and Finnigan and Belcher, 2004

The adjustment length, *Lc*, is proportional to (i) the reciprocal of the roughness density (defined to be the frontal area of canopy elements per unit floor area) and (ii) the drag coefficient of individual canopy elements.

Velocity perturbation and total velocity profiles with and without a canopy

H/L=0.1 $L_c=(ca)^{-1}$=10m {*cd*=0.25, h_c=10m, *LAI*=4}

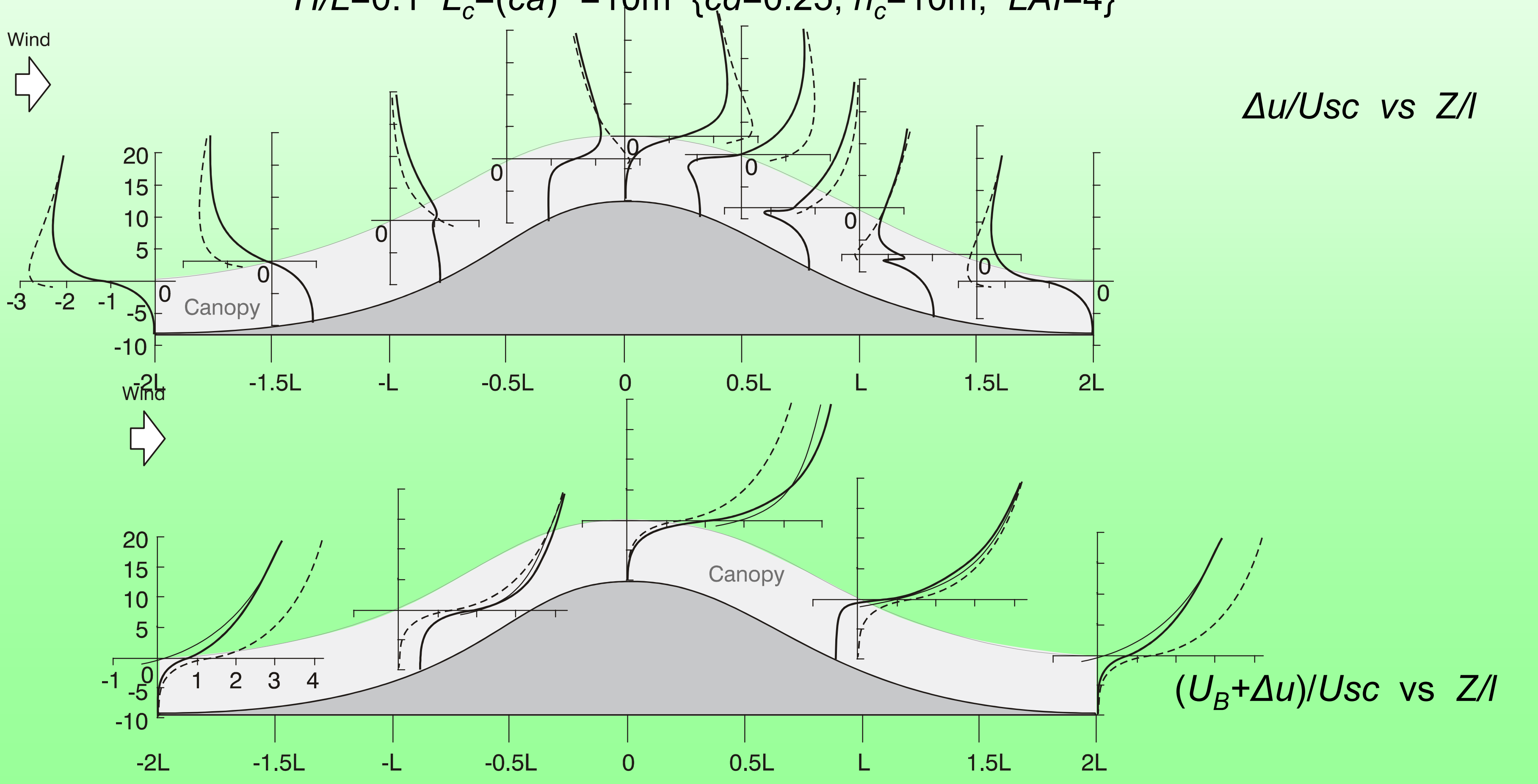

First- and an one-and-a-half closure models

$$\frac{\partial \langle \bar{u}_i \rangle}{\partial x_i} = 0$$

$$E \equiv \tfrac{1}{2} \left\langle \overline{u'_i u'_i} \right\rangle$$

$$\left\langle \overline{u'_i u'_j} \right\rangle = \frac{2}{3} \delta_{ij} E - K \left(\frac{\partial \langle \bar{u}_i \rangle}{\partial x_j} + \frac{\partial \langle \bar{u}_j \rangle}{\partial x_i} \right)$$

$$\frac{\partial \langle \bar{u}_i \rangle}{\partial t} + \langle \bar{u}_j \rangle \frac{\partial \langle \bar{u}_i \rangle}{\partial x_j} + 2\varepsilon_{ijk} \Omega_j \langle \bar{u}_k \rangle = - \frac{\partial \langle \bar{P} \rangle}{\partial x_i} - \frac{\partial \left\langle \overline{u'_i u'_j} \right\rangle}{\partial x_j} + S_i.$$

$$K_M = \ell^2 \frac{\partial U}{\partial z}$$

$$S_i = - c_d A \langle \bar{u}_i \rangle |U|$$

$$\frac{\partial E}{\partial t} + \langle \bar{u}_j \rangle \frac{\partial E}{\partial x_j} = \frac{\partial}{\partial x_i} \left(\frac{K}{\sigma_E^{\varphi}} \frac{\partial E}{\partial x_i} \right) + P_E - \varepsilon + S_E$$

$$K = C_0 l E^{1/2}$$

$$C_0 = C_\mu^{1/4} \qquad \varepsilon = C_0^4 E^2 / K, \qquad S_E = \beta_p c_d A |U|^3 - \beta_d c_d A |U| E$$

$$\frac{\partial \varphi}{\partial t} + \langle \bar{u}_j \rangle \frac{\partial \varphi}{\partial x_j} = \frac{\partial}{\partial x_i} \left(\frac{K}{\sigma_\varphi} \frac{\partial \varphi}{\partial x_i} \right) + \frac{\varphi}{E} \left(C_{\varphi 1} P_E - C_{\varphi 2} \varepsilon F_\varphi W \right) + S_\varphi$$

$$S_\varphi = \alpha_{\varphi p} \frac{\varphi}{E} S_p - \alpha_{\varphi d} \frac{\varphi}{E} S_d \qquad l = \frac{C_\mu^{3/4} E^{3/2}}{\varepsilon} \qquad K = C_\mu \frac{E^2}{\varepsilon}$$

(Raupach and Shaw, 1982 Sanz, 2003; Sogachev and Panferov, 2006)

Kondo and Akashi (1976) derive ℓ from Karman's ratio subject to some constrains.

$$\frac{d}{dz}\left[l^2\left|\frac{d\mathbf{U}}{dz}\right|\frac{d\mathbf{U}}{dz}\right]=\frac{1}{2}ca|\mathbf{U}|\mathbf{U}+if(\mathbf{U}-\mathbf{V}_g)$$

$$C_D(z)=\frac{hca(z)}{2}$$

$$\frac{l(z)}{h}=\frac{4k^3}{hca}=\frac{2k^3}{C_D}$$

$$l(z)\le l_i=kz$$

$$\frac{dl}{dz}\le k,$$

$$l(z)=\frac{\sqrt{\tau/\rho}}{\frac{du}{dz}}.$$

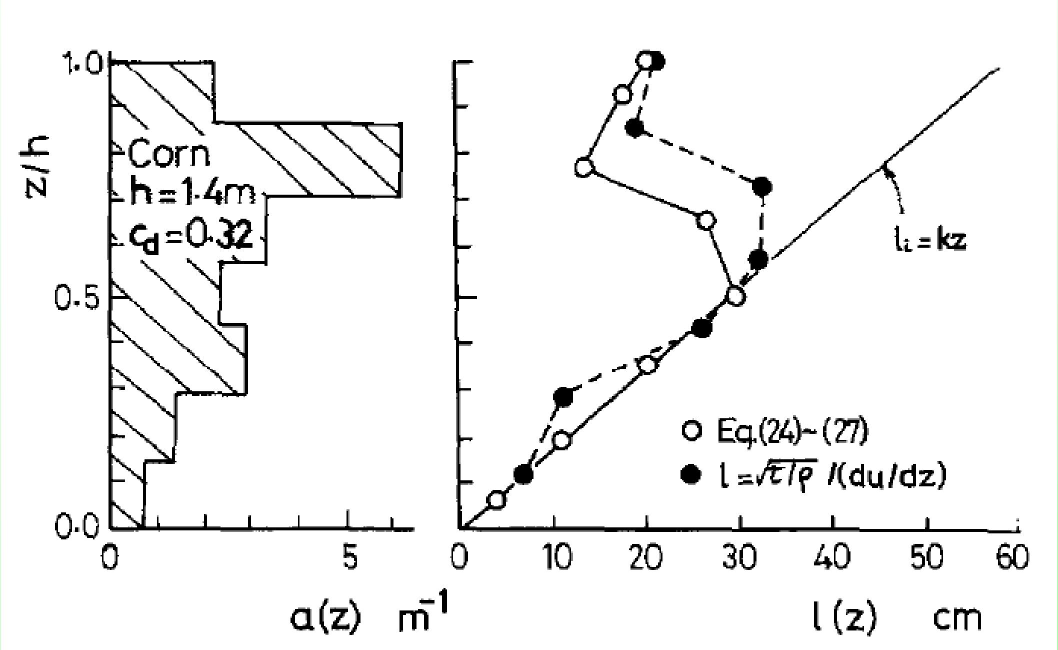

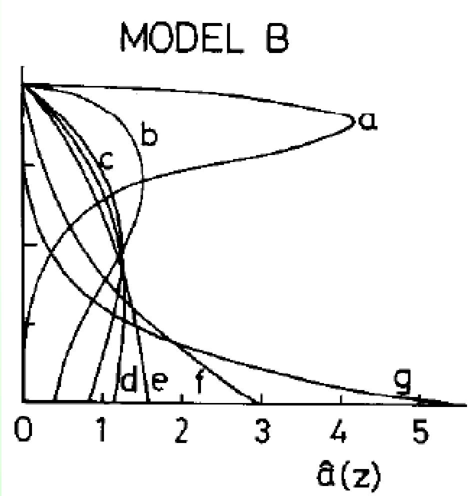

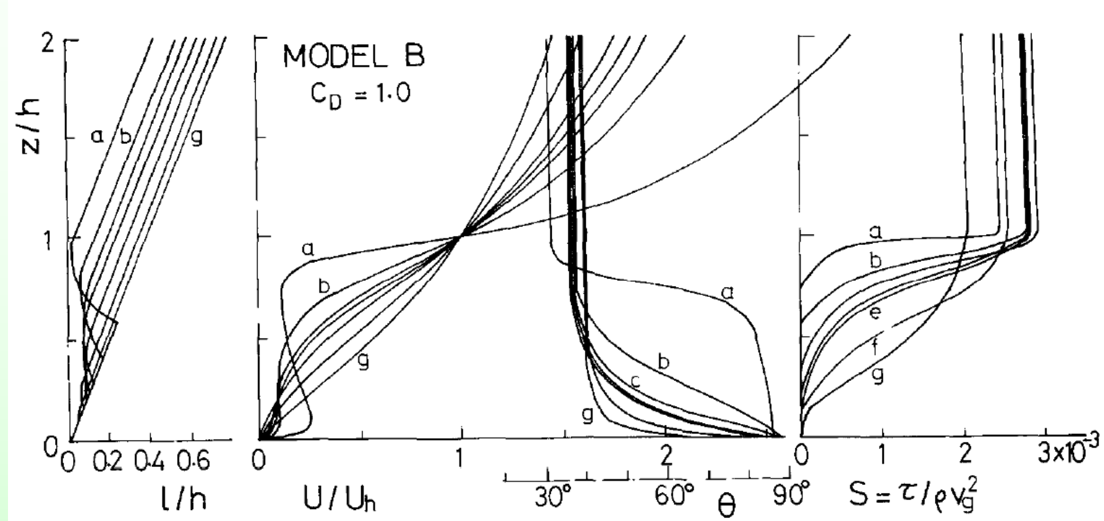

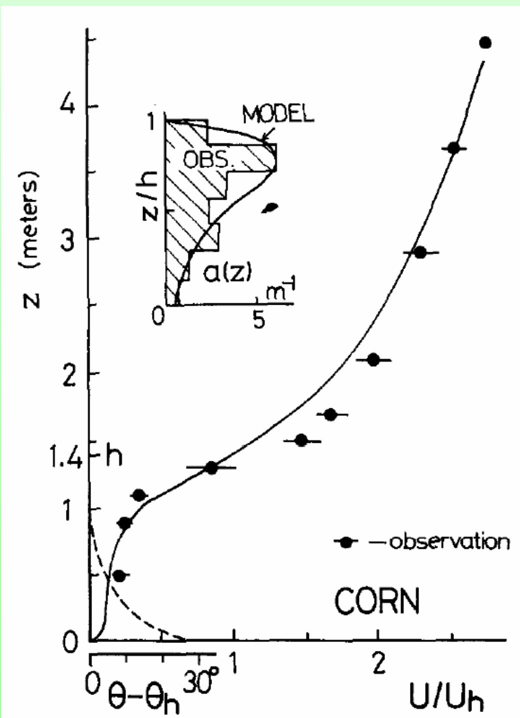

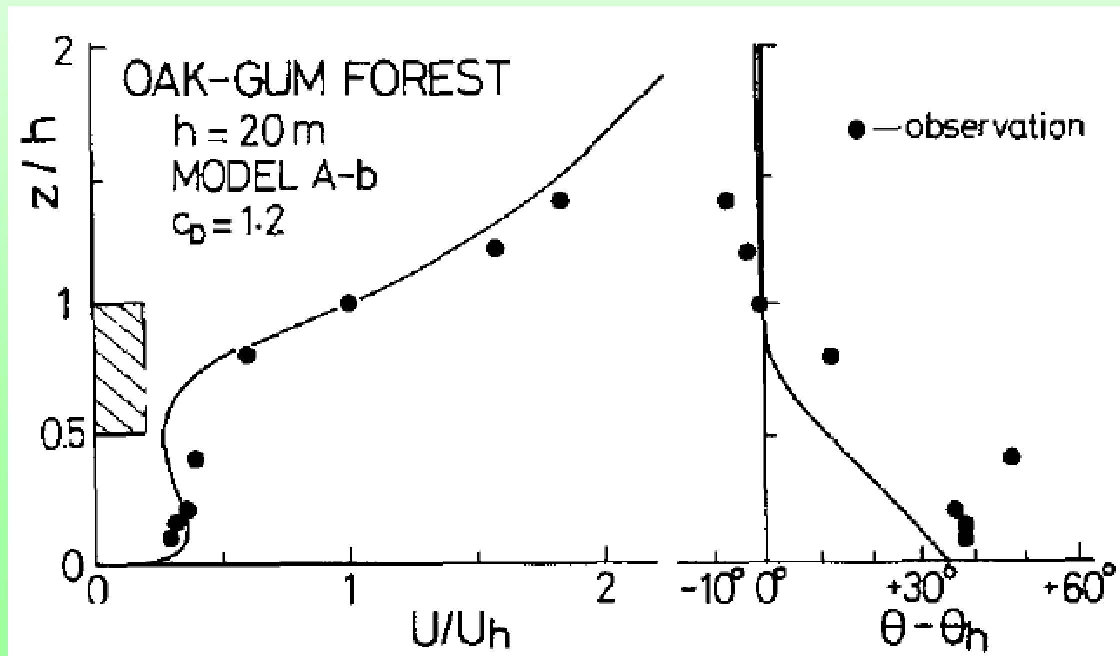

Kondo and Akashi (1976)

Parameterizations of mixing length

Perrier (1967) $l(z) = \frac{0.6}{a(z)}$

Wilson and Shaw (1977)

$$l=0 \quad \text{at} \quad z=0,$$

$$\left|\frac{dl}{dz}\right| \leqslant k,$$

$$l \leqslant \frac{\alpha}{C_d A},$$

(Tjernstrom, 1989)

$$l(z) = 2.25/a(z)$$

Menzhulin (1970, 1974)

$$\frac{1}{l} = \frac{s}{0.40 d_f} + \frac{1}{l_{LZ}}, \qquad l_{LZ} = -0.40 \frac{\psi}{(\partial\psi/\partial z)}$$

$$\psi = \frac{\sqrt{e}}{l_{LZ}}.$$

´Li et al. (1990)

$$l(z) = \frac{l_h z}{(1+0.4A)h}$$

$$K = C_0 l E^{1/2}$$

$$\varepsilon = C_0^4 E^2 / K,$$

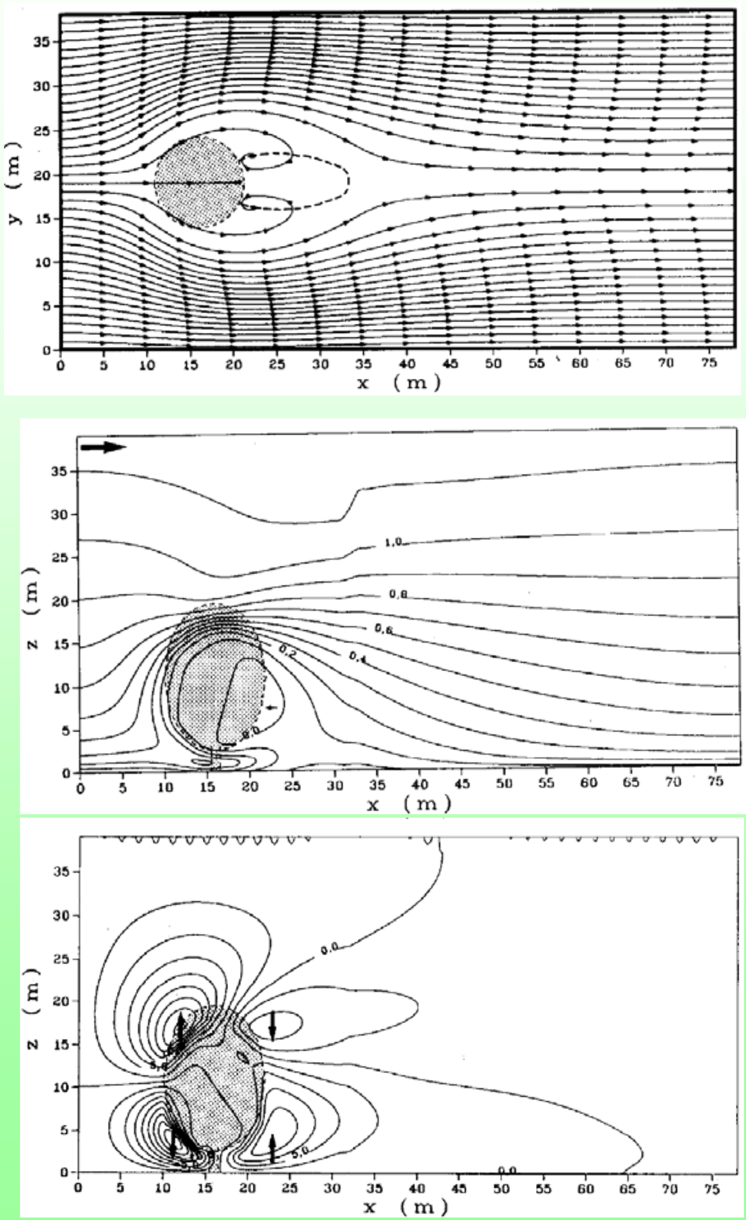

Gross 1987, 1993

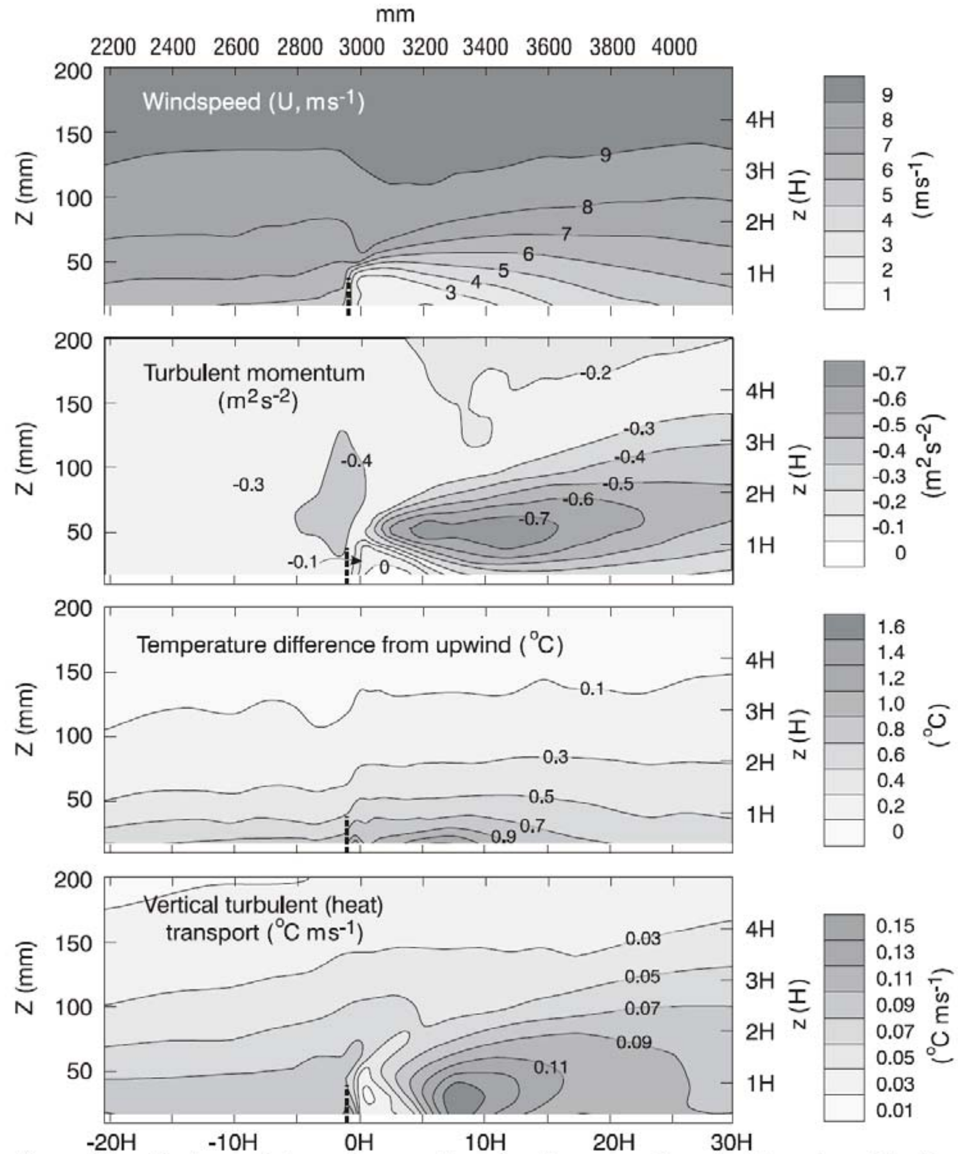

Figure 9.4 Contour plots on the x-z plane for flow around a wind tunnel model of a porous windbreak. (a) Mean windspeed, $U = \overline{u}(x,z)$; (b) Momentum flux, $\overline{u'w'}(x,z)$; Temperature, $\overline{\theta}$; Heat flux, $\overline{w'\theta'}$. Figure from Cleugh and Hughes (2001).

Weaknesses in the local-diffusion assumption

Conceptual legitimacy of the flux-gradient approach at the canopy scale requires that turbulence within the canopy be composed of small, high frequency eddies, such that the transport process occurs along length scales that match the scalar concentration gradient. In reality, turbulence in many canopies is composed of large, lower frequency eddies that traverse the entire length of the canopy, or a sizeable fraction of the canopy height. In the left figure, the vertical profile of the scalar concentration gradient is provided as the heavy solid line.

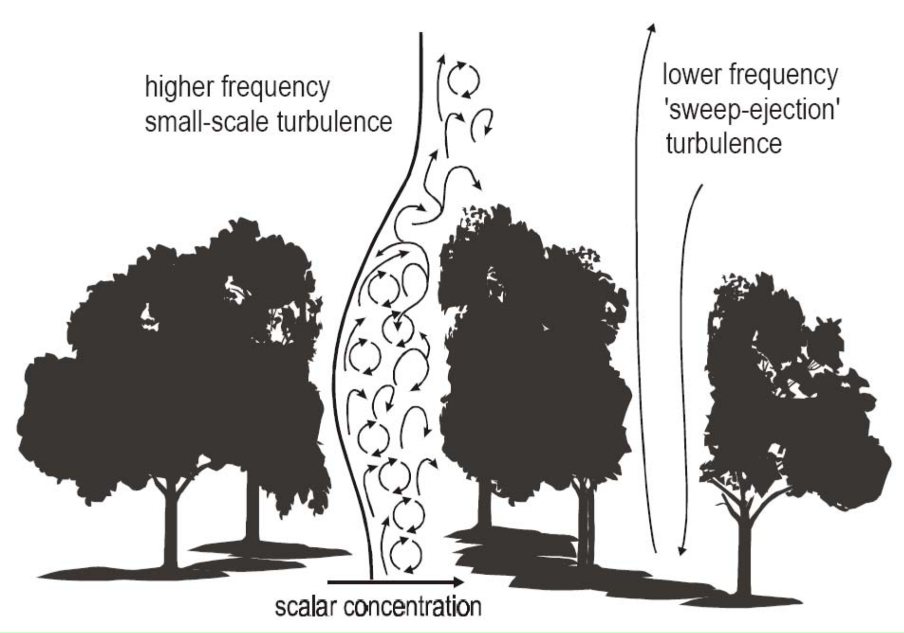

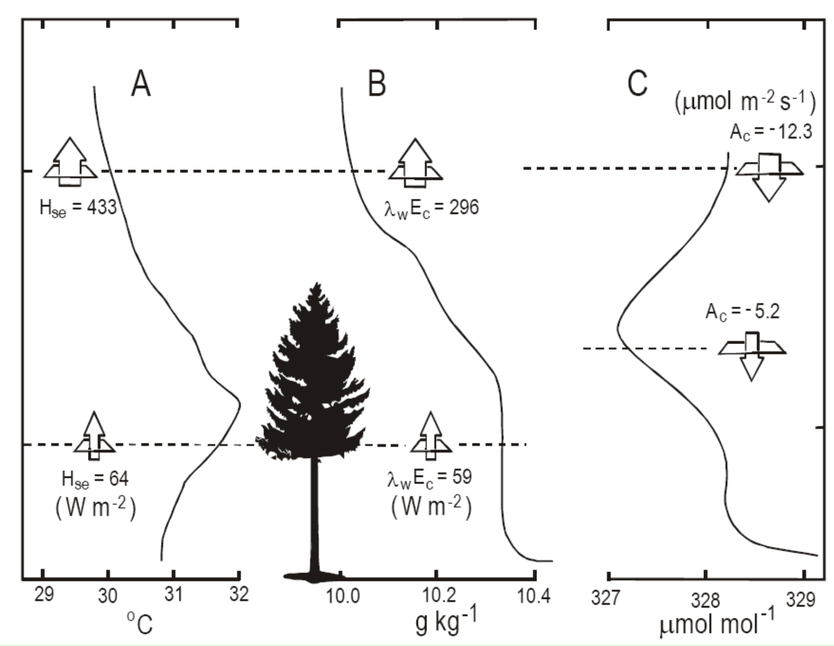

Redrawn from Monson, 2004 and Denmead and Bradley (1985).

Attempt of K-theory improving

$$-\frac{\partial}{\partial z}\left\langle \overline{u''}\,\overline{w''} + \overline{u'\,w'} \right\rangle = \frac{\partial}{\partial z}\left(l^2 \left|\frac{\partial \overline{u}}{\partial z}\right| \frac{\partial \overline{u}}{\partial z}\right) + \frac{\alpha(\overline{u}_h - \overline{u})}{1 + \beta A_r}\,\frac{z}{h}$$

When $z \leq h_{\max}$

$l = kz/\{1.5 + 2.5\,A(z)\}$

When $z > h_{\max}$

$l = l_{h_{\max}} + C_2(z - h_{\max})$

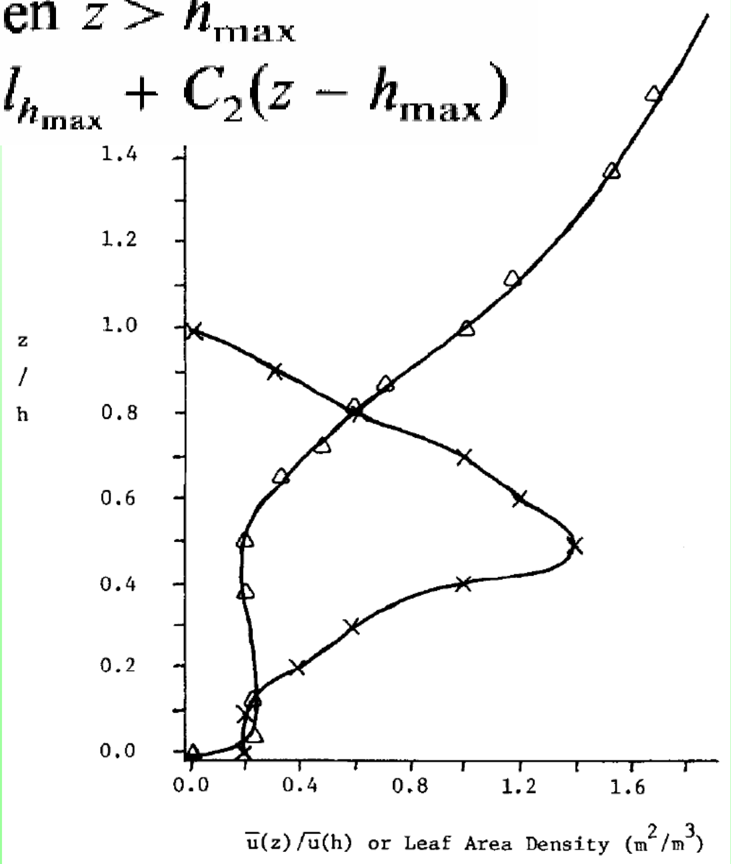

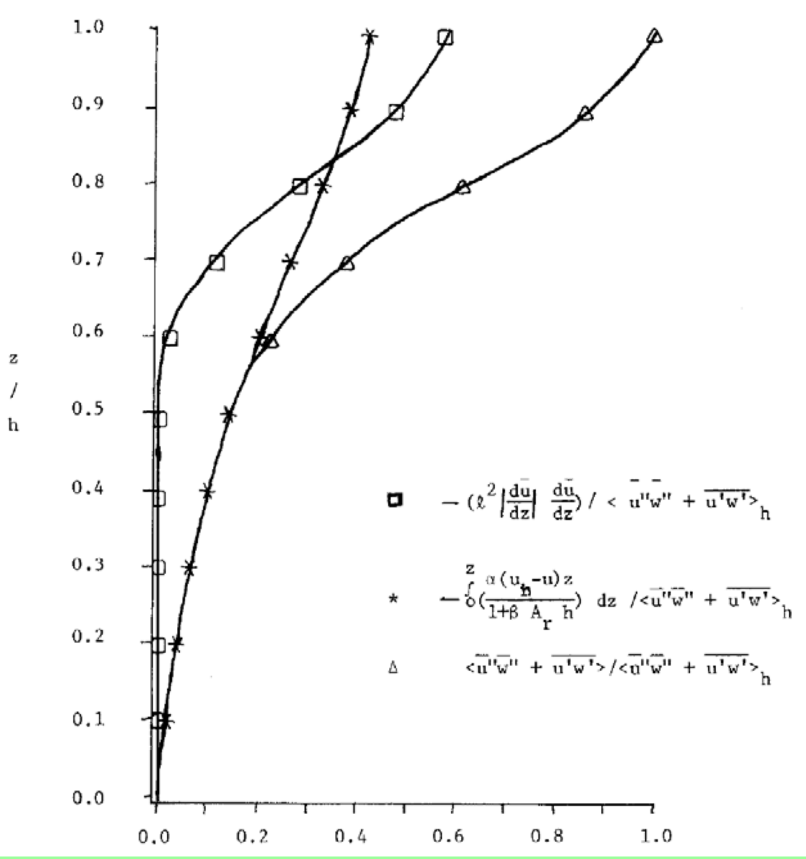

Li et al. (1985)

The Canopy-Mixing Layer Analogy

Raupach et al. (1996) showed that turbulence in and just above plant canopies is better described by a mixing layer analogy than by the common surface layer similarity theory. They concluded that the length scale *Ls* is an important aerodynamic property of plant canopies and is given by *Ls* = *U*(h)/(d*U*/d*z*).

Wilson et al. (1998)

$$K = \lambda(x,z)\sqrt{c_e k(x,z)}$$

$$\lambda = \max\ (\lambda_i, \lambda_o)$$

$$\frac{1}{\lambda_i} = \frac{1}{k_v z} + \frac{1}{\lambda_c}, \frac{1}{\lambda_o} = \frac{1}{k_v(z-d)} + \frac{1}{L_\infty}$$

$$\lambda_c = c\sqrt{k(h)}\left(\frac{\partial S}{\partial z}\right)_h^{-1}$$

$$S = (U^2 + V^2)^{1/2}$$

$$L_\infty = 0.0004\frac{U_G}{f}$$

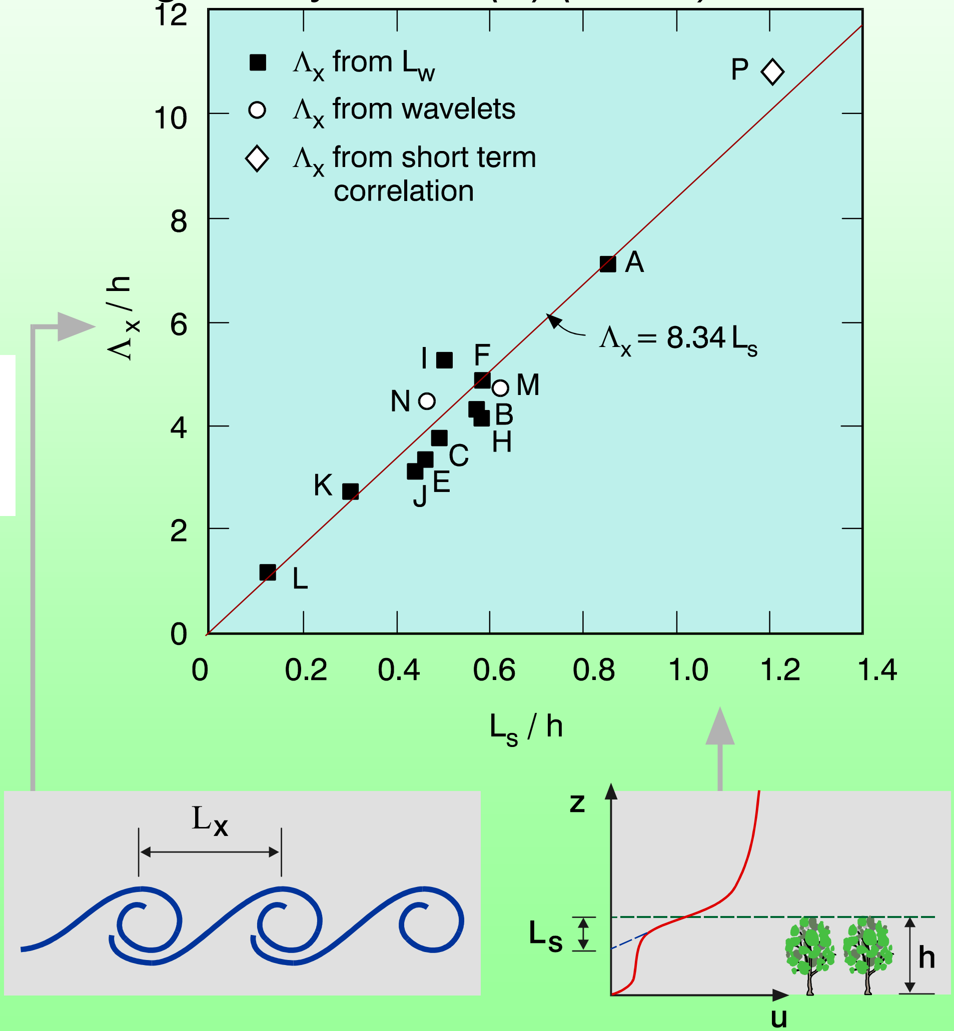

(Redrawn from Finnigan, 2004)

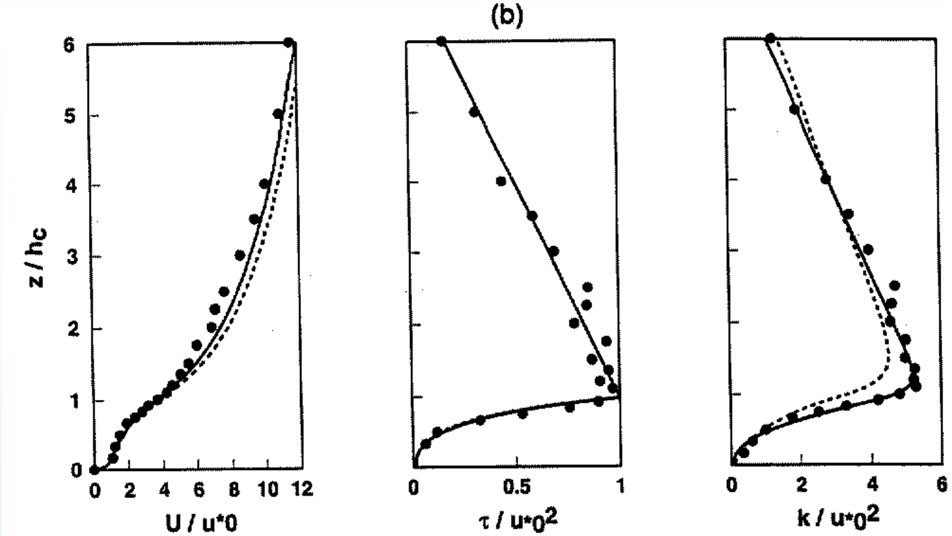

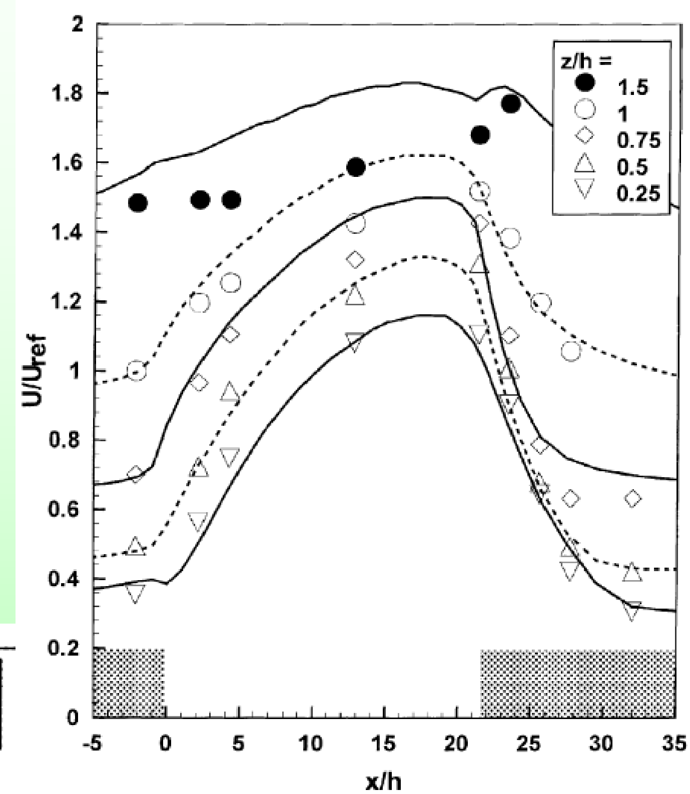

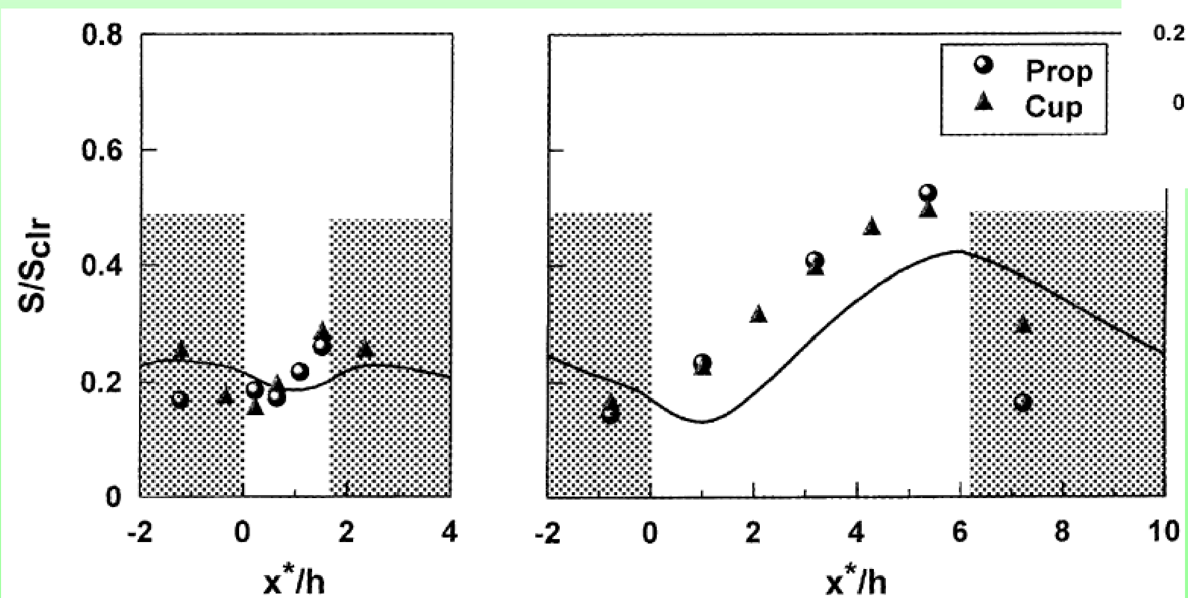

Wilson et al. (1998)

Governing equations for canopy flow

It is impractical to account explicitly for the spatial variability imposed on the airflow by the complexity of the within-canopy airspace. Instead, for many years standard free-air Reynolds equations were adapted for use in canopies by the *adhoc* addition of a source or drag term, which was regarded as a smooth function of space.

Wilson and Shaw (1977) demonstrated that the source and sink terms that appear at any order in continuum treatments of airflow in the vegetation airspace can be formally derived by spatially averaging the Navier–Stokes or Reynolds equations that obtain at a point in the canopy airspace.

This procedure was further developed by Raupach and Shaw (1982) and Finnigan (1985). Solid plant parts are excluded from the averaging volume so that the averaging proceeds over a multiply connected space and source or sink terms appear as the sums of fluxes across the solid boundaries internal to the averaging volume.

In horizontally homogeneous canopies the choice of averaging volume is usually a thin wide horizontal slab that preserves the fundamental vertical heterogeneity of the canopy but reflects its horizontal uniformity on the scale of many plants.

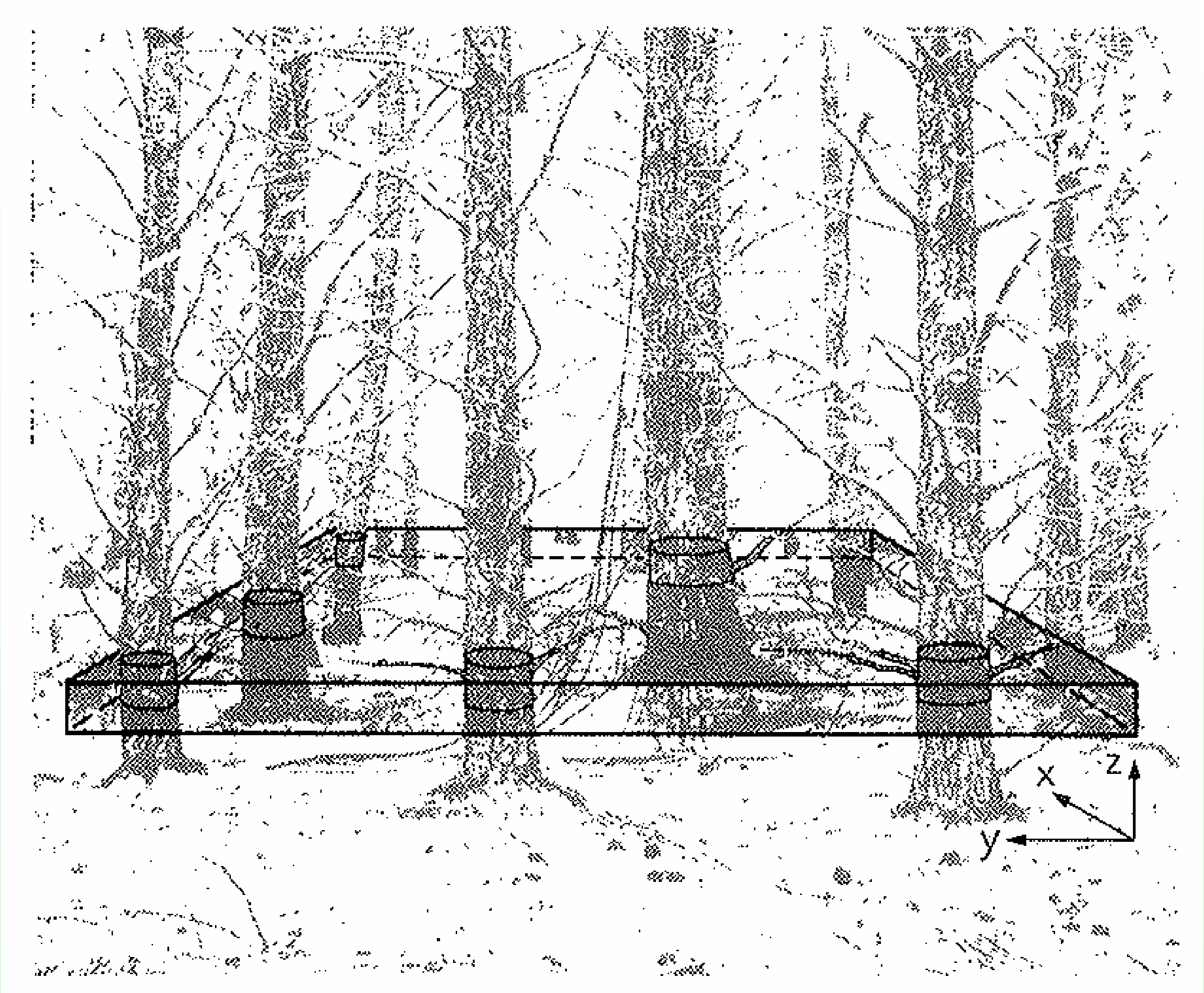

Kaimal and Finnigan, 1994

$$\langle \phi_j \rangle(\mathbf{x}, t) = \frac{1}{V} \int\int\int_V \phi_j(\mathbf{x} + \mathbf{r}, t)\, \mathrm{d}\mathbf{r}$$

$$\overline{\phi}_j(\mathbf{x}) = \frac{1}{T} \int_0^T \phi_j(\mathbf{x}, t)\, \mathrm{d}t$$

Over this multiply connected space, averaging and differentiation do not commute and one result of averaging the flow equations is the appearance of source and sink terms for momentum and scalars

because it is intersected by plant parts. Full analysis shows that if $\overline{\psi}$ is constant at the air-element interfaces, then averaging and differentiation commute, so that $\langle \partial\overline{\psi}/\partial x_i \rangle = \partial\langle \overline{\psi} \rangle / \partial x_i$. Otherwise, they do not commute; in particular, $\langle \partial\overline{\psi}''/\partial x_i \rangle \neq 0$. A simple example is provided by

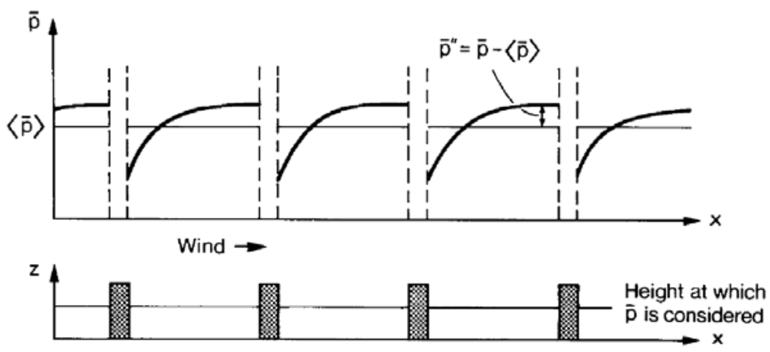

Fig. 2. Schematic pressure field about a series of impermeable fences lying across the wind.

(see Figure 2). A pressure differential exists across each fence because form drag takes place there; therefore, in the space between fences, $\partial\overline{p}/\partial x = \partial\overline{p}''/\partial x > 0$. A horizontal average (within the fluid only) gives $\langle \partial p''/\partial x \rangle > 0$. However, $\partial\langle \overline{p}'' \rangle/\partial x = 0$ by definition, so the operators are non-commutative.

Raupach and Shaw (1982)

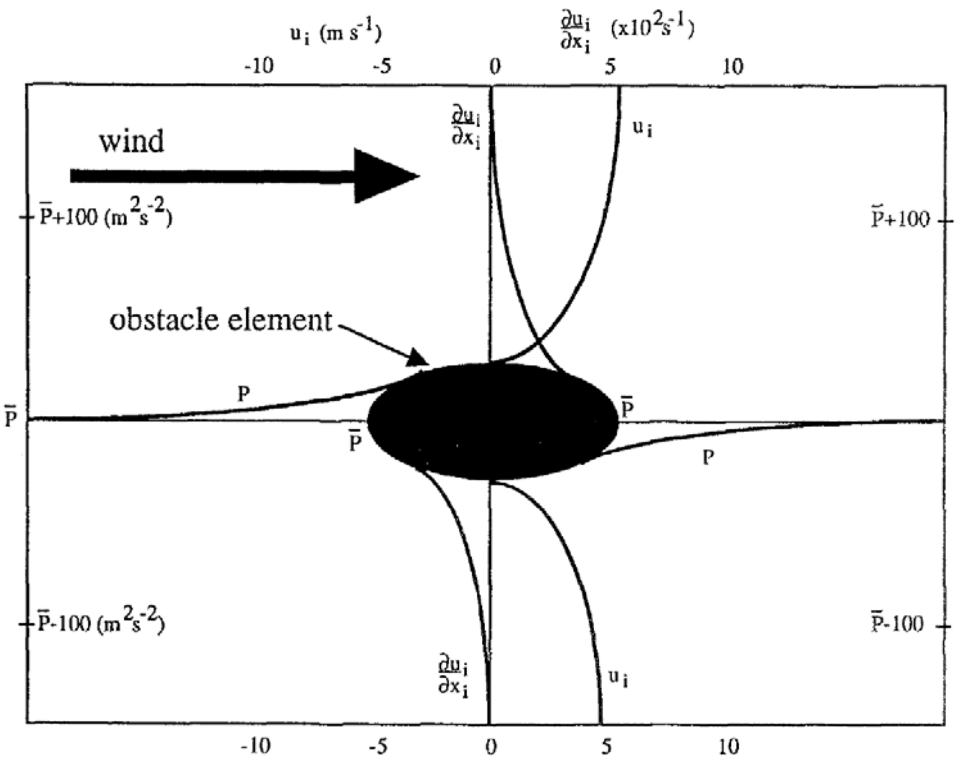

Fig. 1. Sketch of the continuity of dynamic pressure, windspeed, and spatial derivative of windspeed around an obstacle element.

$$\left\langle \frac{\partial \phi_j}{\partial x_i} \right\rangle = \frac{\partial \langle \phi_j \rangle}{\partial x_i} - \frac{1}{V} \iint_{S_I} \phi_j n_i dS,$$

$$\left\langle \frac{\partial \phi_j}{\partial t} \right\rangle = \frac{\partial \langle \phi_j \rangle}{\partial t} - \frac{1}{V} \iint_{S_I} \phi_j v_i n_i dS$$

$$\left\langle \nu \frac{\partial^2 u_i}{\partial x_j^2} \right\rangle = \nu \frac{\partial^2 \langle u_i \rangle}{\partial x_j^2} + \frac{\nu}{V} \iint_S \frac{\partial u_i}{\partial n} \, \mathrm{d}S'$$

$$\left\langle -\frac{\partial p}{\partial x_i} \right\rangle = -\frac{\partial \langle p \rangle}{\partial x_i} - \frac{1}{V} \iint_S p n_i \, \mathrm{d}S'$$

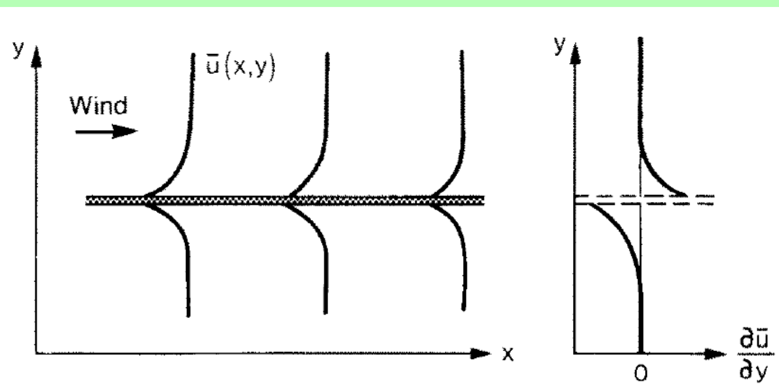

Figure 1. (*a*) Profiles of mean wind adjacent to a *Populus* leaf (from Grace & Wilson, 1976)

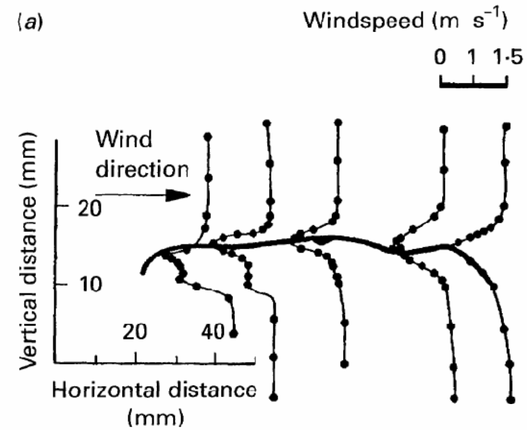

Raupach and Shaw,1982; Wang and Takle ,1995)

$$\frac{\partial u_i}{\partial x_i} = \frac{\partial \langle u_i \rangle}{\partial x_i} = \frac{\partial \langle \overline{u}_i \rangle}{\partial x_i} = \frac{\partial \overline{u}_i''}{\partial x_i} = 0$$

$$\frac{\partial \langle \overline{u}_i \rangle}{\partial t} + \langle \overline{u}_j \rangle \frac{\partial \langle \overline{u}_i \rangle}{\partial x_j} = -\frac{\partial \langle \overline{p} \rangle}{\partial x_i} + \frac{\partial \tau_{ij}}{\partial x_j} + f_{Fi} + f_{Vi}$$

$$f_{Fi} = \frac{1}{V} \int \int_{S_l} \overline{p} n_i dS$$

$$f_{Vi} = -\frac{\nu}{V} \int \int_{S_l} \frac{\partial \overline{u}_i}{\partial n} dS$$

$$\begin{aligned}
\underbrace{\frac{\partial \langle \overline{u_i' u_j'} \rangle}{\partial t}}_{\mathrm{I}} = & -\underbrace{\langle \overline{u}_k \rangle \frac{\partial \langle \overline{u_i' u_j'} \rangle}{\partial x_k}}_{\mathrm{II}} - \underbrace{\left(\langle \overline{u_j' u_k'} \rangle \frac{\partial \langle \overline{u}_i \rangle}{\partial x_k} + \langle \overline{u_i' u_k'} \rangle \frac{\partial \langle \overline{u}_j \rangle}{\partial x_k} \right)}_{\mathrm{III}} \\
& - \underbrace{\frac{\partial \langle \overline{u_i' u_j' u_k'} \rangle}{\partial x_k}}_{\mathrm{IV}} - \underbrace{\left(\frac{\partial \langle \overline{p' u_i'} \rangle}{\partial x_j} + \frac{\partial \langle \overline{p' u_j'} \rangle}{\partial x_i} \right)}_{\mathrm{V}} + \\
& + \underbrace{\left\langle \overline{p' \left(\frac{\partial u_i'}{\partial x_j} + \frac{\partial u_j'}{\partial x_i} \right)} \right\rangle}_{\mathrm{VI}} - 2\nu \underbrace{\left\langle \overline{\frac{\partial u_i'}{\partial x_k} \frac{\partial u_j'}{\partial x_k}} \right\rangle}_{\mathrm{VII}} \\
& - \underbrace{\frac{\partial \langle \overline{u}_k'' \overline{u_i' u_j'} \rangle}{\partial x_k}}_{\mathrm{VIII}} - \underbrace{\left(\left\langle \overline{u_j' u_k'}'' \frac{\partial \overline{u}_i''}{\partial x_k} \right\rangle + \left\langle \overline{u_i' u_k'}'' \frac{\partial \overline{u}_j''}{\partial x_k} \right\rangle \right)}_{\mathrm{IX}} \\
& + \underbrace{\frac{1}{V} \left(\int \int_S \overline{p' (v_i' n_j + v_j' n_i)} \, \mathrm{d}S - \int \int_S \left(\overline{v_j' \frac{\partial u_i'}{\partial n} + v_i' \frac{\partial u_j'}{\partial n}} \right) \mathrm{d}S \right)}_{\mathrm{X}} .
\end{aligned}$$

f_{Fi} is (minus) the sum of the form or pressure drag forces and f_{Vi} is (minus) the sum of the viscous drag forces exerted on every surface element that intersects the averaging volume *V.*

Together they constitute the aerodynamic drag on unit mass of air within *V.*

Raupach and Shaw,1982; Finnigan, 2000)

Non-local closure models

Reynolds - stress transport models

Wilson and Shaw (1977)

$$0 = \frac{\mathrm{d}\langle\overline{u'w'}\rangle}{\mathrm{d}z} - C_d A \langle\bar{u}\rangle^2$$

$$0 = -\langle\overline{w'^2}\rangle \frac{\mathrm{d}\langle\bar{u}\rangle}{\mathrm{d}z} + 2\frac{\mathrm{d}}{\mathrm{d}z}\left(q\lambda_1 \frac{\mathrm{d}\langle\overline{u'w'}\rangle}{\mathrm{d}z}\right) - \frac{q\langle\overline{u'w'}\rangle}{3\lambda_2} + Cq^2 \frac{\mathrm{d}\langle\bar{u}\rangle}{\mathrm{d}z}$$

$$\begin{aligned} 0 &= -2\langle\overline{u'w'}\rangle \frac{\mathrm{d}\langle\bar{u}\rangle}{\mathrm{d}z} + \frac{\mathrm{d}}{\mathrm{d}z}\left(q\lambda_1 \frac{\mathrm{d}\langle\overline{u'^2}\rangle}{\mathrm{d}z}\right) \\ &\quad + 2C_d A \langle\bar{u}\rangle^3 - \frac{q}{3\lambda_2}\left(\langle\overline{u'^2}\rangle - \frac{q^2}{3}\right) - \frac{2}{3}\frac{q^3}{\lambda_3} \end{aligned}$$

$$0 = \frac{\mathrm{d}}{\mathrm{d}z}\left(q\lambda_1 \frac{\mathrm{d}\langle\overline{v'^2}\rangle}{\mathrm{d}z}\right) - \frac{q}{3\lambda_2}\left(\langle\overline{v'^2}\rangle - \frac{q^2}{3}\right) - \frac{2}{3}\frac{q^3}{\lambda_3}$$

$$0 = \frac{\mathrm{d}}{\mathrm{d}z}\left(3q\lambda_1 \frac{\mathrm{d}\langle\overline{w'^2}\rangle}{\mathrm{d}z}\right) - \frac{q}{3\lambda_2}\left(\langle\overline{w'^2}\rangle - \frac{q^2}{3}\right) - \frac{2}{3}\frac{q^3}{\lambda_3},$$

with

$$\lambda_j = a_j L(z); \quad j = 1, 2, 3$$

$$L(z) = \max \begin{cases} L(z - \mathrm{d}z) + k\,\mathrm{d}z \\ \dfrac{\alpha}{C_d A} \end{cases}$$

$$L(0) = 0,$$

where $q = \sqrt{\langle\overline{u_i' u_i'}\rangle}$ is a characteristic turbulent velocity

Meyers and Paw U (1986)

$$0 = -\frac{\mathrm{d}\langle\overline{u'w'}\rangle}{\mathrm{d}z} - C_d A \langle\bar{u}\rangle^2$$

$$0 = -\langle\overline{w'^2}\rangle \frac{\mathrm{d}\langle\bar{u}\rangle}{\mathrm{d}z} - \frac{\mathrm{d}}{\mathrm{d}z}(\langle\overline{w'u'w'}\rangle) - \frac{q\langle\overline{u'w'}\rangle}{3\lambda_2} + Cq^2 \frac{\mathrm{d}\langle\bar{u}\rangle}{\mathrm{d}z}$$

$$\begin{aligned} 0 &= -2\langle\overline{u'w'}\rangle \frac{\mathrm{d}\langle\bar{u}\rangle}{\mathrm{d}z} - \frac{\mathrm{d}}{\mathrm{d}z}(\langle\overline{w'u'u'}\rangle) + 2C_d A \langle\bar{u}\rangle^3 \\ &\quad - \frac{q}{3\lambda_2}\left(\langle\overline{u'^2}\rangle - \frac{q^2}{3}\right) - \frac{2}{3}\frac{q^3}{\lambda_3} \end{aligned}$$

$$0 = -\frac{\mathrm{d}}{\mathrm{d}z}(\langle\overline{w'v'v'}\rangle) - \frac{q}{3\lambda_2}\left(\langle\overline{v'^2}\rangle - \frac{q^2}{3}\right) - \frac{2}{3}\frac{q^3}{\lambda_3}$$

$$0 = -\frac{\mathrm{d}}{\mathrm{d}z}(\langle\overline{w'w'w'}\rangle) - \frac{q}{3\lambda_2}\left(\langle\overline{w'^2}\rangle - \frac{q^2}{3}\right) - \frac{2}{3}\frac{q^3}{\lambda_3}$$

$$\langle\overline{w'u'u'}\rangle = -\frac{\tau}{C_8}\left(2\langle\overline{w'u'w'}\rangle \frac{\mathrm{d}\langle\bar{u}\rangle}{\mathrm{d}z} + \langle\overline{w'^2}\rangle \frac{\mathrm{d}\langle\overline{u'^2}\rangle}{\mathrm{d}z} - 4\langle\overline{u'w'}\rangle C_d A \langle\bar{u}\rangle^2\right)$$

$$\langle\overline{w'u'w'}\rangle = -\frac{\tau}{C_8}\left(2\langle\overline{w'w'w'}\rangle \frac{\mathrm{d}\langle\bar{u}\rangle}{\mathrm{d}z} + \langle\overline{w'u'}\rangle \frac{\mathrm{d}\langle\overline{w'^2}\rangle}{\mathrm{d}z} - 3\langle\overline{w'^2}\rangle C_d A \langle\bar{u}\rangle^2\right)$$

$$\langle\overline{w'w'w'}\rangle = -\frac{\tau}{C_8}\left(3\langle\overline{w'^2}\rangle \frac{\mathrm{d}\langle\overline{w'^2}\rangle}{\mathrm{d}z}\right)$$

$$\langle\overline{w'v'v'}\rangle = -\frac{\tau}{C_8}\left(\langle\overline{w'^2}\rangle \frac{\mathrm{d}\langle\overline{v'^2}\rangle}{\mathrm{d}z}\right).$$

Comparative analysis

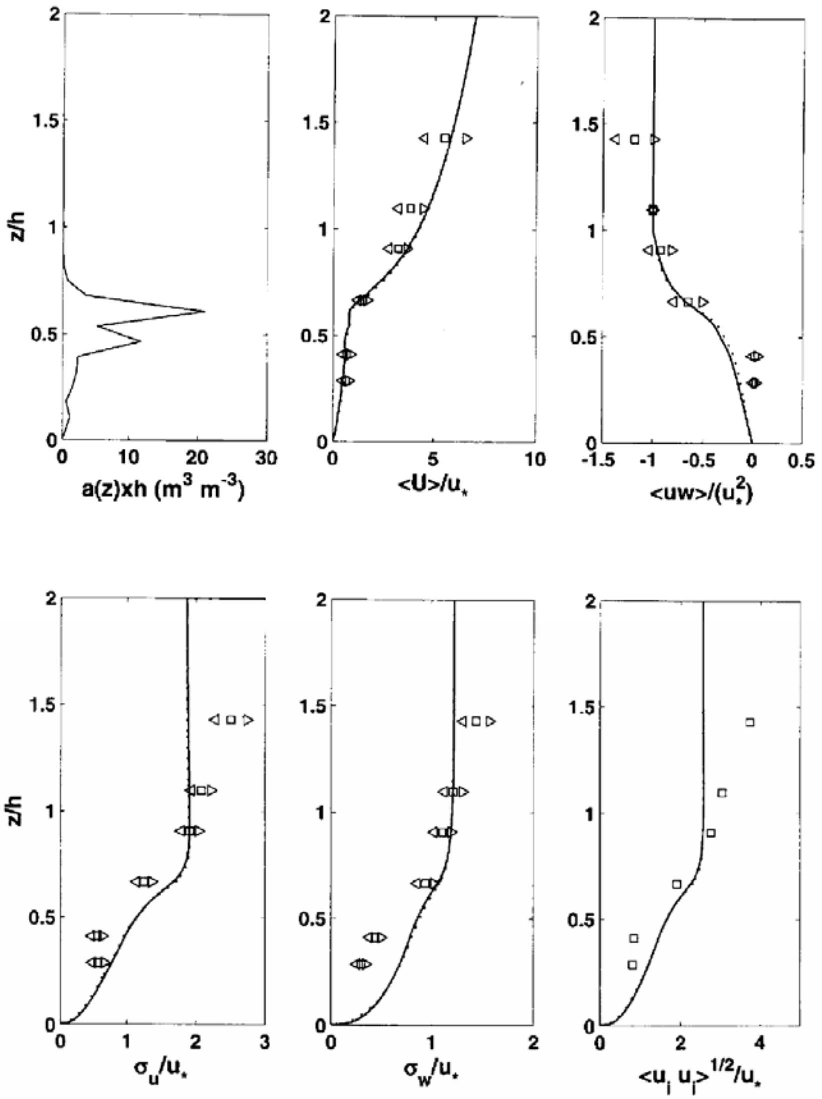

Figure 1. Comparison between modeled and measured profiles of $\langle \bar{u} \rangle$, $\langle \overline{u'w'} \rangle$, $\langle \overline{u'^2} \rangle^{1/2}$, $\langle \overline{w'^2} \rangle^{1/2}$, and q. The solid line is for third-order closure, the dotted line is for second-order closure, u_* is defined at the canopy top ($z/h = 1$), and the squares are ensemble measurements from the 69 runs. The triangles are ± 1 standard deviation of normalized flow variables. The leaf area index profile (LAI) normalized by canopy height (h) is also shown (top left panel).

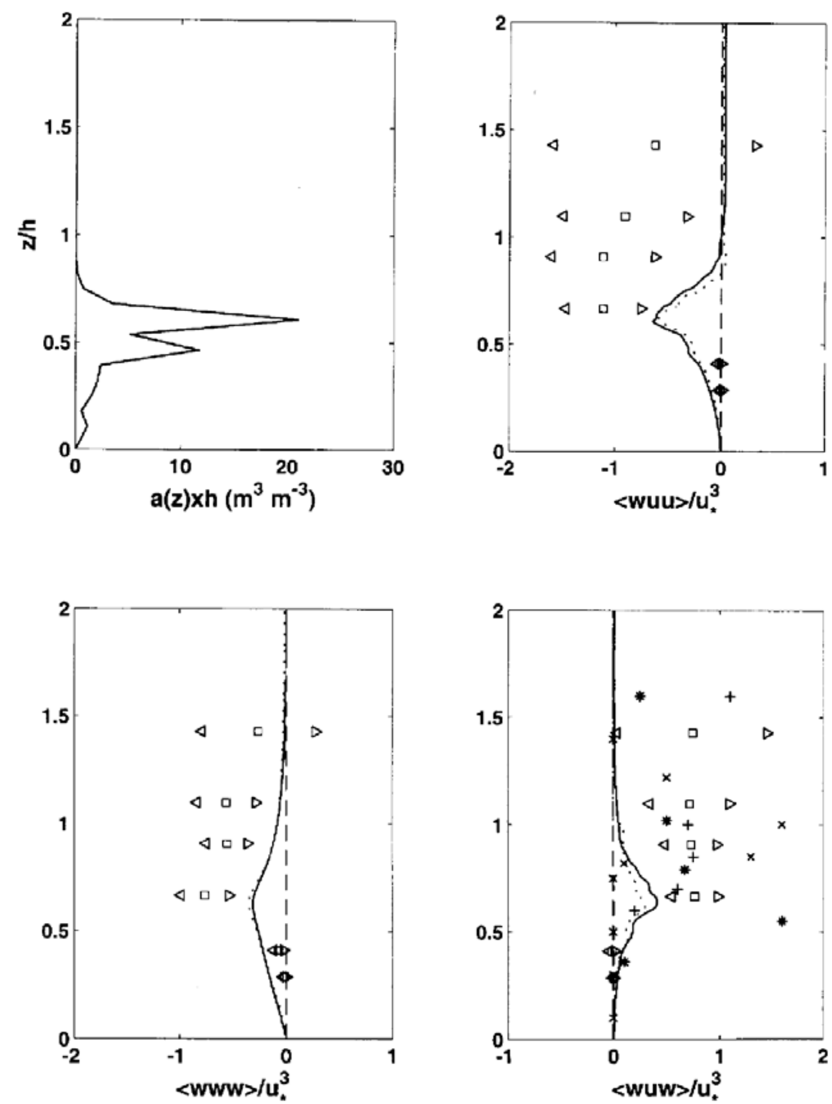

Figure 2a. Same as Figure 1 but for $\langle \overline{w'u'w'} \rangle$, $\langle \overline{w'u'u'} \rangle$, and $\langle \overline{w'^3} \rangle$. The '+' symbols represent the maize measurements in Meyers and Paw U (1986), the '$*$' symbols represent the corn measurements of Shaw and Seginer (1987), and the '$\times$' symbols represent the measurements of Meyers and Baldocchi (1991).

Katul and Albertson, 1998

Ayotte et al, 1999

"In particular, the turbulent length scale or time scale must be calculated as a dynamic variable in any model that aims to simulate inhomogeneous canopy flows."

$$\tau = \frac{E}{\varepsilon} \quad = 1/ \quad \frac{q}{3\lambda_2}$$

$$U_i = \overline{U}_i + u_i$$

$$\begin{aligned} |U| &= \left\{(\overline{U}_1 + u_1)^2 + (\overline{U}_2 + u_2)^2 + (\overline{U}_3 + u_3)^2\right\}^{1/2} \\ |\overline{U}| &= (\overline{U}_1^2 + \overline{U}_2^2 + \overline{U}_3^2)^{1/2}, \\ |u| &= |U| - |\overline{U}|. \end{aligned}$$

$$f_{Fi} + f_{Vi} = f_i = c_d A(x_3) U_i |U|$$

$$\epsilon_{ij} = \frac{2}{3}\epsilon_1 \delta_{ij} + d_{ij}$$

$$\frac{\partial \epsilon_1}{\partial t} + \overline{U}_k \frac{\partial \epsilon_1}{\partial x_k} = c_\epsilon \frac{\partial}{\partial x_k}\left(\frac{k}{\epsilon}\overline{u_k u_l}\frac{\partial \epsilon_1}{\partial x_l}\right) - c_{\epsilon 1}\frac{\epsilon_1 \overline{u_i u_k}}{k}\frac{\partial \overline{U}_i}{\partial x_k} - c_{\epsilon 2}\frac{{\epsilon_1}^2}{k}$$

Ayotte et al, 1999

$$\frac{\partial U_i}{\partial t} = \cdots - c_d A(x_3)|U|U_i$$

$$\begin{aligned}\frac{\partial \overline{u_i u_j}}{\partial t} &= \cdots - (\overline{u'_i f'_j} + \overline{u'_j f'_i}) \\ &= \cdots - c_d A(x_3)(|\overline{u}|\overline{u_i u_k} + \overline{u_i}\,\overline{|u|u_k} + \overline{u_k}\,\overline{|u|u_i} + \overline{|u|u_i u_k}) \\ &= \cdots - d_{ij}.\end{aligned}$$

$$|u|u_i = \left\{ \underline{\left(|\overline{U}|^2 + 2\overline{U}_j u_j + u_j u_j\right)^{1/2}} - |\overline{U}| \right\} u_i$$

$$|u|u_i \approx \left(\frac{\overline{U}_j u_j}{|\overline{U}|} + \frac{u_k u_k}{2|\overline{U}|} \right) u_i$$

$$\overline{|u|u_i} \approx \frac{\overline{U}_j \overline{u_j u_i}}{|\overline{U}|} + \frac{\overline{u_k u_k u_i}}{2|\overline{U}|}$$

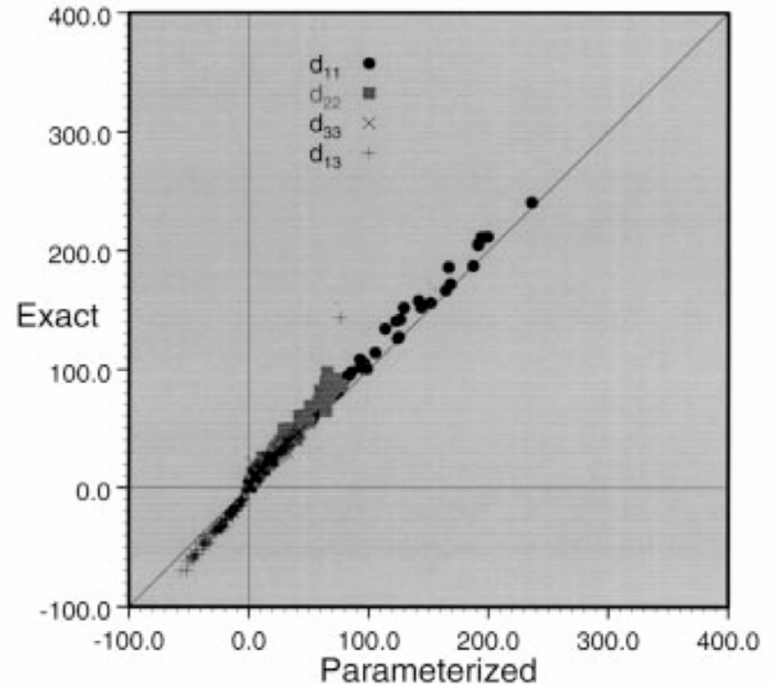

Figure 2. Exact and parameterised dissipation (d_{ij}) terms calculated using (28) and (32) respectively. Data used are from a eucalypt forest (Raupach et al., 1996).

$$d_{ij} = -c_d A(x_3) \left(|\overline{U}|\overline{u_i u_j} + \frac{\overline{U_i U_k}\,\overline{u_k u_j}}{|\overline{U}|} + \frac{\overline{U_j U_k}\,\overline{u_k u_i}}{|\overline{U}|} \right)$$

Ayotte et al, 1999

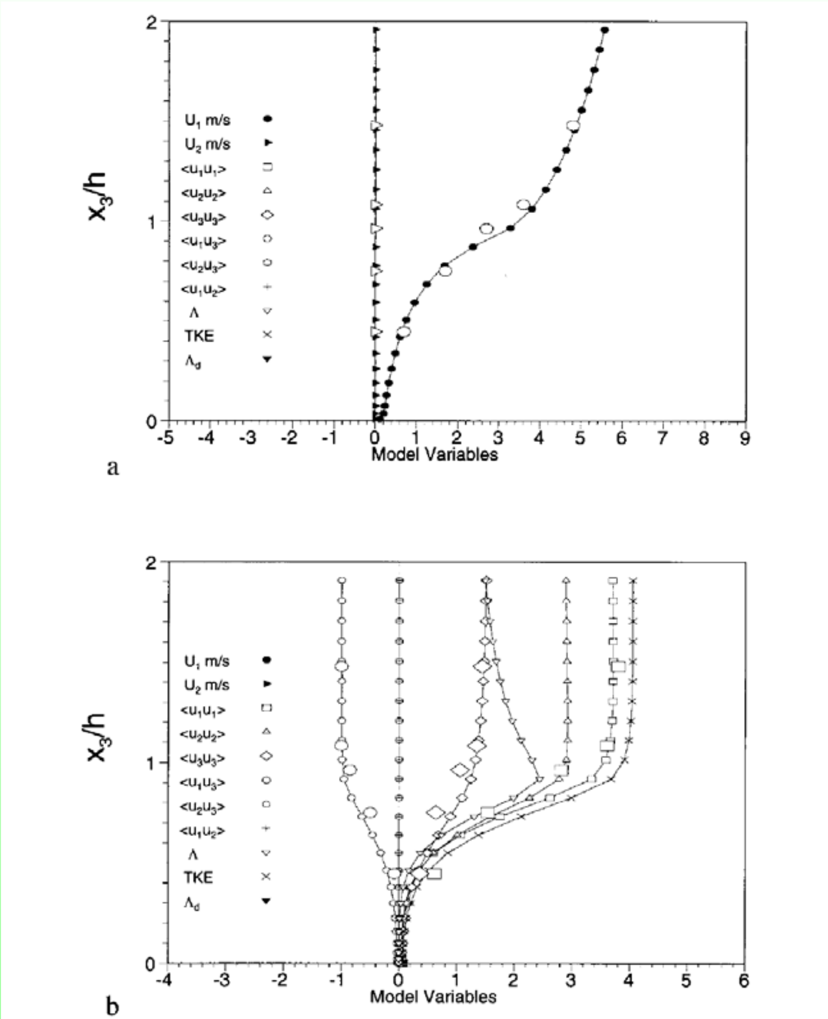

Figure 6. Mean (a) and turbulent (b) profiles in a eucalypt canopy. Large open symbols are measurements with modelled mean and turbulent profiles shown in (a) and (b) respectively plotted as smaller connected symbols. Quantities enclosed in angle braces (⟨ ⟩) are ensemble averaged Reynolds stresses, equivalent to overlined quantities elsewhere.

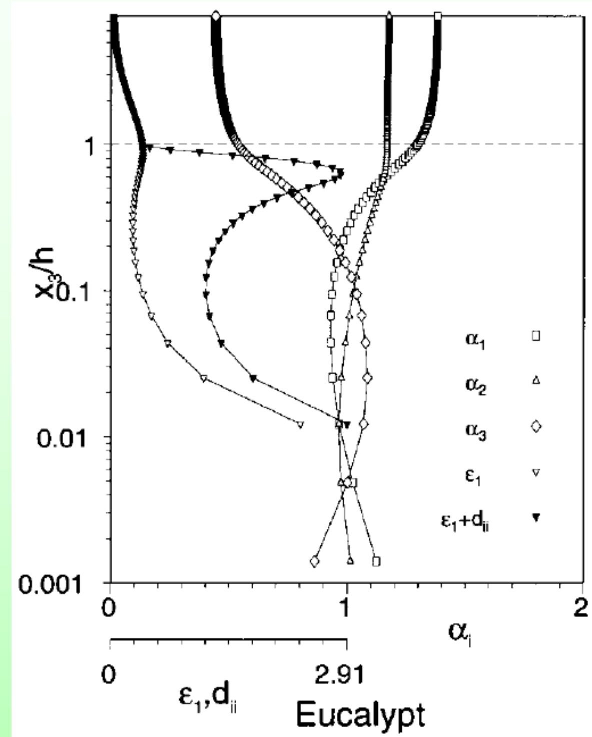

$$\tau = \frac{E}{\varepsilon} = \frac{E}{\varepsilon_1 + d}$$

Ayotte et al, 1999

TABLE I

Canopy geometric and turbulence parameters.

Canopy type	h	$c_d A_0$	t_c	$\alpha_1 : \alpha_2 : \alpha_3$	Profile
Eucalypt	12 m	0.04 m^{-1}	0.3	0.40 : 0.35 : 0.25	SL

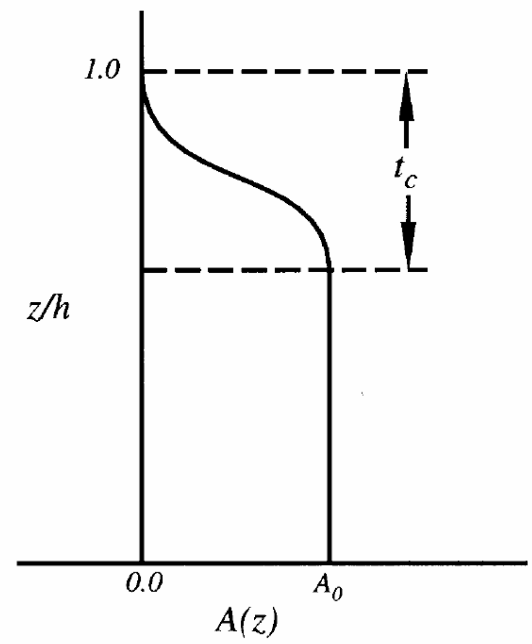

$$\alpha_1, \alpha_2, \alpha_3 = \frac{\overline{u_1 u_1}, \overline{u_2 u_2}, \overline{u_3 u_3}}{\overline{u_k u_k}}$$

$$\left(2\alpha_1 - \frac{2}{3}\right) c_1 - \frac{4}{11} c_2 = \frac{8}{11},$$

$$\left(2\alpha_2 - \frac{2}{3}\right) c_1 - \frac{6}{11} c_2 = -\frac{10}{33},$$

$$\left(2\alpha_3 - \frac{2}{3}\right) c_1 + \frac{10}{11} c_2 = -\frac{2}{33},$$

$$\left(\frac{4}{11} - \frac{16}{11} c_2\right) \alpha_1 + \left(\frac{6}{11} - \frac{2}{11} c_2\right) \alpha_1 + \frac{6}{11} c_2 - \frac{2}{55} = c_1 \alpha^2$$

Inclan et al, 1996

Contrary to other formulations of first order closure, the transilient turbulence theory allows large-size eddies to transport fluid across finite distances before the smaller eddies effect the mixing with the rest of the environment.

Stull's transilient turbulence theory (T-theory) was originally developed to study turbulent air flow in the planetary boundary layer (PBL).

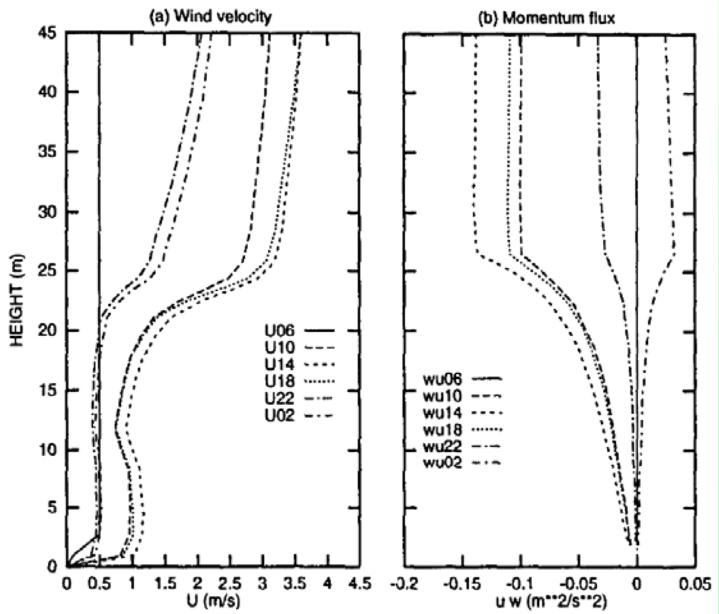

Modelled profiles of wind velocity(a) and momentum flux (b) within the canopy.

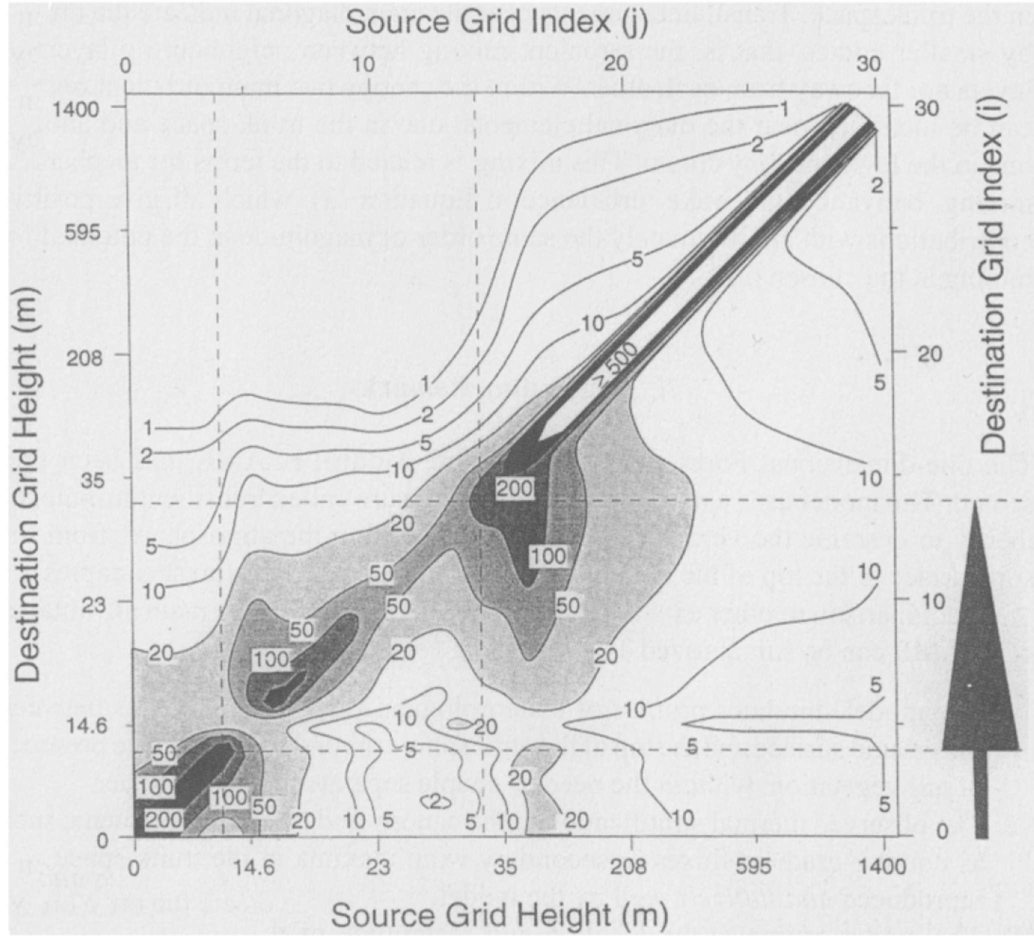

Figure 9. Contoured transilient matrix at 1400, showing the fraction of air reaching any destination location that came from each source location. Height scale is non-linear along each axis due to unequal grid spacing.Transilient elements have been multiplied by 1000 only for display purposes.

Wenge Ni, 1997

The present work extends this model to study the interaction of turbulent air flow within a plant canopy and in the PBL.

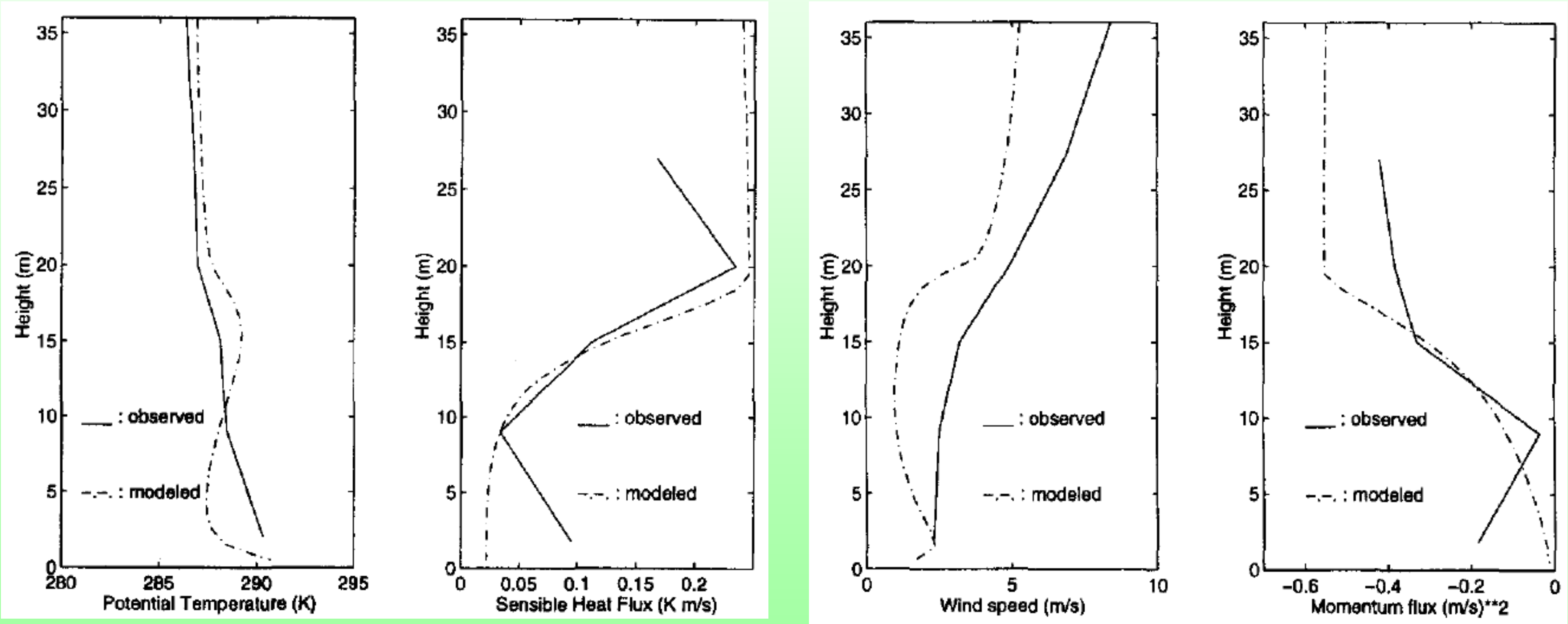

Comparison of modeled parameters within and just above Black Moshannon Forest, PA, and observations at 13:00 on 30 May 1990.

LES models

These difficult inhomogeneous situations demand two- and three-dimensional deployment of instruments to capture their character properly, and for field experiments in tall canopies especially, this is a daunting prospect.

One of the most promising recent developments in canopy studies, therefore, is the use of LES models. The pioneering efforts of Shaw & Schumann (1992) have been followed by several other studies that show excellent correspondence with measured field and wind tunnel data. Dwyer et al (1997) illustrated the power of LES models to calculate essentially unobservable terms like p', while Su et al (1998) tackled a sparse forest canopy and Patton et al (1998) showed the ability of the technique to deal with truly inhomogeneous situations in their simulation of windbreak flows.

There is little doubt that a hallmark of the next two decades of canopy studies will be increasing reliance on such simulations to augment measurement.

Finnigan, 2000

Shaw & Schumann (1992)

$$\frac{\partial \bar{u}_j}{\partial x_j} = 0 ,$$

$$\frac{\partial \bar{u}_i}{\partial t} + \frac{\partial(\bar{u}_j \bar{u}_i)}{\partial x_j} = -\frac{1}{\rho}\frac{\partial \bar{p}}{\partial x_i} + \frac{\partial}{\partial x_j}\left(\nu \frac{\partial \bar{u}_i}{\partial x_j} - \overline{u_i'' u_j''}\right) + \beta g \bar{T} \delta_{i3} + F_i$$

$$\frac{D\overline{E''}}{Dt} = -\overline{u_i'' u_j''}\frac{\partial \bar{u}_i}{\partial x_j} + \beta g \overline{w'' T''} + \frac{\partial}{\partial x_i}\left[\frac{5}{3} l c_{3m} \overline{E''}^{1/2} \frac{\partial \overline{E''}}{\partial x_i}\right] - c_{\epsilon m}\frac{\overline{E''}^{3/2}}{l} - 2\frac{\overline{E''}}{\tau}$$

In a large-eddy simulation, the grid-volume-average momentum equation explicitly includes the action of canopy drag on the resolved turbulent velocities. The net effect on subgrid-scale turbulence is less obvious.

$$F_i = -c_d a V \bar{u}_i = -\bar{u}_i / \tau$$

$$l = \min(\Delta, c_l z)$$

$$0 = -(1 - c_{GM})^{2/3}\,\overline{E''}\left(\frac{\partial \bar{u}_i}{\partial x_j} + \frac{\partial \bar{u}_j}{\partial x_i}\right) + (1 - c_{Bm})$$
$$\times\left[\beta g\left(\delta_{13}\,\overline{u_j'' T''} + \delta_{j3}\,\overline{u_i'' T''} - \tfrac{2}{3}\delta_{ij}\,\overline{u_3'' T''}\right)\right] - c_{Rm}\frac{\overline{E''}^{1/2}}{l}\overline{A_{ij}''}$$

LES examples

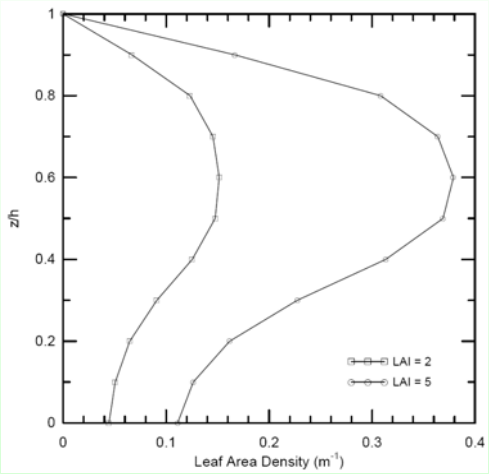

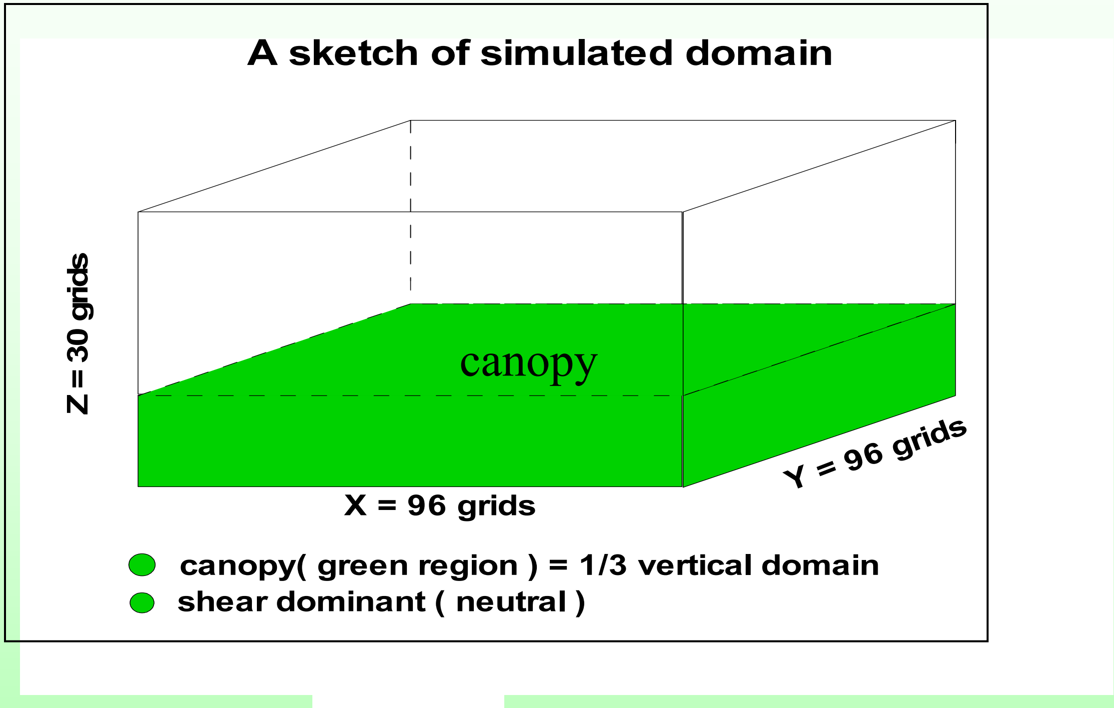

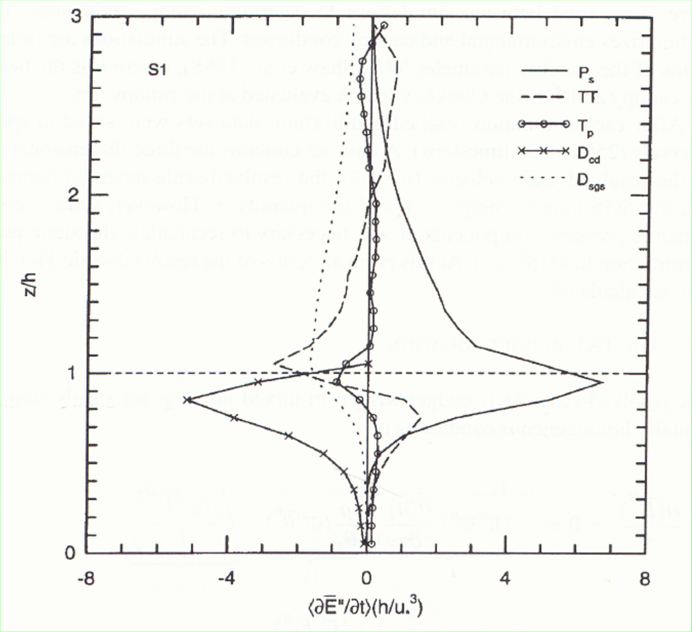

Typical conditions

- periodic horizontal boundary conditions
- frictionless lid at upper boundary (no flux)
- uniform force to drive the flow
- scalar source through depth of canopy

Finnigan and Shaw (2000), Shaw (2004)

LES examples

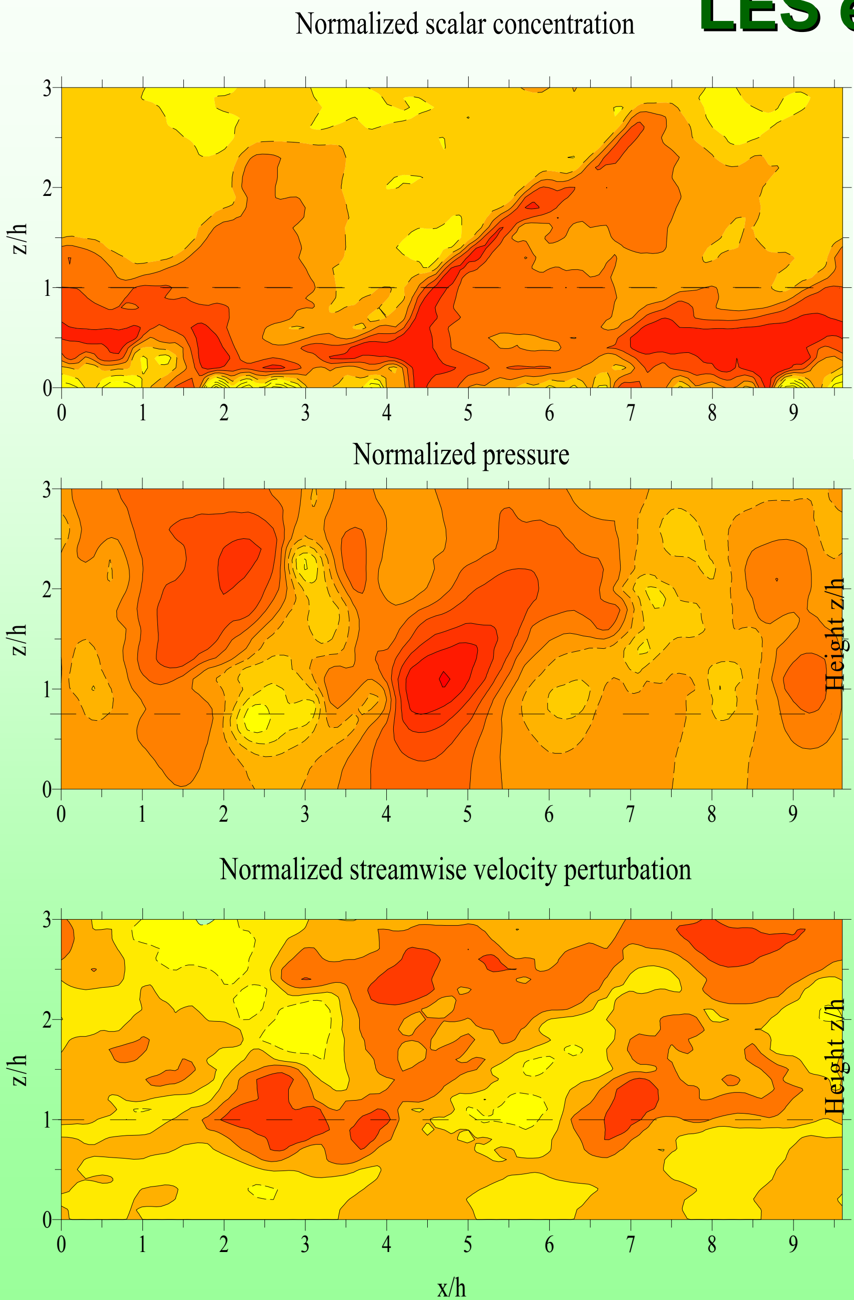

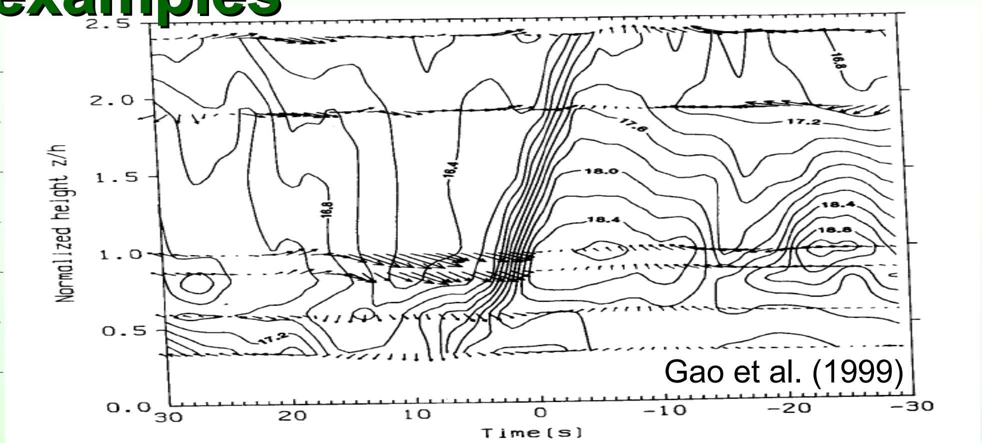

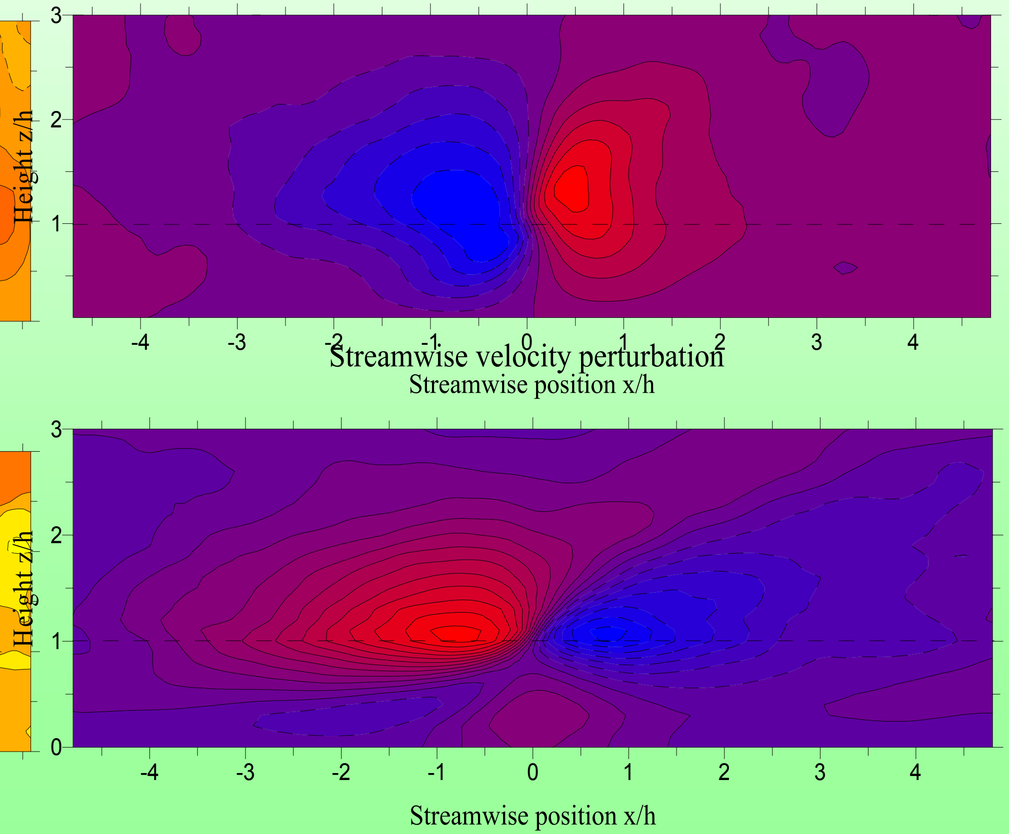

Finnigan and Shaw (2000), Shaw (2004)

Xie and Li, (2005)

LES examples

Yang et al. (2006)

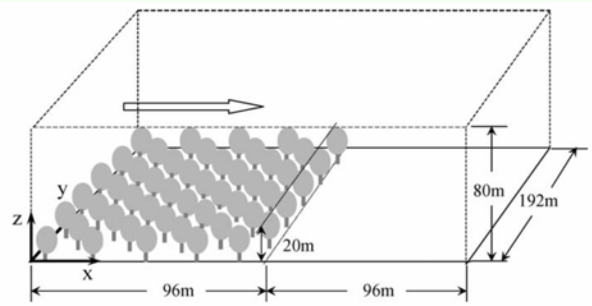

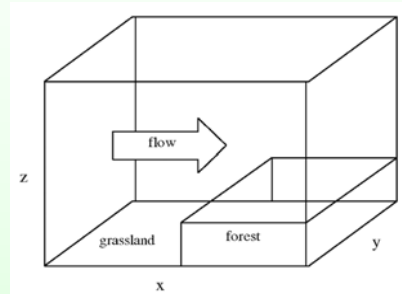

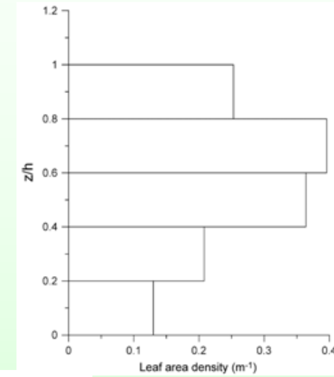

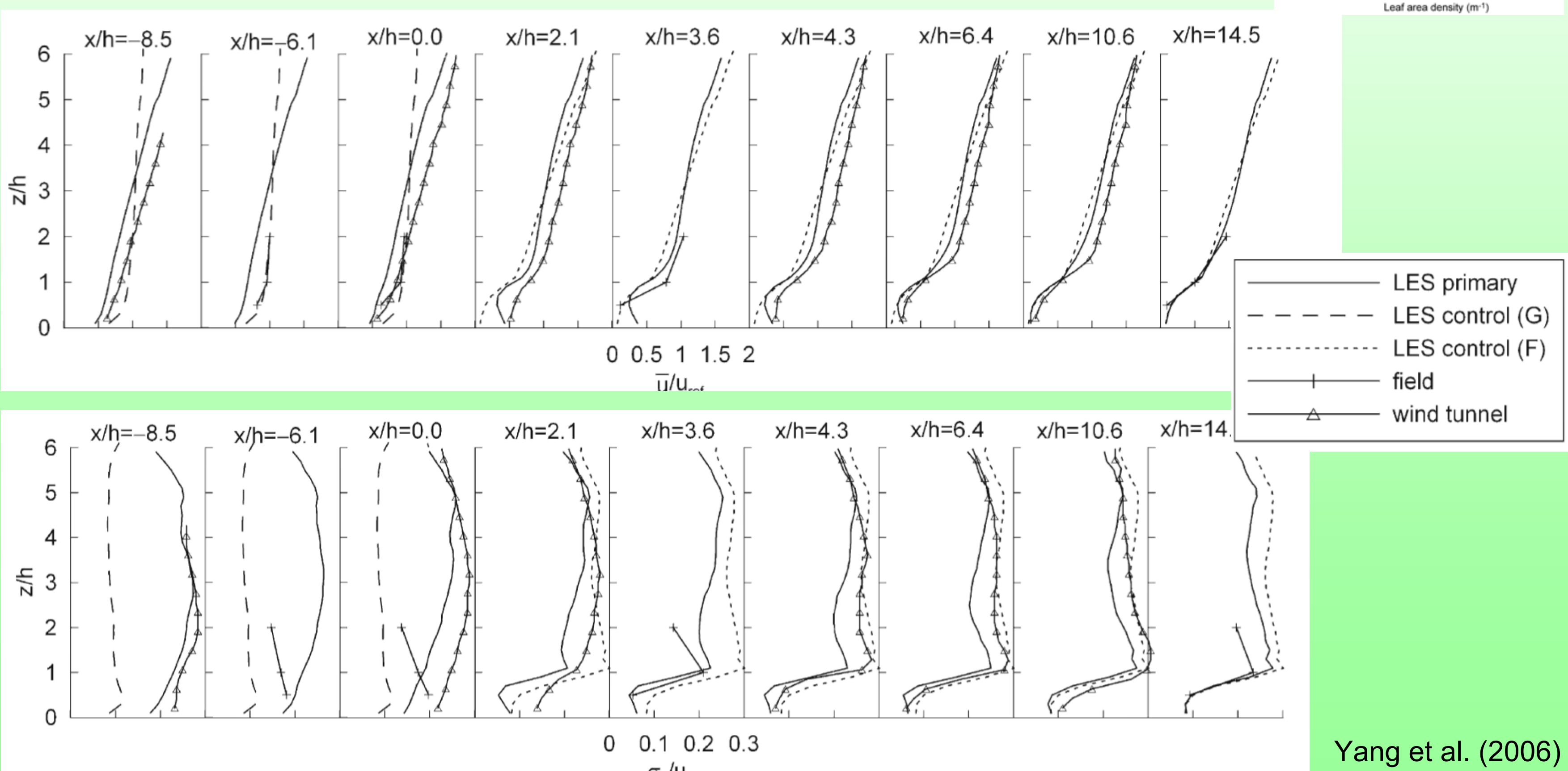

Yang et al. (2006)

LES examples

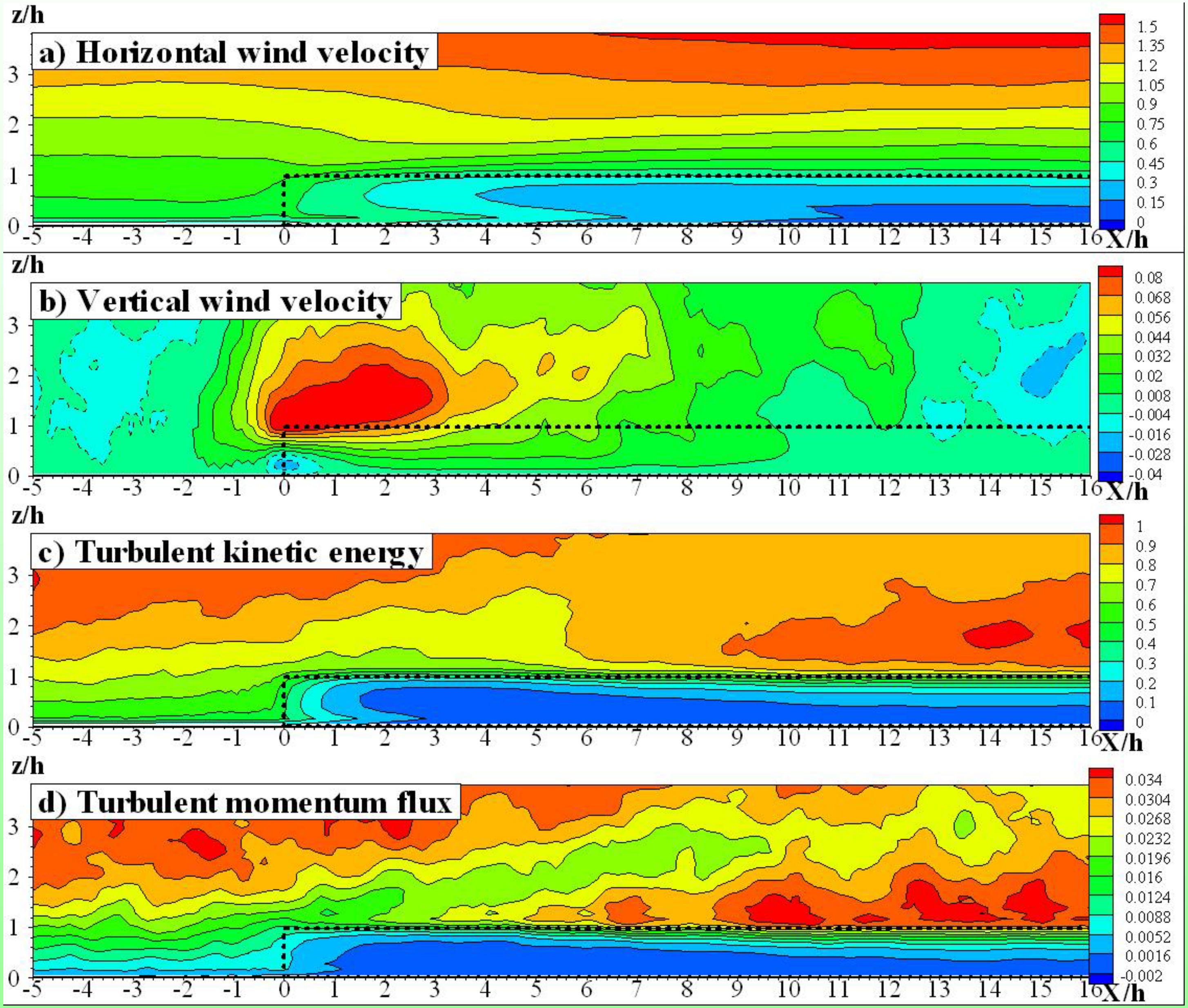

Thanks to Barry Gardiner, 2007

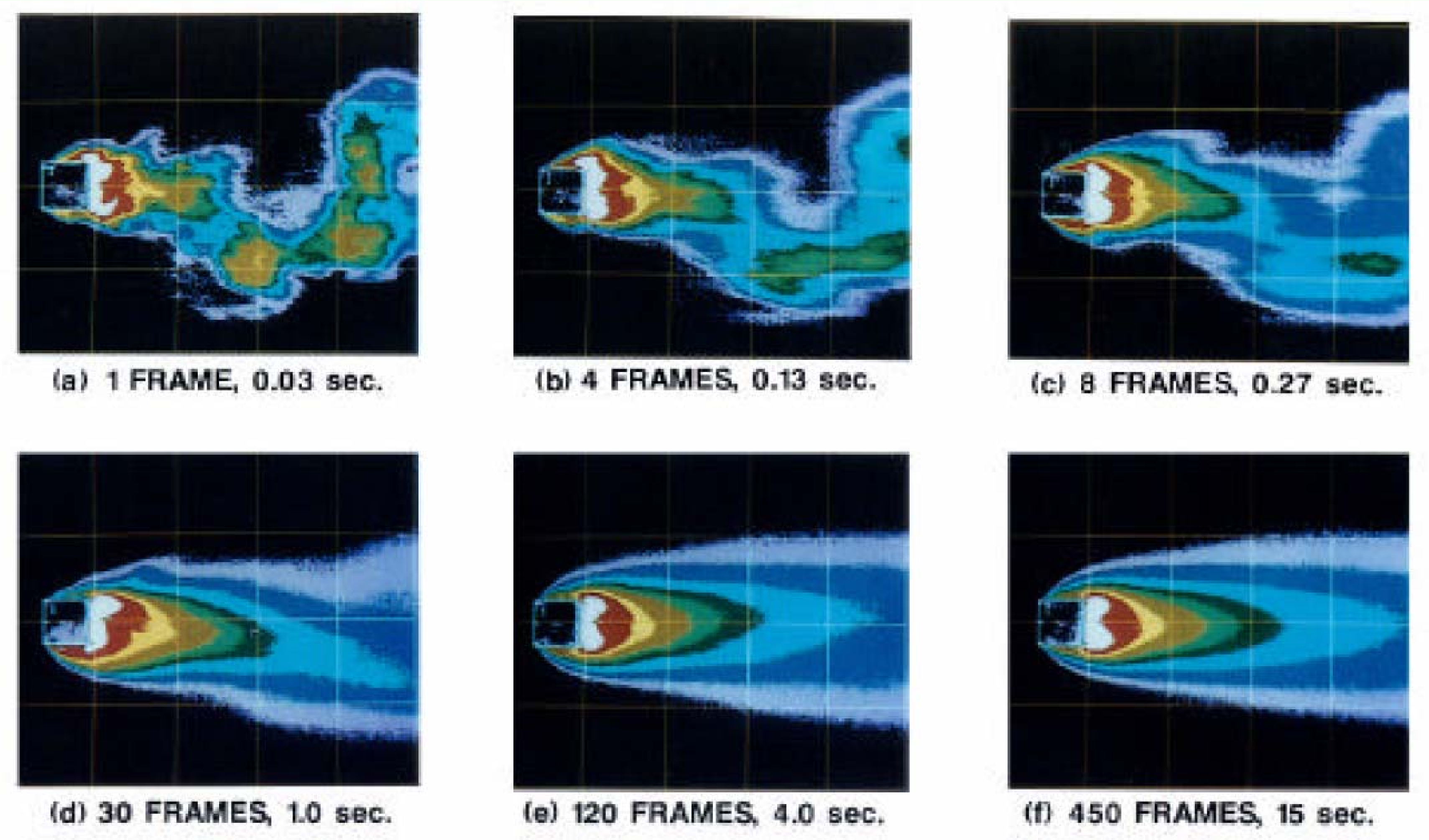

(Lee et al., 1991)

Uncertainties of Reynolds - stress transport and LES models

“Meyers and Paw U (1986) obtained a drag coefficient (*Cd*) for their canopies by matching the model prediction of mean wind against observation while Wilson (1988) obtained *Cd* from the observed shear stress divergence. Thus *Cd* in the first case was used as an adjustable model parameter and in the second as a data input. This points to one of the major weaknesses in our current understanding of canopy flows: we cannot predict the drag on the foliage from knowledge of the canopy geometry and the behaviour of the plant elements in isolation”.

(Ayotte et al., 1999).

… ”the merit of LES models for disturbed flows very much remains to be demonstrated”…

(Wilson and Yee, 2003).

Canopy description uncertainties

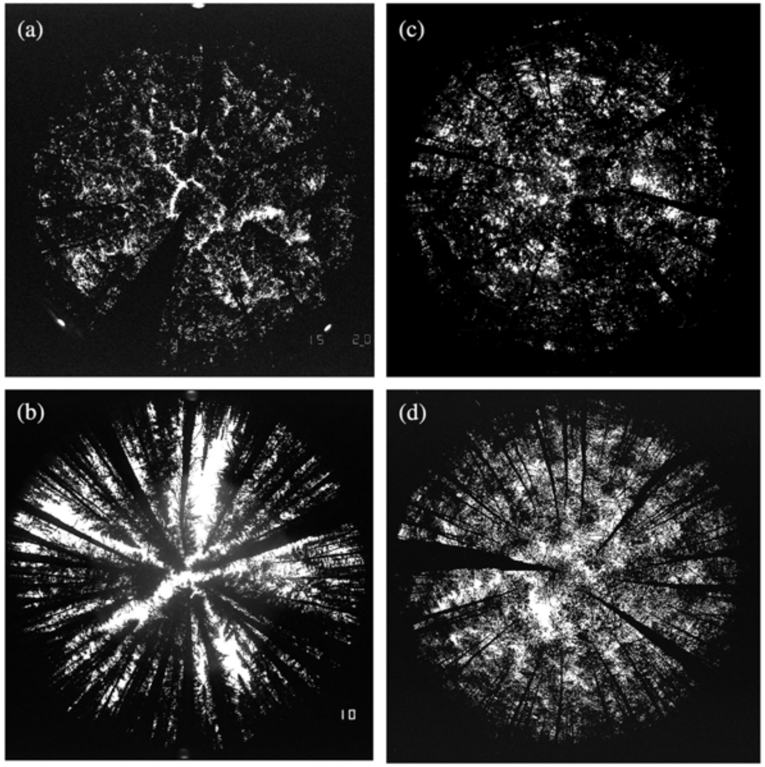

Figure 1. Hemispherical photographs from the selected experiment sites: (a) St-Gilles, Quebec, Canada; (b) Candle Lake, Saskatchewan, Canada; (c) Haguenau, Alsace, France; and (d) Hartheim, Germany.

Walter et al. 2003

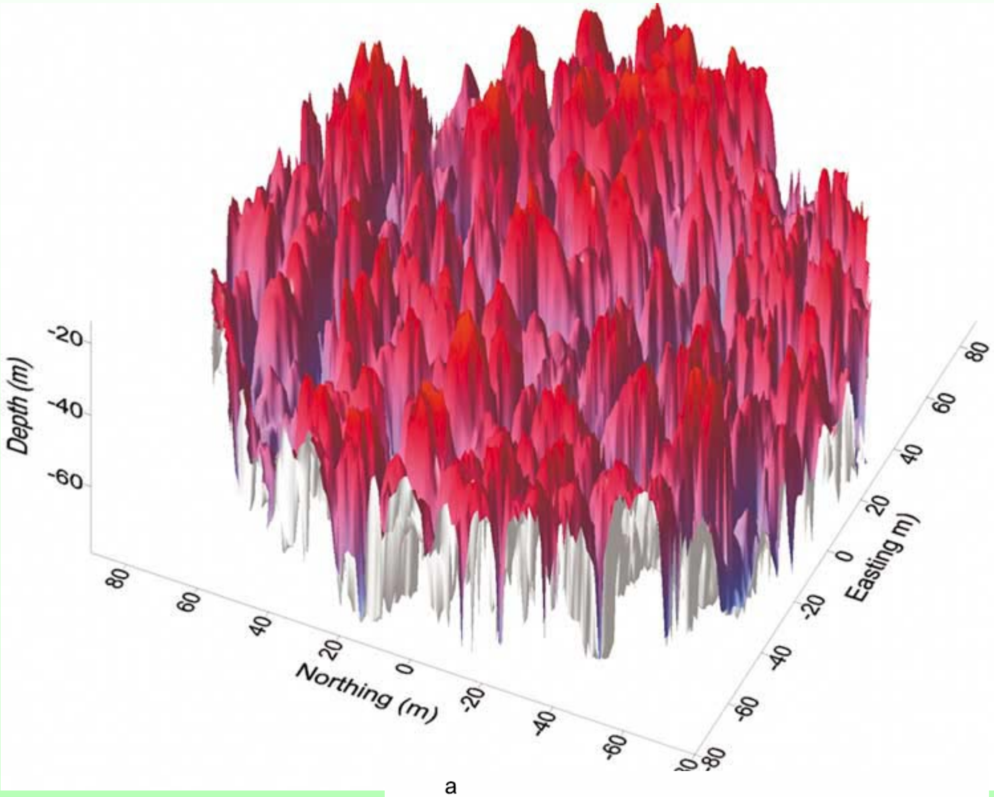

Figure 6. Topography of the outer surface of the Wind River old-growth canopy within the crane circle. The vertical axis gives depth below the crane jib. The horizontal resolution is 1 m.

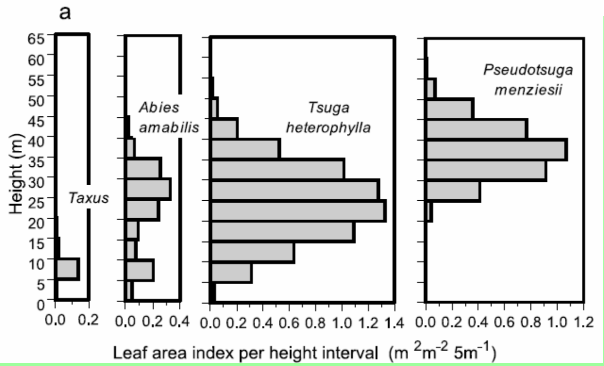

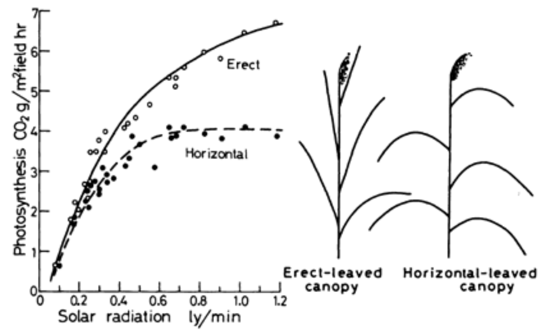

Figure 3 Rice photosynthesis as influenced by leaf arrangement (cultivar Nihonbare) (Tanaka 147).

Monsi et al. 1973

Parker et al. 2004

How to specify turbulence in the model?

Pinard and Wilson (2001) concluded that, "most often, uncertainty in the drag coefficient will limit the accuracy of modelled wind statistics, regardless of the turbulence closure chosen." This is why, "bearing in mind that for two- and three-dimensional flows a higher-order model is laborious, one ought not to overlook the competence of the simpler first-order model."

Katul et al. (2004) have shown that the 1.5-order closure (as a logical compromise between first- and second-order closures) is sufficient for most practical tasks.

Ayotte et al. (1999) argued that the turbulent length scale or time scale must be calculated as a dynamic variable in any model that aims to simulate inhomogeneous canopy flows.

Turbulence closure approaches

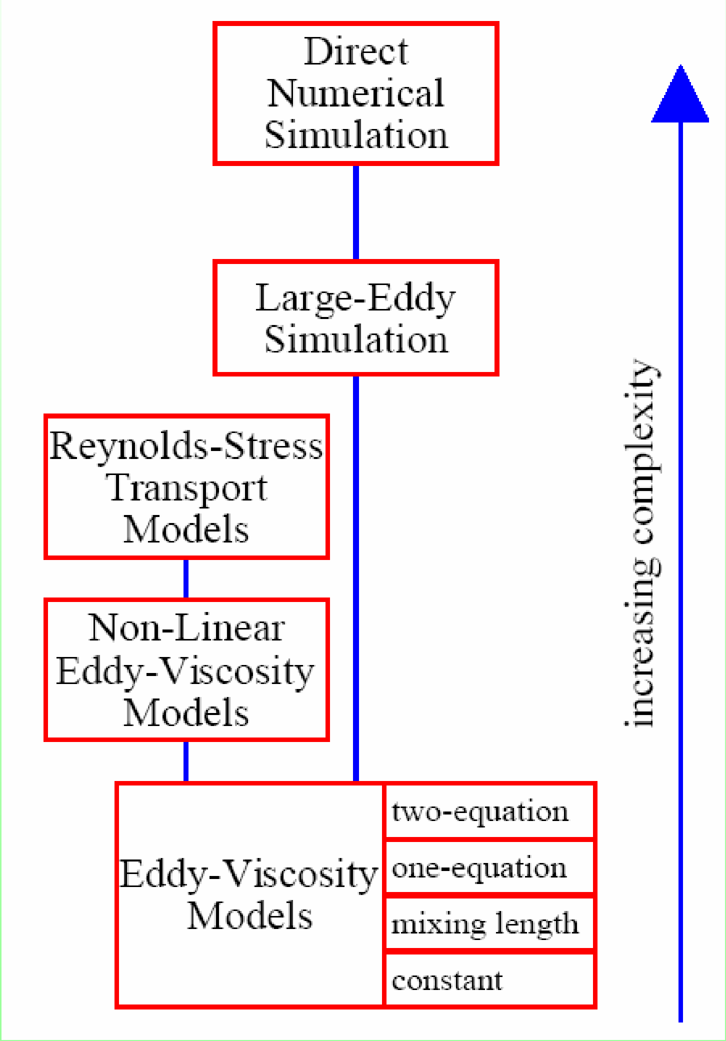

Two – equation models

Governing equations

$$\frac{\partial \overline{U}_i}{\partial x_i} = 0.$$

$$\frac{\partial \overline{U}_i}{\partial t} + \overline{U}_j \frac{\partial \overline{U}_i}{\partial x_j} + 2\varepsilon_{ijk}\Omega_j \overline{U}_k = -\frac{1}{\rho_0}\frac{\partial \overline{P}}{\partial x_i} - \frac{\partial \overline{u_j u_i}}{\partial x_j}$$

with $U_i = \overline{U}_i + u_i$

$$\frac{\partial E}{\partial t} + \overline{U}_j \frac{\partial E}{\partial x_j} = \frac{\partial}{\partial x_i}\left(\frac{K}{\sigma_E}\frac{\partial E}{\partial x_i}\right) + P_E - \varepsilon$$

$$E \equiv \tfrac{1}{2}\overline{u_i u_i} \qquad P_E \equiv -\overline{u_i u_j}\frac{\partial \overline{U}_i}{\partial x_j} \qquad \varepsilon = C_\mu^{3/4}\frac{E^{3/2}}{l}$$

$$\overline{u_i u_j} = \frac{2}{3}\delta_{ij}E - K\left(\frac{\partial \overline{U}_i}{\partial x_j} + \frac{\partial \overline{U}_j}{\partial x_i}\right) \qquad \frac{u_L^2}{E} = C_\mu^{1/2}\frac{P_E}{\varepsilon} \qquad u_L = \sqrt[4]{\overline{u_1 u_3}^2 + \overline{u_2 u_3}^2}$$

To close the system certain assumptions concerning *K* are needed

(Pielke, 2002)

Closure equations

E-l model

Blackadar (1962), Laykhtman (1970), Zilitinkevich (1970)

$$l = \left(\frac{1}{kz} + \frac{1}{l_{\max}} \right)^{-1} \quad l = \left(\frac{1}{l_{LZ}} + \frac{1}{l_{\max}} \right)^{-1} \qquad K = C_\mu^{1/4} l \sqrt{E} \qquad l_{LZ} = -k \frac{\sqrt{E}/l_{LZ}}{\frac{\partial}{\partial z}\left(\sqrt{E}/l_{LZ}\right)}$$

E-El model

Mellor and Yamada (1974)

$$\frac{\partial El}{\partial t} + \overline{U}_j \frac{\partial El}{\partial x_j} = \frac{\partial}{\partial x_i}\left(\frac{K}{\sigma_E} \frac{\partial El}{\partial x_i} \right) + l\left(C_1 P_E - C_2 \varepsilon F_{wall}\right) \qquad K = C_\mu^{1/4} l \sqrt{E}$$

$\sigma_E = 1$, $C_1 = 0.9$, $C_2 = 0.5$, and near-wall correction term $F_{wall} = (1 + 1.33 * (l / kz)^2)$

E-ε model

Jones and Launder (1972)

$$\frac{\partial \varepsilon}{\partial t} + \overline{U}_j \frac{\partial \varepsilon}{\partial x_j} = \frac{\partial}{\partial x_i}\left(\frac{K}{\sigma_\varepsilon} \frac{\partial \varepsilon}{\partial x_i} \right) + \frac{\varepsilon}{E}\left(C_{\varepsilon 1} P_E - C_{\varepsilon 2} \varepsilon\right) \qquad K = C_\mu \frac{E^2}{\varepsilon} \qquad l = \frac{C_\mu^{3/4} E^{3/2}}{\varepsilon}$$

$C_{\varepsilon 1} = 1.44$, $C_{\varepsilon 2} = 1.92$, $\sigma_E = 1$, and $\sigma_\varepsilon = 1.3$.

E-ω model $(\omega = \varepsilon / E)$

Kolmogorov (1942), Wilcox (1998)

$$\frac{\partial \omega}{\partial t} + \overline{U}_j \frac{\partial \omega}{\partial x_j} = \frac{\partial}{\partial x_i}\left(\frac{K}{\sigma_\omega} \frac{\partial \omega}{\partial x_i} \right) + \frac{\omega}{E}\left(C_{\omega 1} P_E - C_{\omega 2} \varepsilon\right) \qquad K = C_\mu \frac{E}{\omega} \qquad l = \frac{C_\mu^{3/4} E^{1/2}}{\omega}$$

$C_{\omega 1} = 0.52$, $C_{\omega 2} = 0.8$, $\sigma_E = 2.$, $\sigma_\omega = 2.$

Simulations "free-air" flow in ABL

Cabauw case

$$C_1 = \left[C_1 + (C_2 - C_1)\frac{l}{l_{\max}} \right] \qquad l_{\max} = \frac{0.00027G}{f} \qquad \sigma = \frac{k^2}{C_\mu^{1/2}(C_2 - C_1)}$$

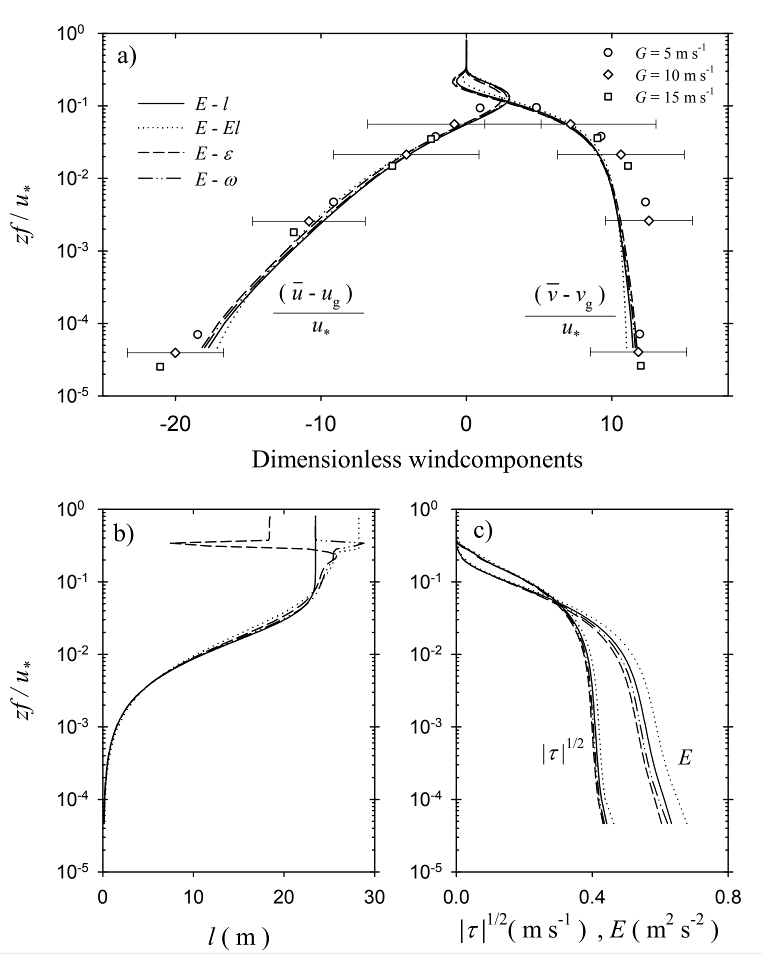

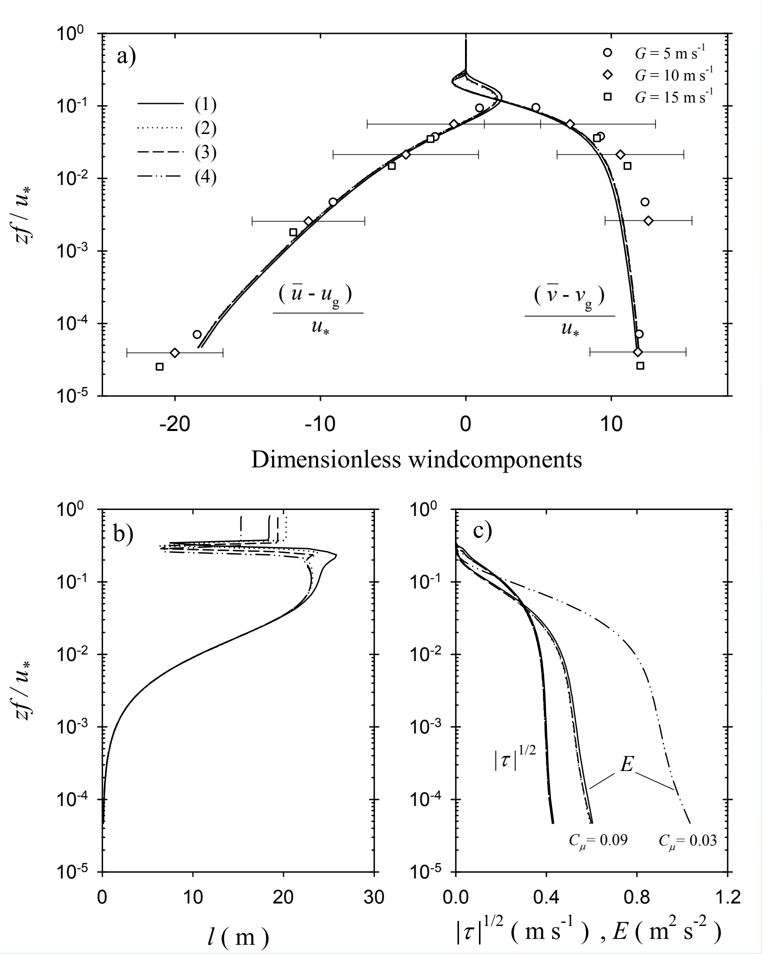

(Apsley and Castro, 1997; Sogachev and Panferov, 2006)

Accounting for a plant drag

$$\frac{\partial \overline{U}_i}{\partial t} + \overline{U}_j \frac{\partial \overline{U}_i}{\partial x_j} + 2\varepsilon_{ijk}\Omega_j \overline{U}_k = -\frac{1}{\rho_0}\frac{\partial \overline{P}}{\partial x_i} - \frac{\partial \overline{u_j u_i}}{\partial x_j} + S_i$$

(Raupach and Shaw, 1982)

$$\frac{\partial E}{\partial t} + \overline{U}_j \frac{\partial E}{\partial x_j} = \frac{\partial}{\partial x_i}\left(\frac{K}{\sigma_E}\frac{\partial E}{\partial x_i}\right) + P_E - \varepsilon + S_E$$

$$\frac{\partial El}{\partial t} + \overline{U}_j \frac{\partial El}{\partial x_j} = \frac{\partial}{\partial x_i}\left(\frac{K}{\sigma_E}\frac{\partial El}{\partial x_i}\right) + l\left(C_1 P_E - C_2 \varepsilon F_{wall}\right) + S_{El}$$

$$\frac{\partial \varepsilon}{\partial t} + \overline{U}_j \frac{\partial \varepsilon}{\partial x_j} = \frac{\partial}{\partial x_i}\left(\frac{K}{\sigma_\varepsilon}\frac{\partial \varepsilon}{\partial x_i}\right) + \frac{\varepsilon}{E}\left(C_{\varepsilon 1} P_E - C_{\varepsilon 2}\varepsilon\right) + S_\varepsilon$$

$$\frac{\partial \omega}{\partial t} + \overline{U}_j \frac{\partial \omega}{\partial x_j} = \frac{\partial}{\partial x_i}\left(\frac{K}{\sigma_\omega}\frac{\partial \omega}{\partial x_i}\right) + \frac{\omega}{E}\left(C_{\omega 1} P_E - C_{\omega 2}\varepsilon\right) + S_\omega$$

S_φ $(\varphi = El,\ \varepsilon\ \omega)$

Canopy flow simulation by different models

$$S_E = \beta_p c_d\, A(z)\left|U\right|^3 - \beta_d\, c_d\, A(z)\left|U\right| E$$

$$S_\varphi = \alpha_p \beta_p \frac{\varphi}{E} S_p - \alpha_d\, \beta_d \frac{\varphi}{E} S_d$$

Type	Model	β_p	β_d	$\alpha_{\varphi p}$	$\alpha_{\varphi d}$
$E{-}El$	Analytical	1.0	4.0	1.0	1.0
	Yamada (1982)	1.0	0.0	1.0	0.0
$E{-}\varepsilon$	Analytical	1.0	4.0	1.5	1.5
	Liu et al. (1996)	1.0	4.0	1.5	0.6
	Foudhil et al. (2005)	0.8	4.0	1.875	0.81
$E{-}\omega$	Analytical	1.0	4.0	0.5	0.5
	Neary (2003)	0.05	0.0	3.2	0.0

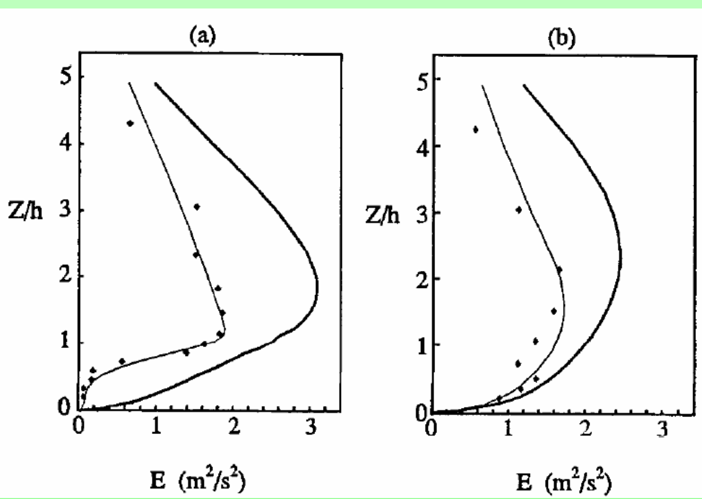

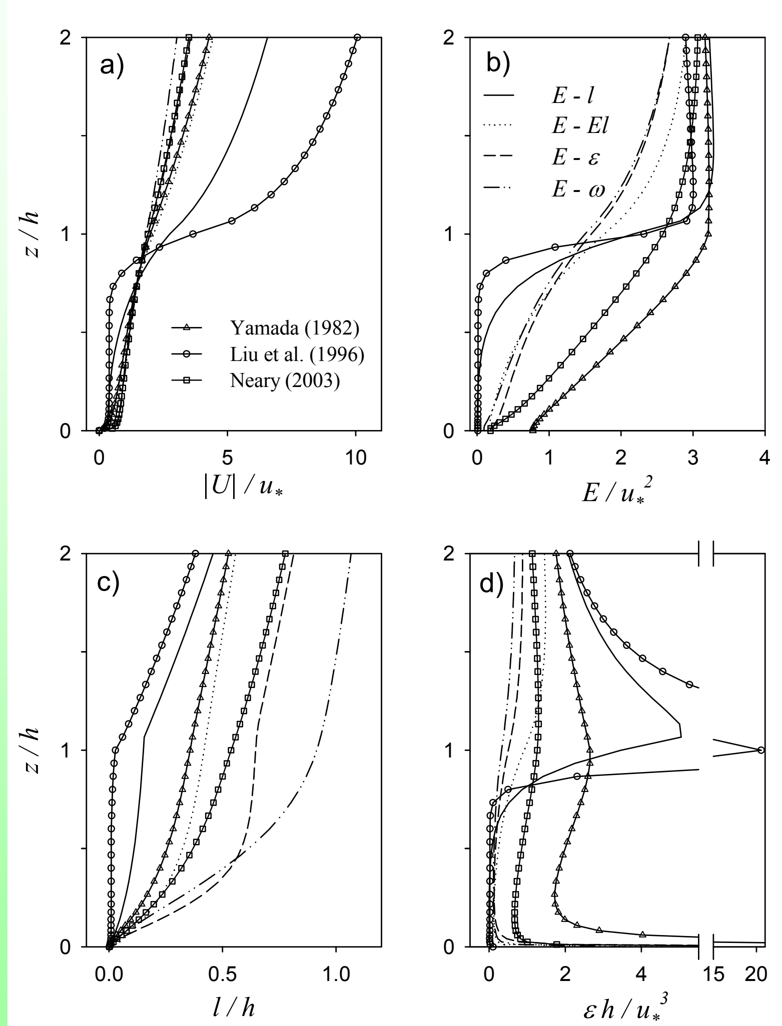

E-l model with vegetation parameterization as in Wilson et al. (1998)

(Sogachev and Panferov., 2006)

What is the reason of diversity?

$$\frac{\partial E}{\partial t} + \overline{U}_j \frac{\partial E}{\partial x_j} = \frac{\partial}{\partial x_i}\left(\frac{K}{\sigma_E}\frac{\partial E}{\partial x_i}\right) + P_E - \varepsilon + S_E$$

$$\frac{\partial \varepsilon}{\partial t} + \overline{U}_j \frac{\partial \varepsilon}{\partial x_j} = \frac{\partial}{\partial x_i}\left(\frac{K}{\sigma_\varepsilon}\frac{\partial \varepsilon}{\partial x_i}\right) + \frac{\varepsilon}{E}\left(C_{\varepsilon 1} P_E - C_{\varepsilon 2}\varepsilon\right) + S_\varepsilon$$

$$K = C_\mu \frac{E^2}{\varepsilon} \longrightarrow K = C_\mu \frac{E^2}{\varepsilon - S_E}$$

(Ayotte et al., 1999)

$$\frac{P_E}{\varepsilon_0} \neq \frac{C_2}{C_1}$$

(Sogachev and Panferov., 2006)

Proposed modification of two-equation models

$$\frac{P_E}{\varepsilon_0} = \frac{C_2 - \gamma}{C_1 - \gamma} = \frac{C_{2\gamma}}{C_{1\gamma}} \qquad [E/\varepsilon](t) = \text{const}$$

For E-El, E-ε and E-ω models
γ are 1.5, 1.0 and 0.0, respectively (Pope, 2000)

$$\frac{P_E + \alpha_{\varphi p} S_p}{\varepsilon_0 + \alpha_{\varphi d} S_d} = \frac{C_{2\gamma}}{C_{1\gamma}}$$

$$\frac{P_E + S_p}{\varepsilon_0 + S_d} = \frac{C^*_{2\gamma}}{C_{1\gamma}} \qquad P_E = C_{2\gamma}\,\varepsilon_0 / C_{1\gamma}$$

$$C_2^* = C_2 - \frac{(C_2 - 1.5) S_d El}{C_\mu^{3/4} E^{5/2}} + \frac{(C_1 - 1.5) S_p El}{C_\mu^{3/4} E^{5/2}}$$

$$C_2^* = C_2 - \frac{(C_2 - 1) S_d}{\varepsilon} + \frac{(C_1 - 1) S_p}{\varepsilon}$$

$$C_2^* = C_2 - \frac{C_2 S_d}{E\omega} + \frac{C_1 S_p}{E\omega}$$

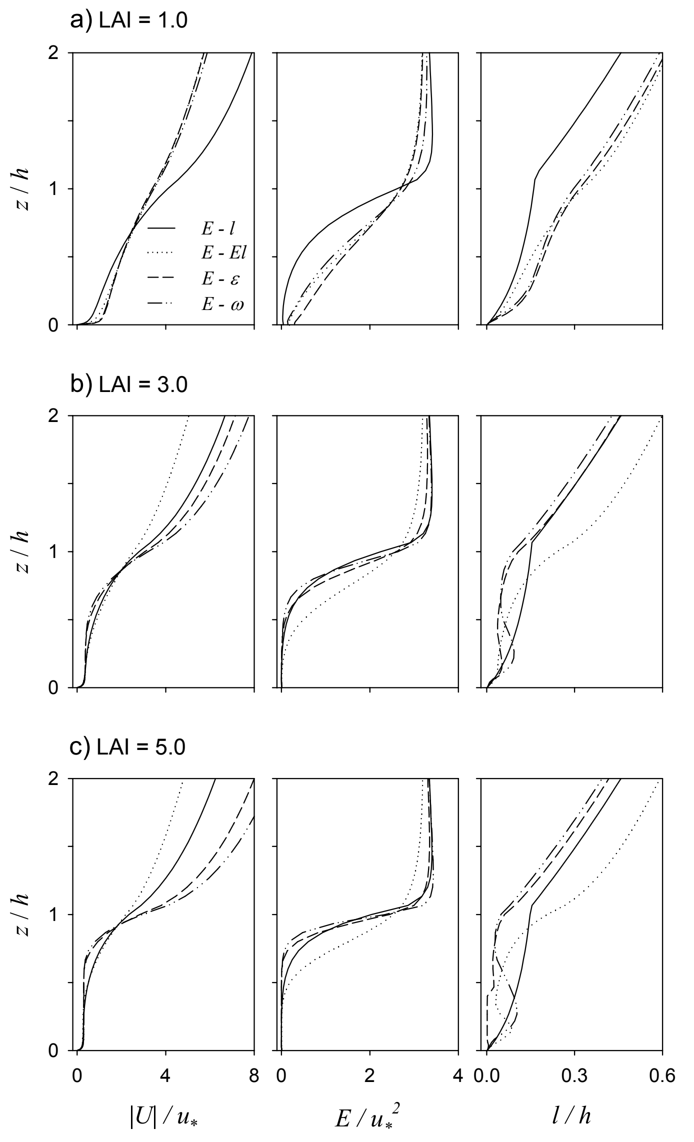

(Sogachev and Panferov., 2006)

Proposed modification …(continued)

With $S_p = S_d$ (Seginer et al., 1976)

$$C_2^* = C_2 - \frac{(C_2 - C_1)S_d El}{C_\mu^{3/4} E^{5/2}}$$

$$C_2^* = C_2 - \frac{(C_2 - C_1)S_d}{\varepsilon}$$

$$C_2^* = C_2 - \frac{(C_2 - C_1)S_d}{E\omega}$$

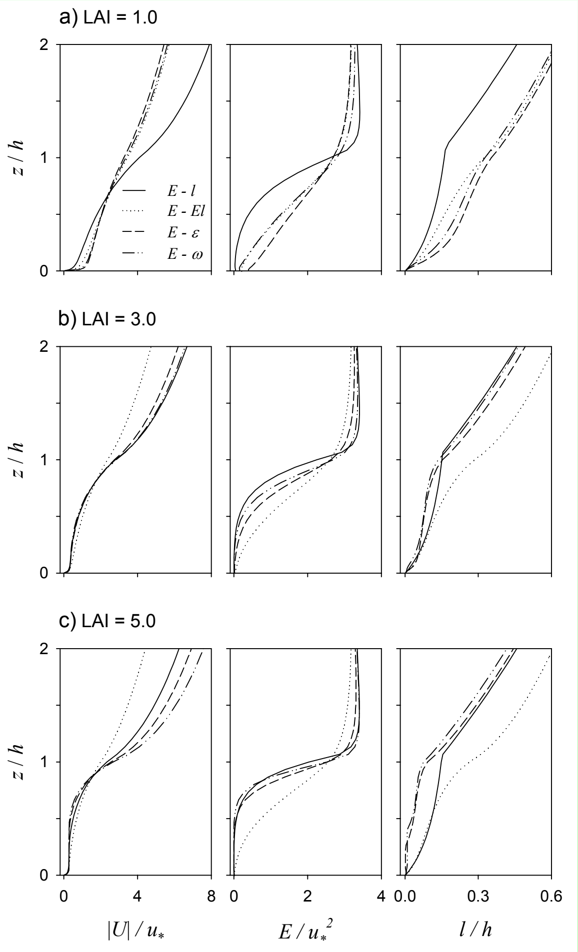

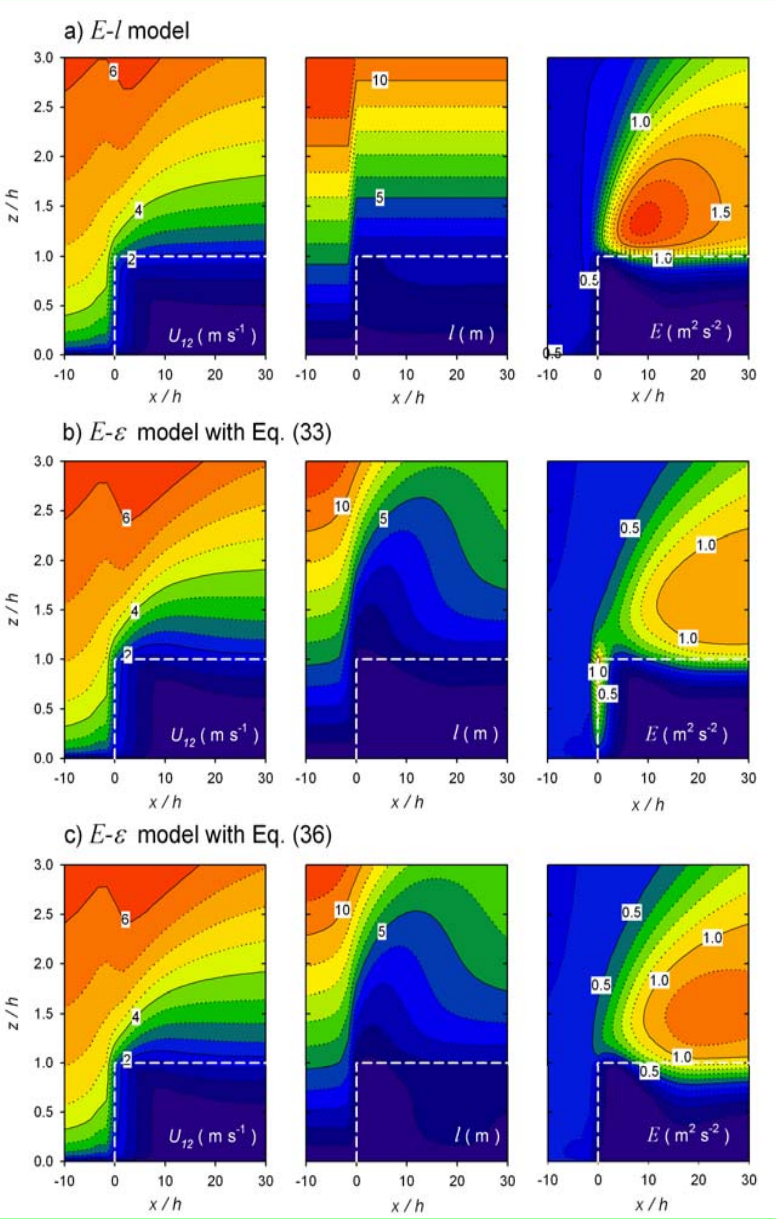

(Sogachev and Panferov., 2006)

Some examples of the model verification with proposed modification and new assumption of S_d

$$S_d \approx \beta_d\left(C_\mu\right)C_d\, A(z)\left|U\right| E$$

based on experimental data of Seginer et al. (1976) and Gardiner (1992)

►The *Elora corn* canopy
(Wilson et al., 1982; Wilson, 1988)

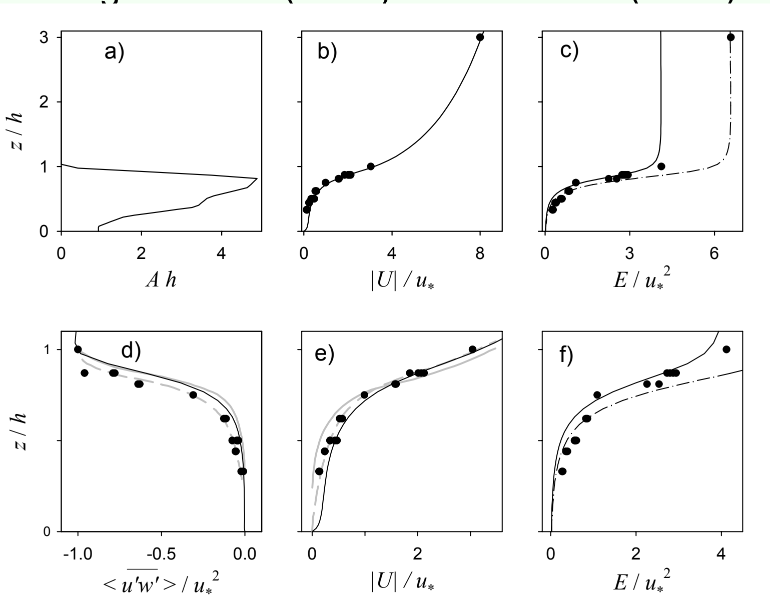

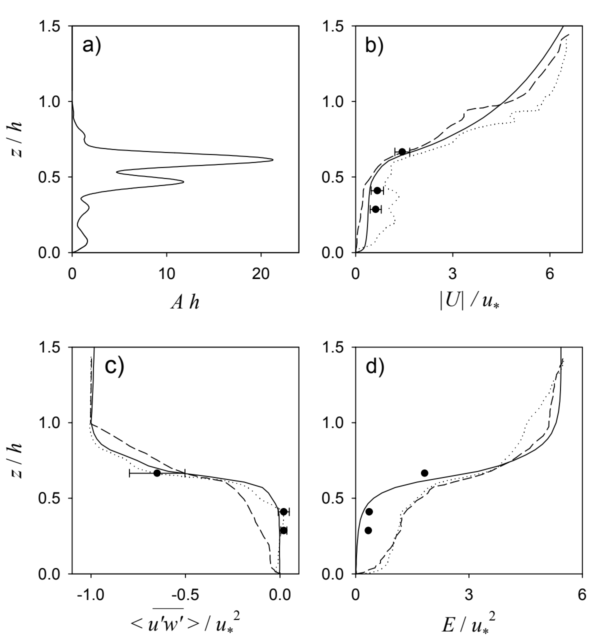

▲The *Pine forest* canopy
(Katul and Chang, 1999)

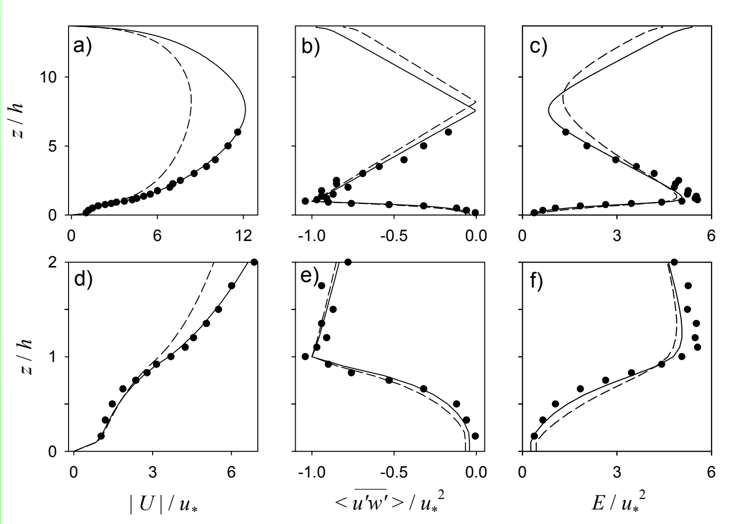

◄*Furry hill* wind-tunnel experiment
(Finnigan and Brunet, 1995)

(Sogachev and Panferov, 2006)

Turbulence regime study

Experimental observations of turbulence downwind of a forest edge (Kruijt, 1994):
-The turbulent diffusivity strongly decreased (to 60% of the equilibrium value)
- This drop was correlated with deficits of low-frequency (large eddy) turbulence
-The spectral analysis showed that turbulent length scales were smaller on average than in equilibrium conditions. This variation in length scales appeared to explain the variation in diffusivity.

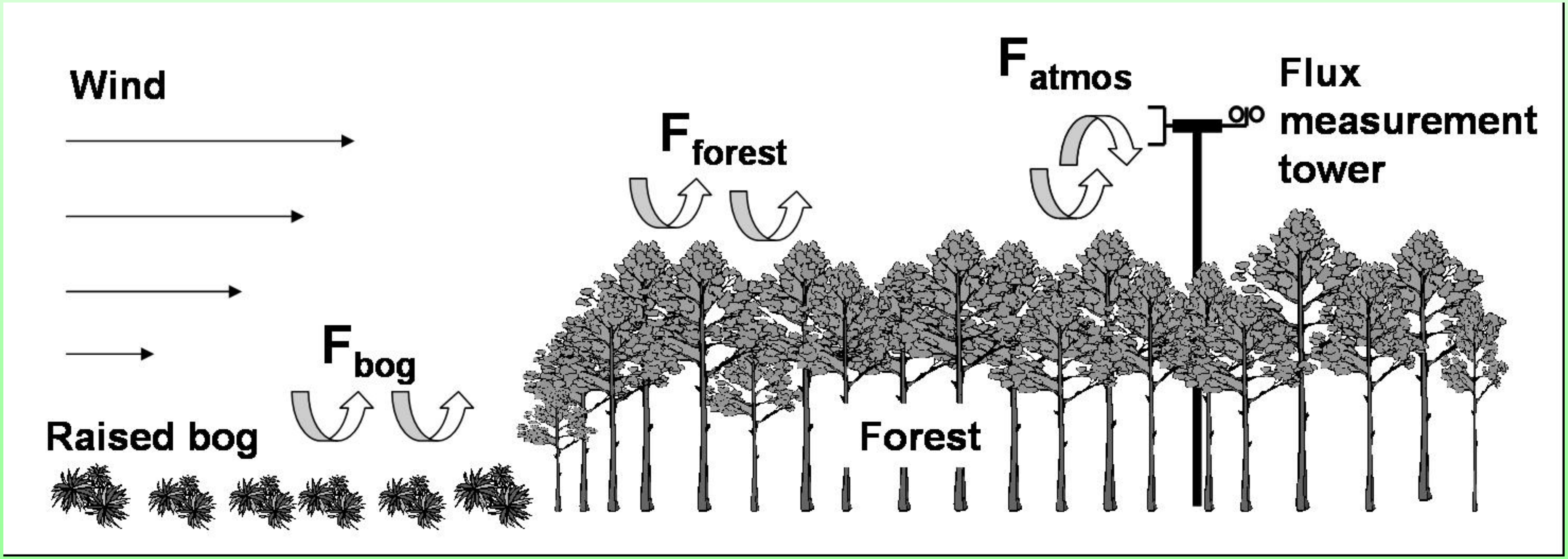

(Kruijt, 1994)

Forest edge effect

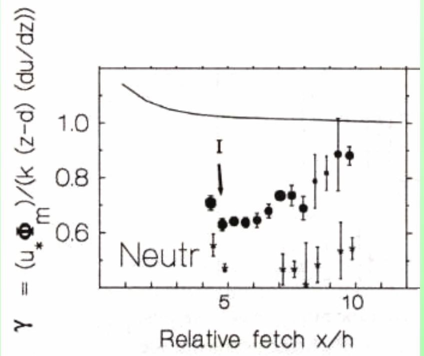

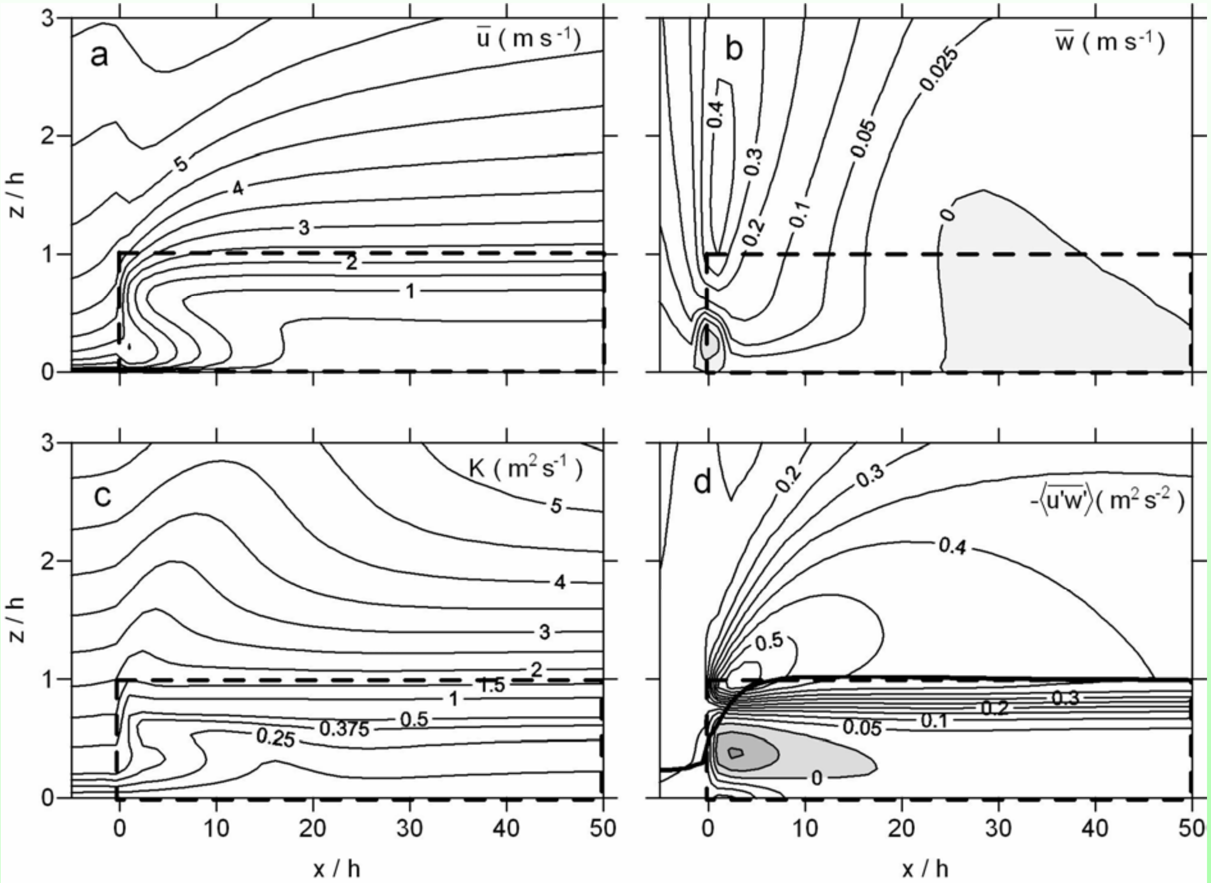

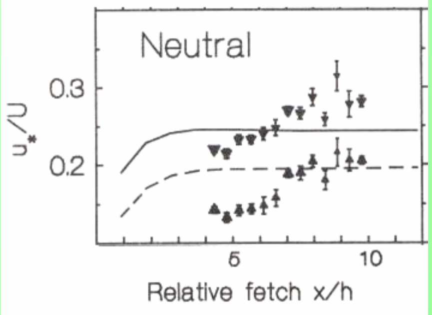

(Kruijt, 1994, Sogachev et al. 2007)

Turbulence regime
(qualitative comparison with measurements)

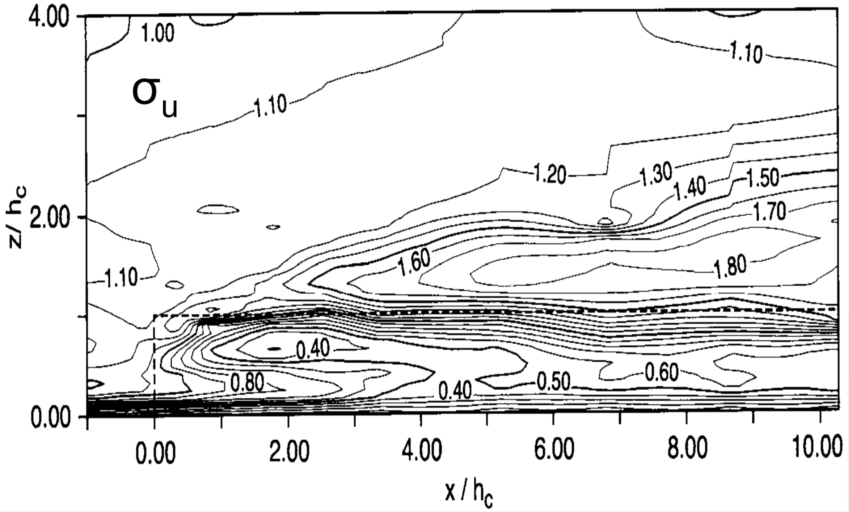

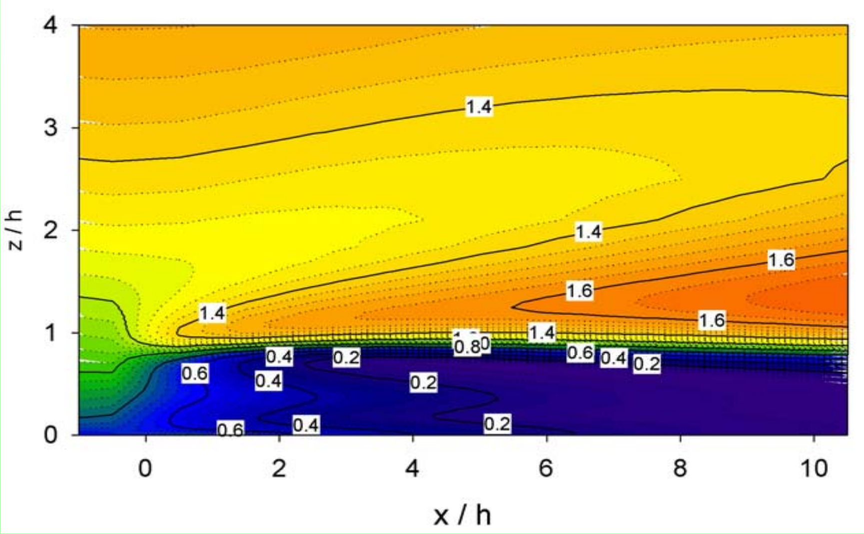

(Morse et al., 2002)

Turbulence regime
(comparison SCADIS with wind-tunnel measurements)

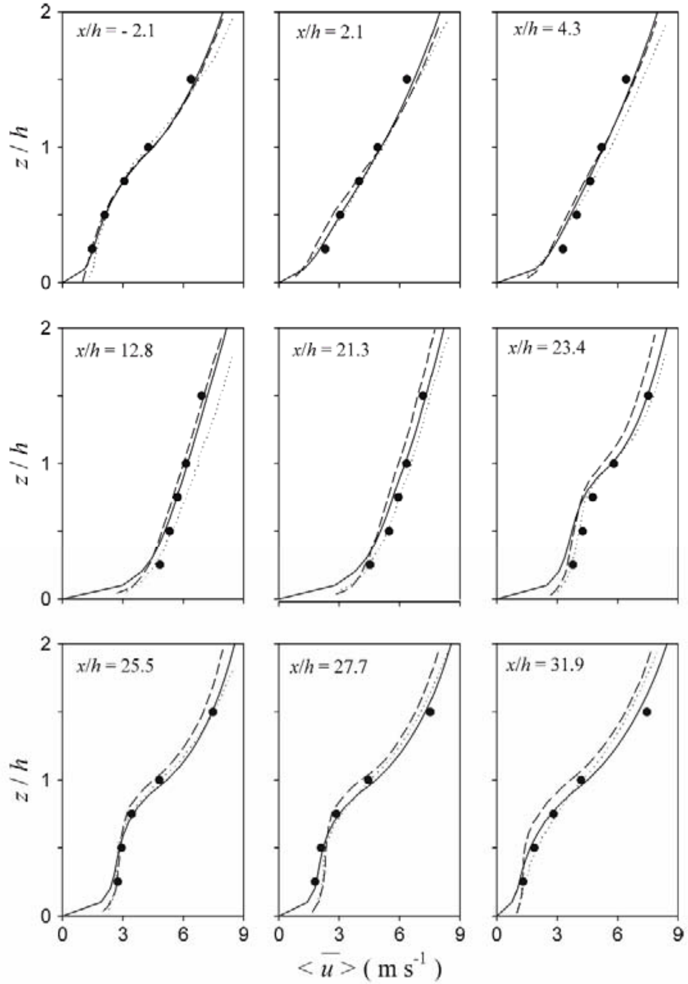

Fig. 13 Comparison between vertical profiles of measured (symbols) and modelled (lines) mean horizontal wind, $\langle \bar{u} \rangle$ across a clearing of width $21.3h$ in a model forest. The position at $x/h = 0$ corresponds to the beginning of the clearing. The solid line represents E–ω model, the dotted line shows Wilson and Flesch's (1999) model and the dashed line — Foudhil's et al. (2005) model

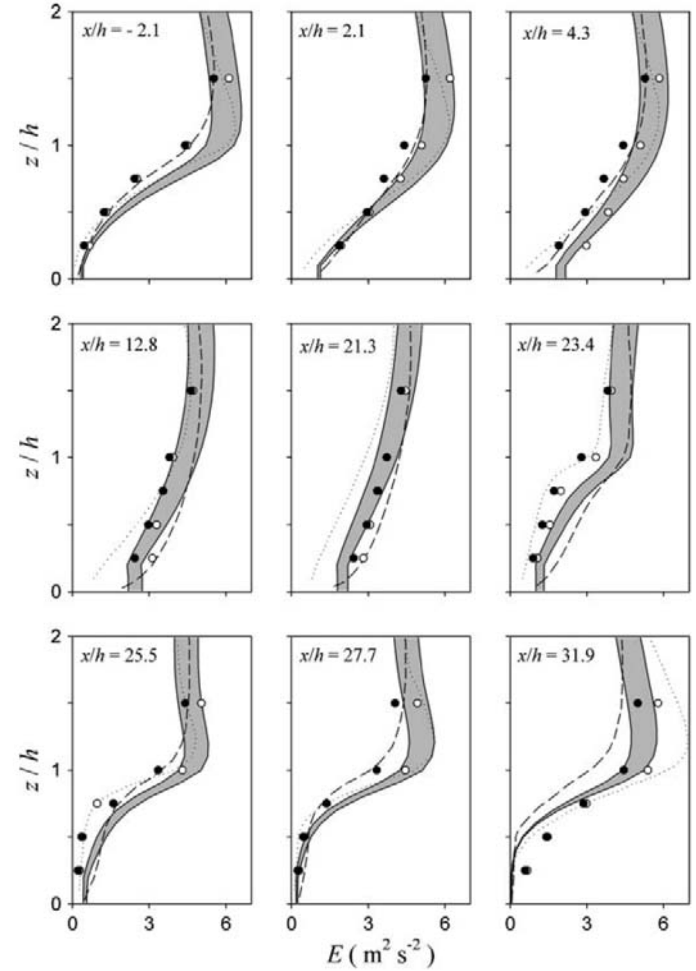

Fig. 14 Comparison between vertical profiles of measured (symbols) and modelled (lines) turbulent kinetic energy, E across a clearing of width $21.3h$ in a model forest. The position at $x/h = 0$ corresponds to the beginning of the clearing. The solid line represents E–ω model, the dotted line Wilson and Flesch's (1999) model, and the dashed line Foudhil et al.'s (2005) model. Symbols (○) and (●) indicate different estimates of E derived by Wilson and Flesch (1999) and Foudhil et al. (2005), respectively. Grey zones show the range of E values modelled by E–ω model with C_μ values ranging between 0.0324 and 0.0524, which are associated with the E estimates of Wilson and Flesch (1999) and Foudhil et al. (2005), respectively

(Sogachev and Panferov, 2006)

Some examples of the model verification

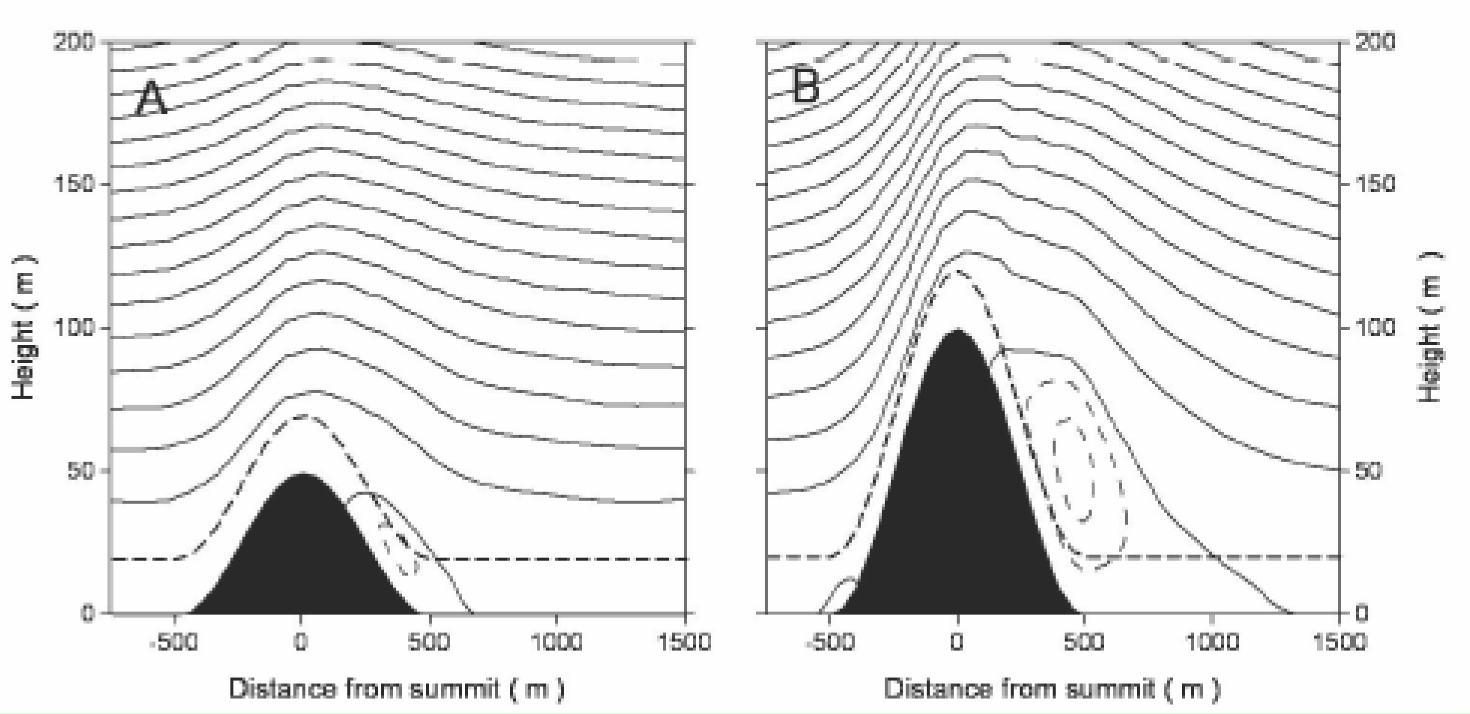

(Finnigan and Brunet, 1995, Sogachev et al., 2004)

SCADIS model and its applications

Scheme of the SCADIS (scalar distribution) model

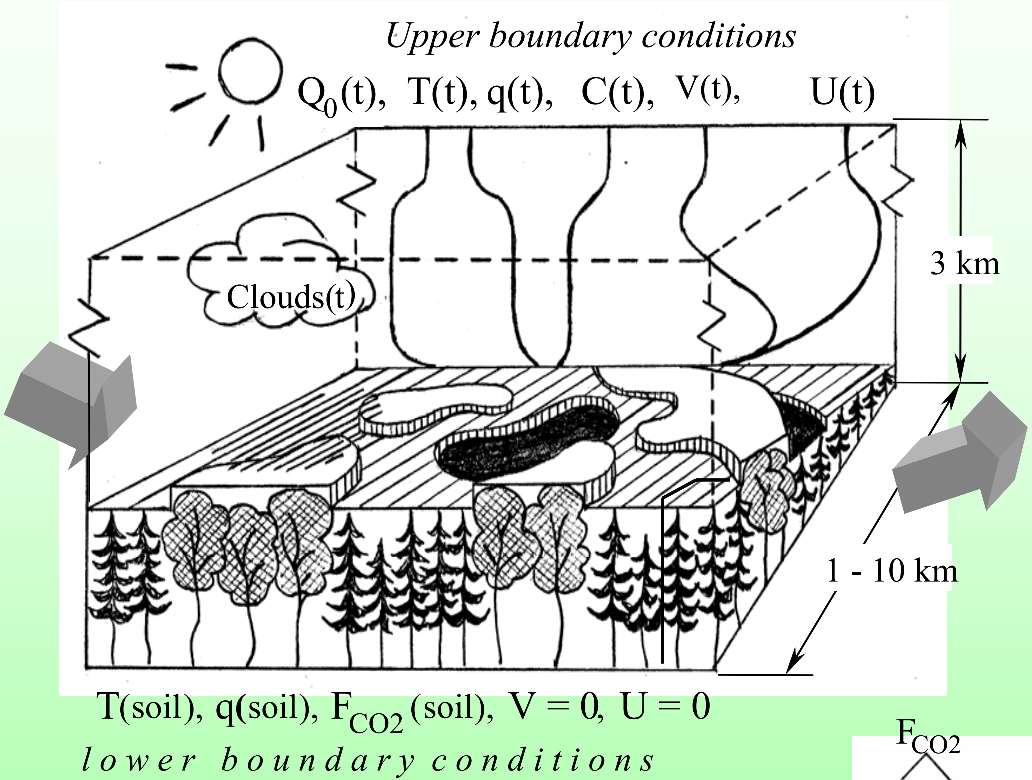

SCADIS is high resolution 3-D numerical model capable of computing the physical processes within both plant canopy and atmospheric boundary layer simultaneously.

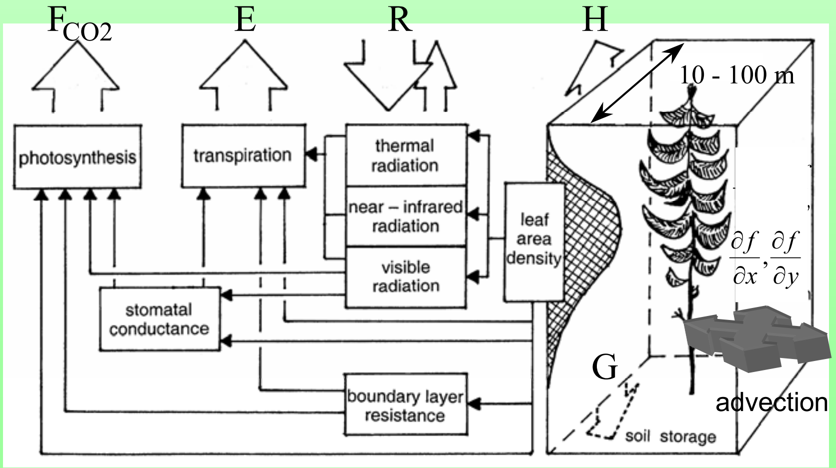

(Sogachev et al., 2002)

Vegetation description in the SCADIS model

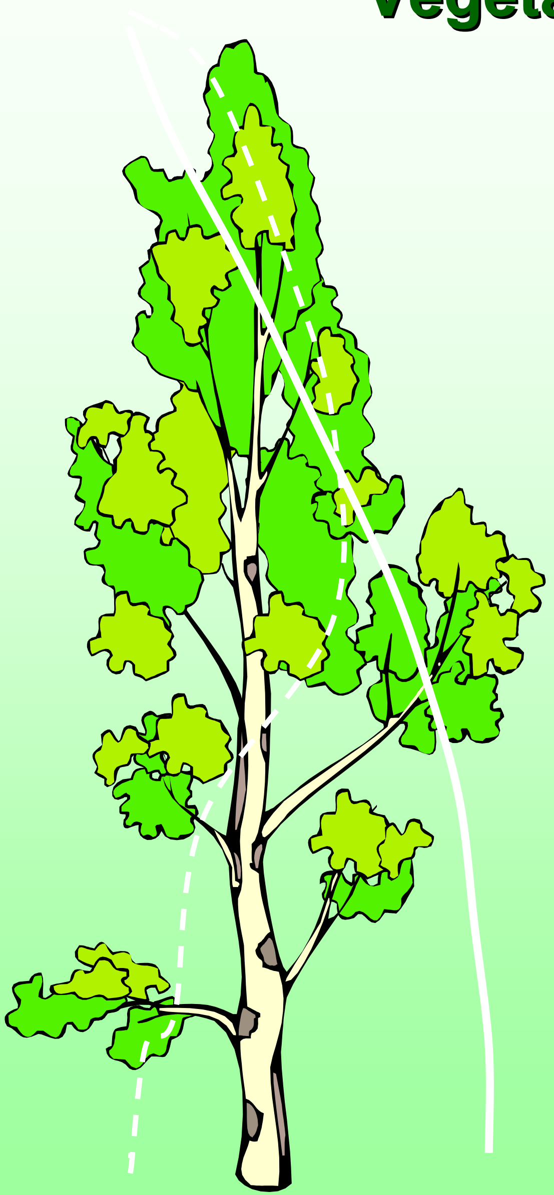

A(z) [м^2 м$^{-3}$]　　LAI [м^2 м$^{-2}$]

Structure of vegetation…

Sources caused by vegetation in equations :

momentum

$$S_i = -c_d\, A(z)\,\overline{U}_i\,|U|,$$ (Raupach and Shaw, 1982)

turbulent kinetic energy

$$S_E = 0. \qquad \frac{\partial E}{\partial t} + \overline{U}_j \frac{\partial E}{\partial x_j} = \frac{\partial}{\partial x_i}\left(\frac{K}{\sigma_E}\frac{\partial E}{\partial x_i}\right) + P_E - \varepsilon$$

closure

$$S_\omega = 0. \qquad \frac{\partial \omega}{\partial t} + \overline{U}_j \frac{\partial \omega}{\partial x_j} = \frac{\partial}{\partial x_i}\left(\frac{K}{\sigma_\omega}\frac{\partial \omega}{\partial x_i}\right) + \frac{\omega}{E}\left(C_{\omega 1} P_E - C_{\omega 2}\varepsilon\right)$$

$$C^*_{\omega 2} = C_{\omega 2} - \frac{\left(C_{\omega 2} - C_{\omega 1}\right) S_d}{E\omega} \qquad S_d \approx \beta_d\left(C_\mu\right) C_d\, A(z)\,|U|\, E$$

(Sogachev and Panferov, 2006)

Clear-cut study site in Solling, Germany

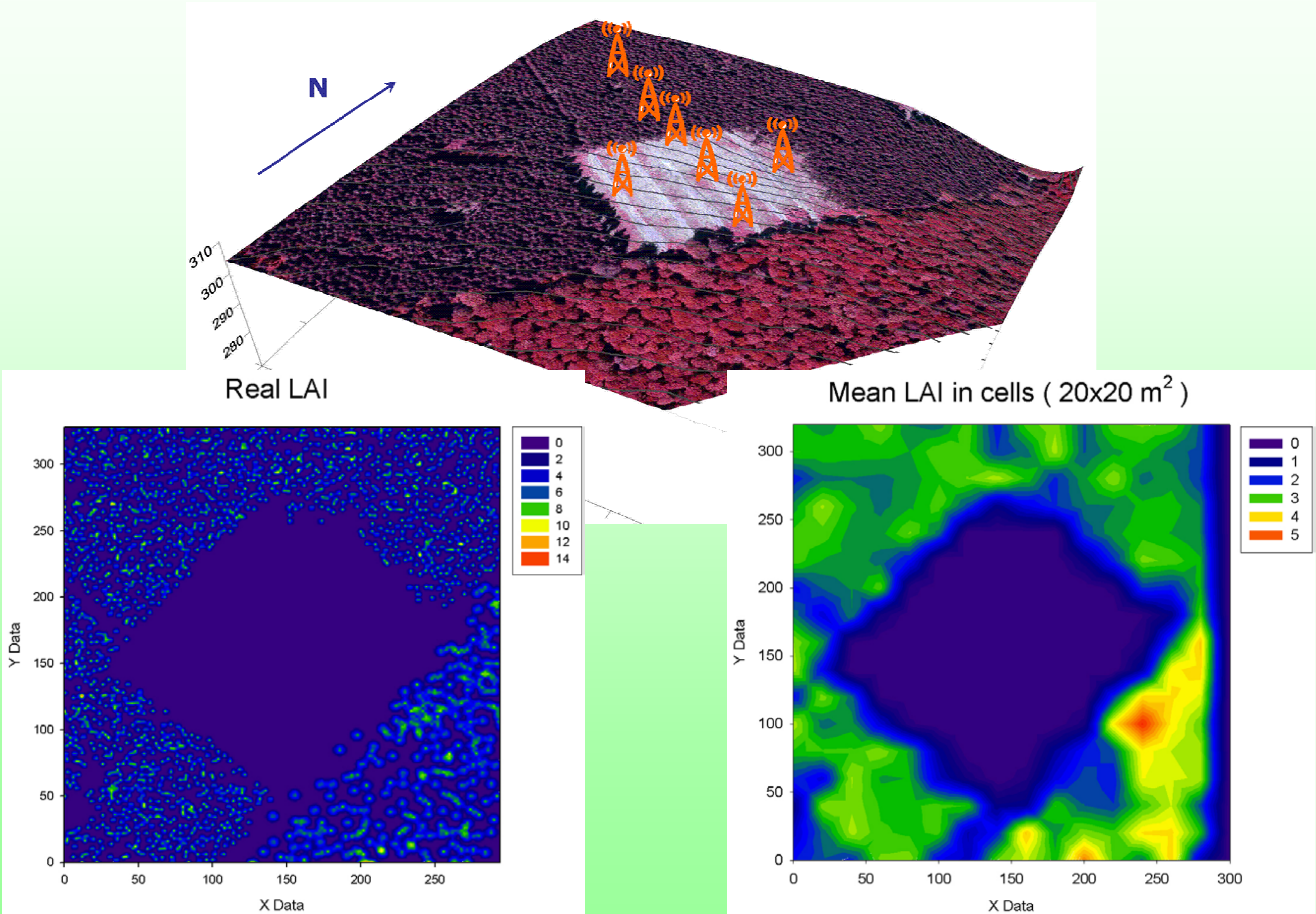

(Oltchev et al., 2005; DFG Crant Gr 738/16-1)

Modelled airflow over study area in Solling

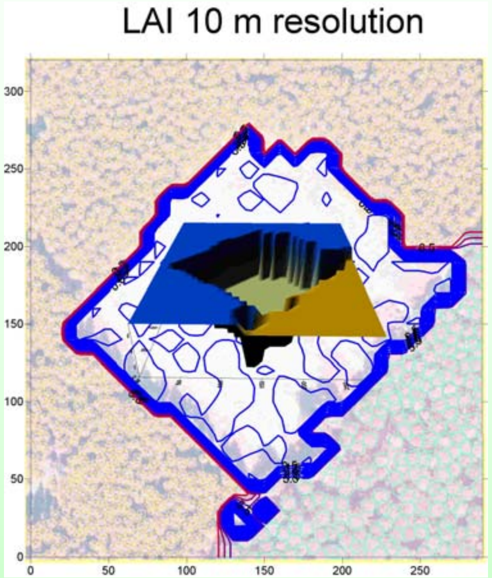

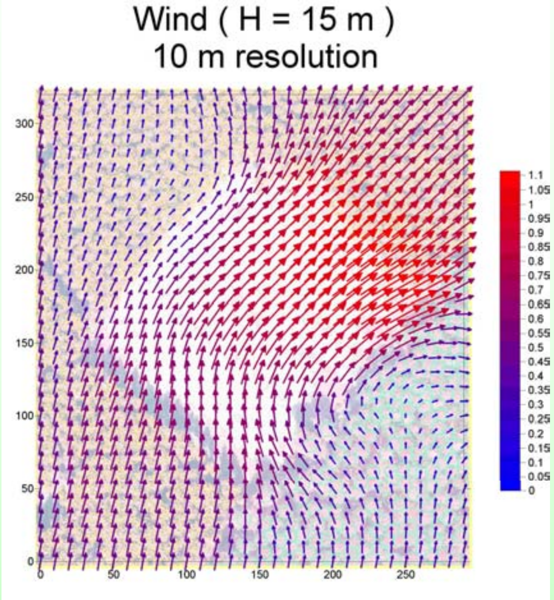

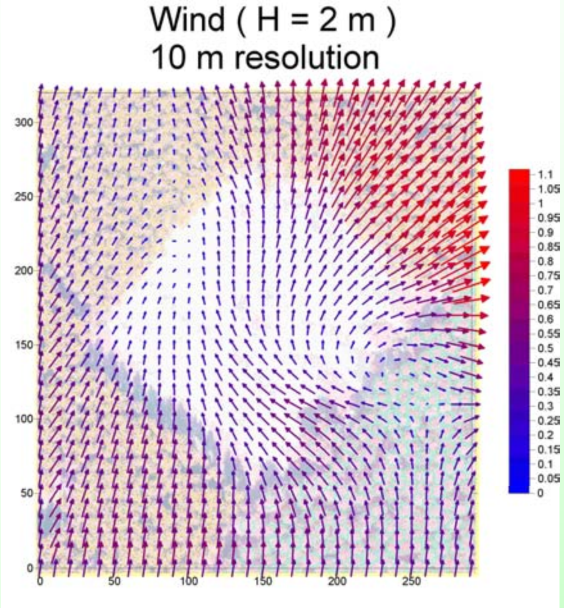

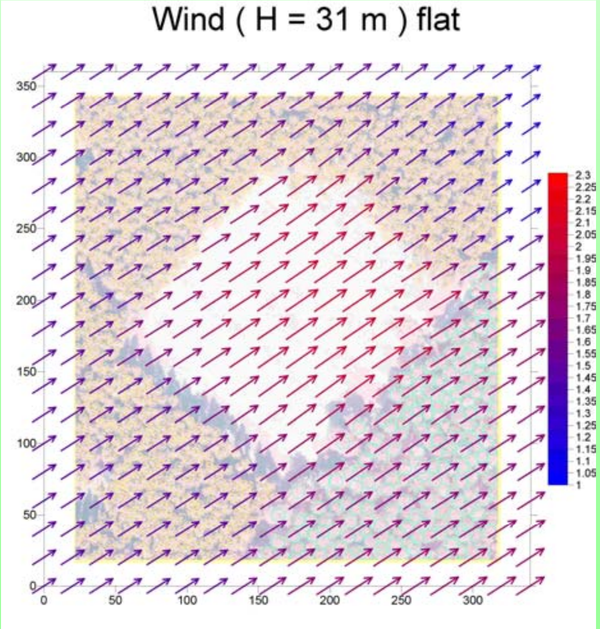

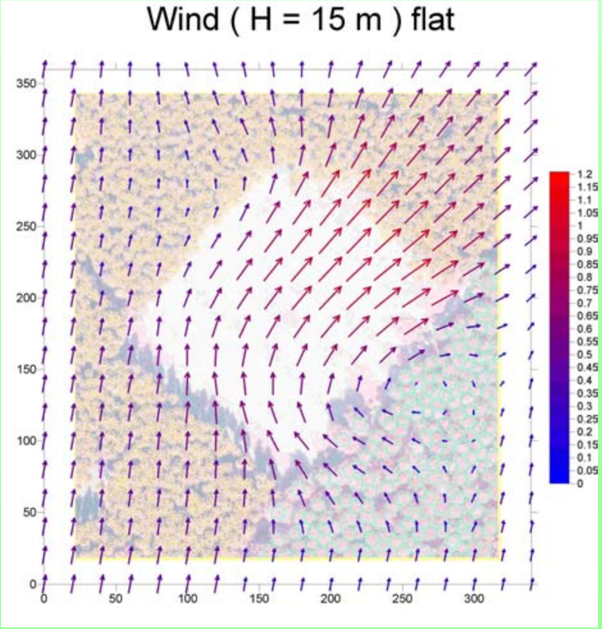

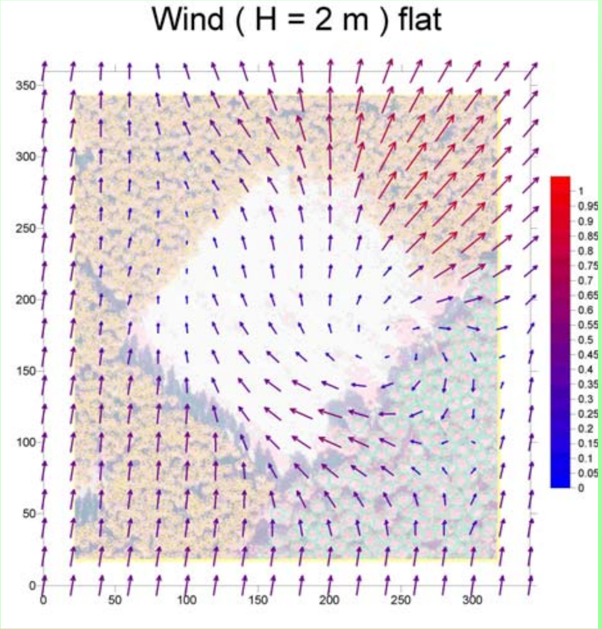

Source weight function or flux footprint

Definition

In a simple form «footprint» or «source weight function» $f\ (x,y,z_m)$ is the transfer function between the measured value at a certain point $F(0,0,z_m)$ and the set of forcings on the surface-atmosphere interface $F(x,y,0)$ (Schuepp et al., 1990, Schmid, 2002).

$$F(0,0,z_m) = \int_{-\infty}^{\infty}\int_{0}^{\infty} F(x,y,0)\,f(x,y,z_m)\,dxdy$$

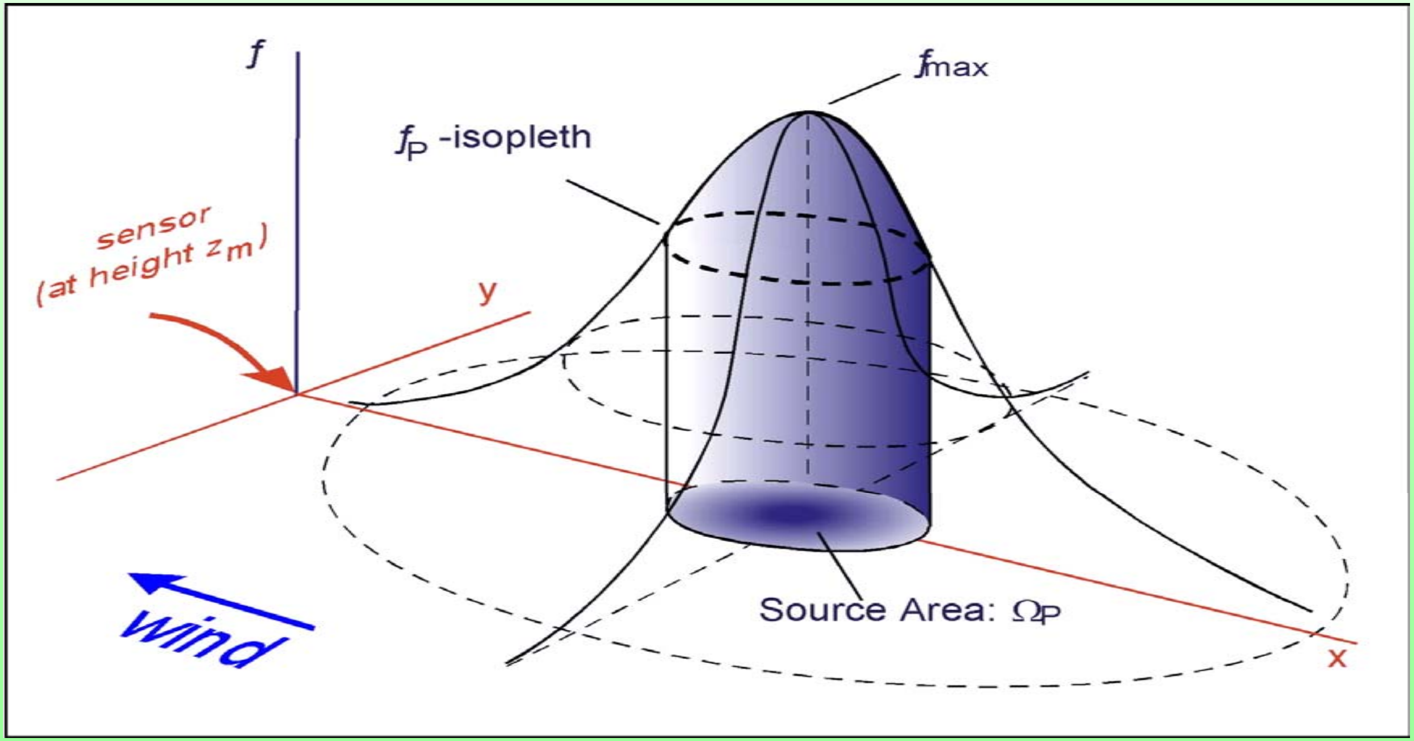

(Schmid, 2002)

Footprint prediction for urban terrain in Helsinki, Finland

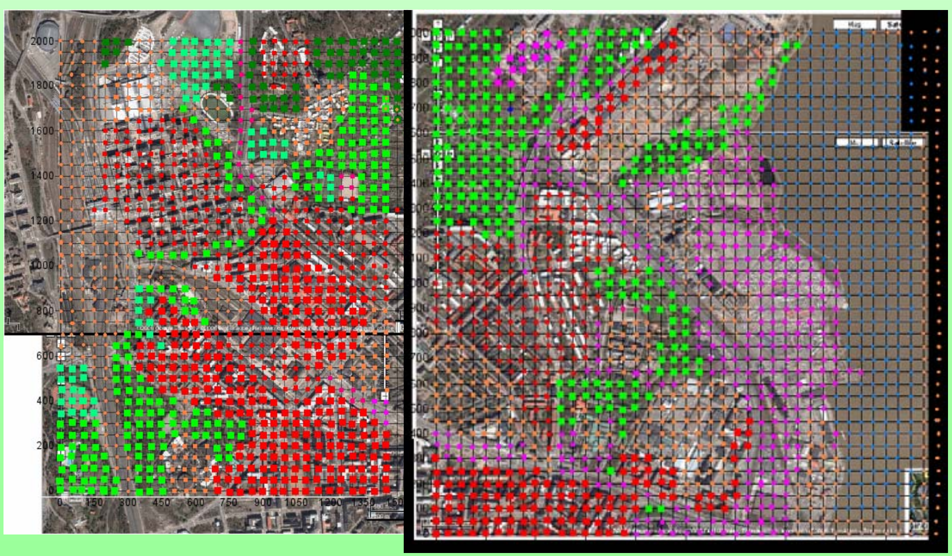

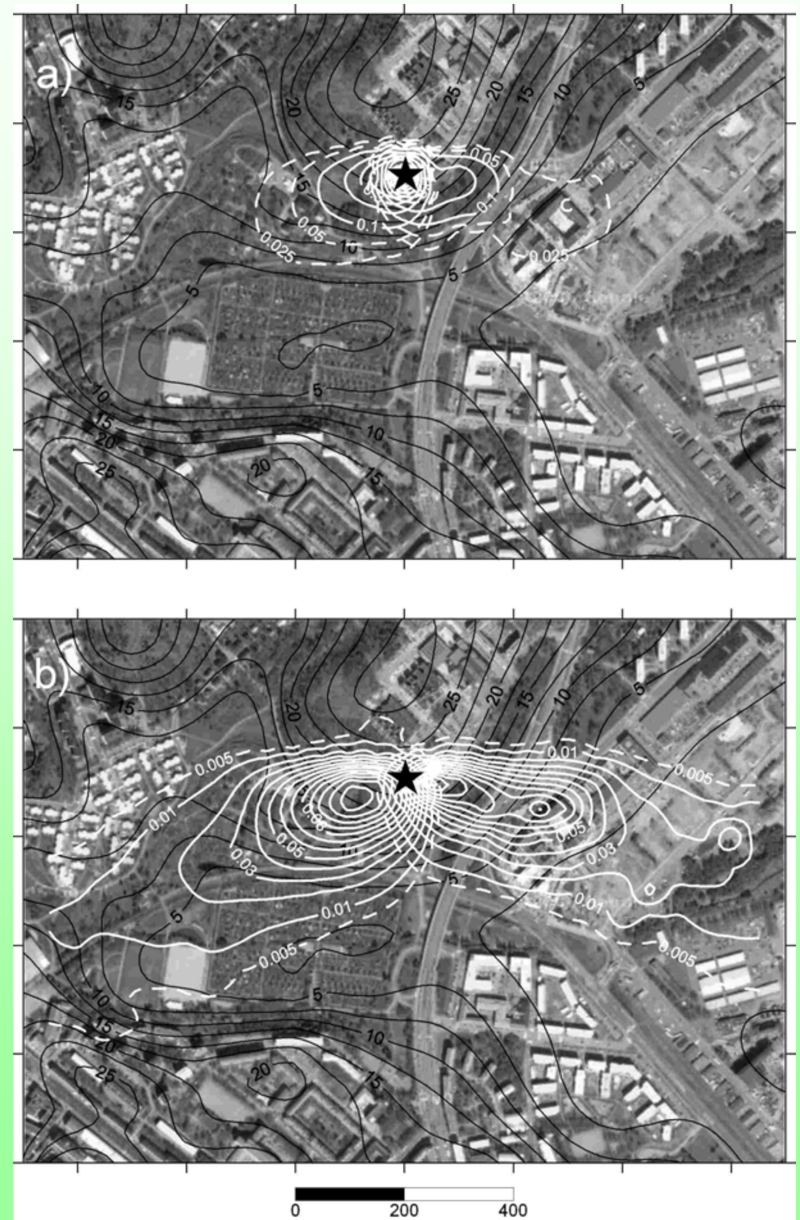

(Vesala et al., 2007)

Footprint prediction for Lake tower, Sweden

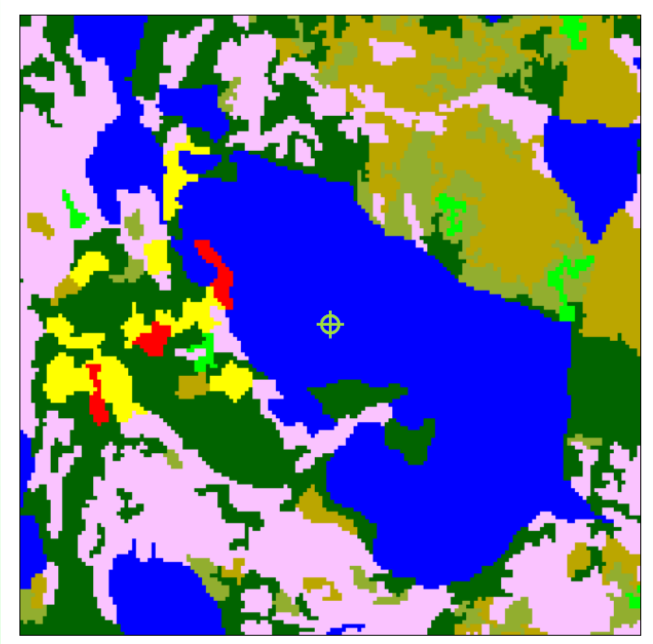

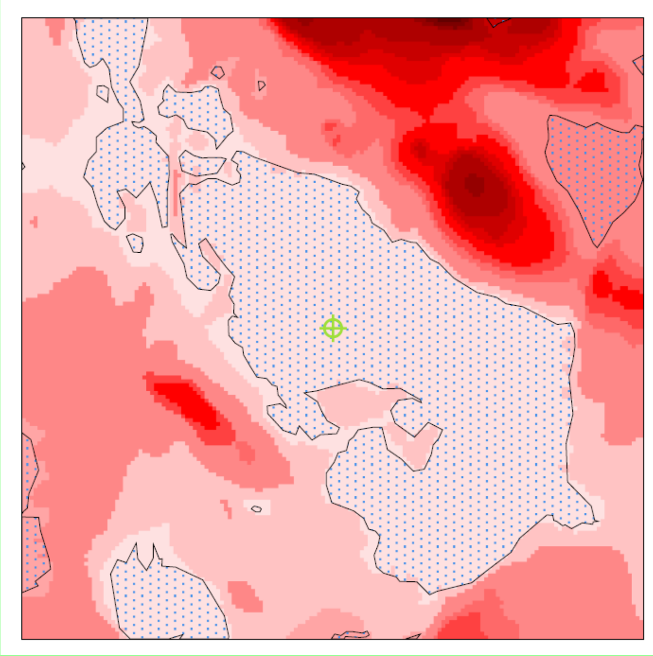

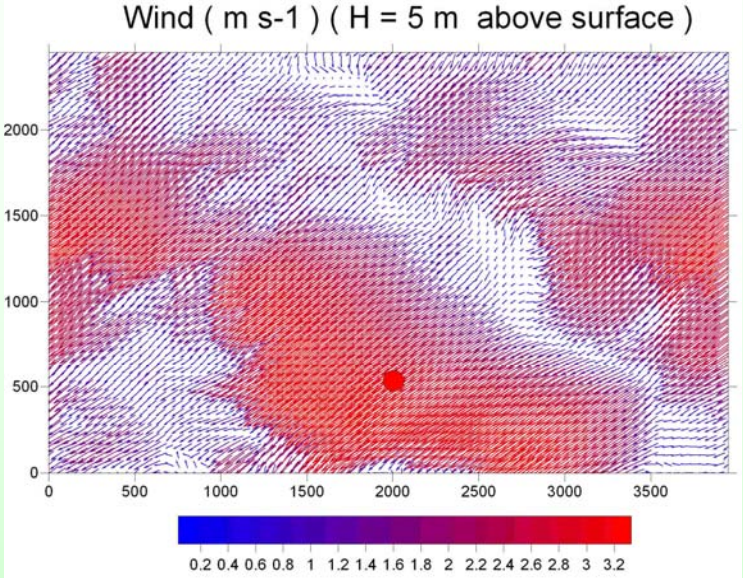

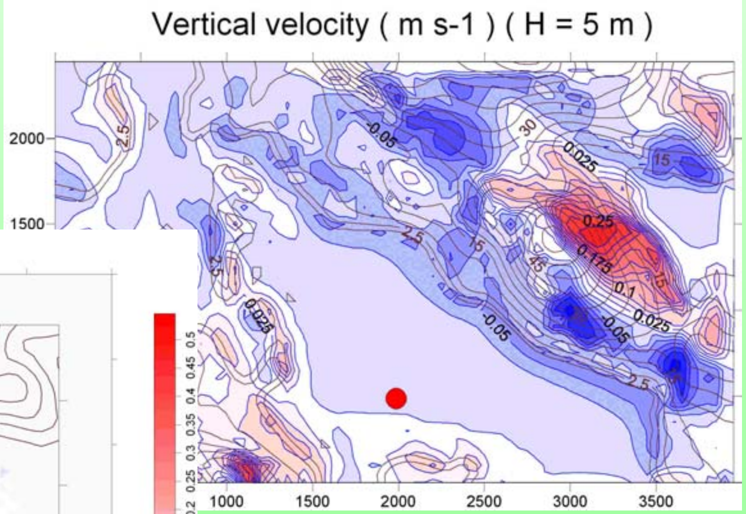

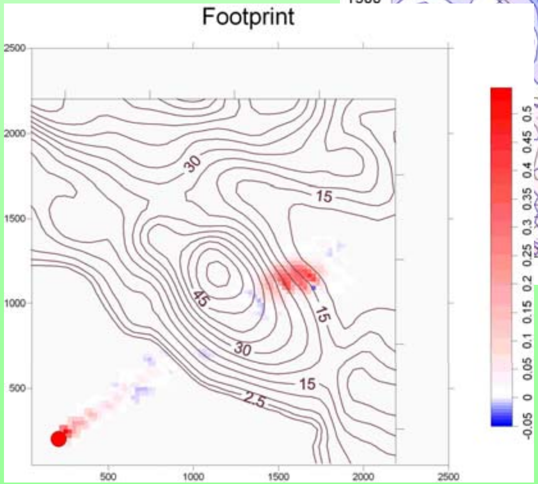

ABL dynamics

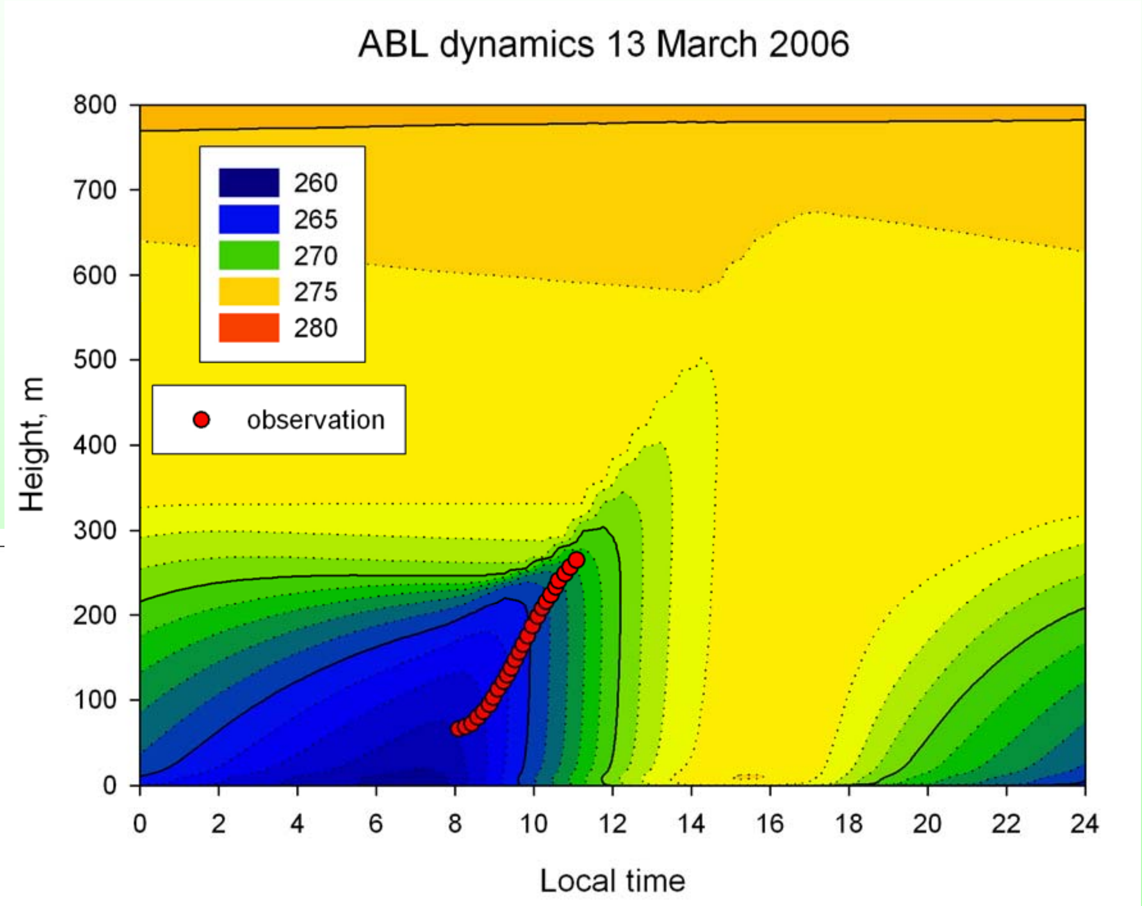

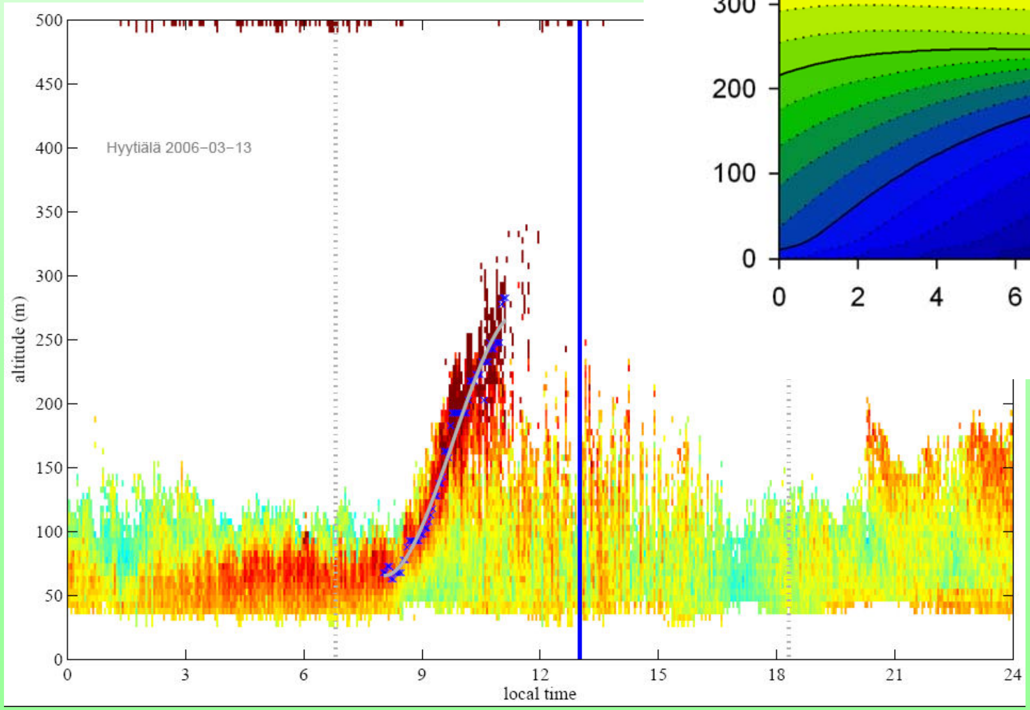

(Lasko et al., 2007)

Snow cover depletion

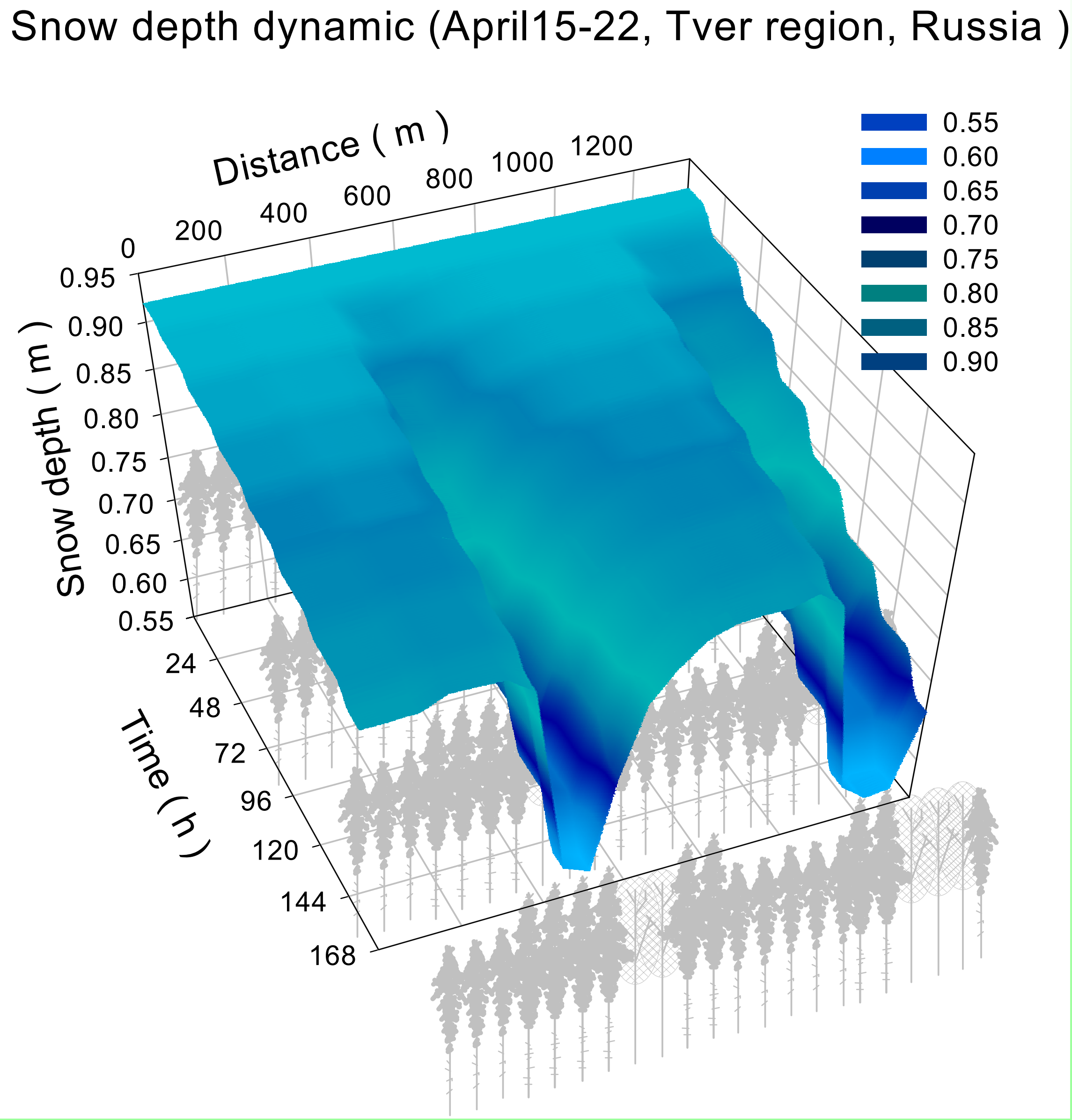

Summary

Vegetation is important factor in interaction between underlying surface and atmosphere.

The variety of turbulence models exists to describe this interaction

High-resolution models, which are able to describe canopy-PBL layer in a realistic manner without resort to vast computing expenses, can serve as efficient analysis tools to describe the key points of the heterogeneous surface-atmosphere system.

The two-equation closure model is a compromise between time consuming LES- and higher-order closure models and simple E-l models.

SCADIS model based on E-ω scheme has the potential to be widely applied for many problems. A number of applications have been shown.

Though present model approach seems to represent an economical and physically sound way to describe the atmosphere-vegetation interaction, it is unable to take into account all nuances of processes occurring in the gap-forest transition zone. Additional efforts are needed to improve the model.


Thank you for your attention !